The biology of *Asparagopsis armata* for closed-life cycle cultivation in New Zealand

A thesis

submitted in partial fulfilment

of the requirements for the degree

of

Doctor of Philosophy in Biological Science

at

The University of Waikato

by

Alisa Andrea Mihaila

THE UNIVERSITY OF
WAIKATO
Te Whare Wānanga o Waikato

2024

Abstract

The red seaweed *Asparagopsis armata* is a target species for aquaculture due to its efficacy as an anti-methanogenic ruminant feed additive. However, limited knowledge regarding its reproductive biology and methods for closed-life cycle cultivation has delayed adoption of this method in aquaculture. This thesis therefore aimed to address these knowledge gaps by investigating (1) reproductive phenology, (2) techniques for inducing life-cycle transitions, (3) nursery requirements, and (4) internal mechanisms regulating reproductive processes in *A. armata*.

A comparative analysis of *A. armata* reproductive phenology in New Zealand from 2021 to 2022, compared to 1978 to 1981, identified potential climate-driven shifts in phenology. Specifically, the occurrence period of gametophytes was shorter, and cystocarp production and viable carpospore release were delayed in comparison to 1978–1981. Discoloration, low reproductive output, and low survival rates in 2022 were likely caused by heat stress. These findings will help guide aquaculture practises and advance our understanding of climate change effects on seaweed reproductive phenology through future comparative studies.

Mass production and release of tetraspores in domesticated *A. armata* tetrasporophytes was demonstrated through a 14-day exposure to a reduced critical photoperiod of 8 h L:16 h D. Increasing the temperature from 15 to 18 °C resulted in a marked increase in tetraspore release, whereas exposure to 11 and 13 °C, along with lower light intensities and nutrient concentrations, did not initiate tetrasporogenesis. These results highlight the importance of temperature, among other environmental factors, in controlling reproductive output. A distinct bimodal pattern in tetraspore release was

observed, and tetrasporogenesis could be re-induced in the same biomass by adjusting key environmental parameters. These findings collectively offer precise control over tetrasporogenesis, facilitating commercial hatchery production.

Key parameters for enhancing the growth and development of juvenile gametophytes of *A. armata* were identified, notably moderate temperature and water flow, which resulted in substantial biomass productivity increases. Gametophytes developed more rapidly under a 12h L:12h D photoperiod, while growth was enhanced under lower irradiances. Additionally, lowering nutrient concentrations resulted in cleaner cultures without compromising growth. These results elucidate the influence of environmental factors during the early life stages of *A. armata*, providing essential insights to enable large-scale nursery operations.

Finally, an analysis of metabolomic and transcriptomic dynamics during induction of tetrasporogenesis identified marked changes in gene expression. While metabolomic changes were less prominent, accumulation of several metabolites occurred. Multiple pathways and genes, such as those related to polyamine and steroid hormone production, environmental signalling, and carbon metabolism, were upregulated during induction. These results demonstrate a dynamic biochemical and molecular response, particularly in the early stages of initiating tetrasporogenesis, laying the groundwork for identifying candidate genes and metabolites that regulate this process.

In summary, this thesis significantly advances the science and knowledge required for the successful cultivation of *A. armata* by creating foundations to (1) guide the selection of cultivation techniques, (2) develop climate-resilient management strategies, (3) enable the implementation of streamlined commercial hatcheries and nurseries, and (4) direct

future research aimed at deciphering the fundamental internal mechanisms of reproductive transitions in seaweed.

Acknowledgements

Completing my PhD has been a significant academic endeavour, yet it has also been an immensely transformative personal journey, largely shaped by the exceptional guidance of those around me. Firstly, I want to wholeheartedly thank my supervisors – Marie Magnusson, Rebecca Lawton, and Christopher Glasson. Your belief in my abilities has always motivated me to aim for high standards, and I feel that I've gained so much more than a PhD thanks to all that I've learned from you. Marie, I will forever be grateful for the opportunities, endless support, and guidance you have provided me over the years. Thank you for being an exemplary mentor and champion chief supervisor, whom I truly admire and look up to. Rebecca, thank you for always finding time for me, your positive encouragement, and for being a constant source of inspiration through your mind-blowing organisation and efficiency. Chris, your insightful comments, advice, and ideas during this journey have been greatly valued, and I'm particularly thankful for your encouragement to push my boundaries with the last chapter of this thesis.

This thesis would not have been possible without those who generously sacrificed their time to help me. A special thanks to Holly Roberston, Logan Forsythe, Jacob Nepper-Davidsen, Peter Randrup, Chris Blake, Ariana Brandenburg, and Nethmie Jayasooriya for their invaluable support in field work, lab assistance, and culture maintenance. A big thanks also to my friends Dr Christina Praeger, for making all my time in the microscope room so much more enjoyable, and Dr Roger Huerlimann for his expert guidance in transcriptomics and willingness to offer solid advice.

I would like to sincerely thank the University of Waikato, and Sam Elsom and Professor Emeritus Rocky De Nys at Sea Forest Limited, who through their financial support, have made this research possible. The collaborative environment generated by the partnership with Sea Forest has been an invaluable part of this journey. I'd like to express additional thanks to Dr Masayuki Tatsumi (Sea Forest Limited) for facilitating valuable knowledge exchange through our insightful discussions and reciprocal lab visits, which I thoroughly enjoyed. I also wish to acknowledge the Waikato Graduate Women Educational Trust for recognising my doctoral study with a merit award.

Thanks to the amazing students and technicians at CMFS for their ongoing positive encouragement and the engaging discussions we shared. A special thanks to the downstairs office crew for keeping me motivated (even if it meant occasional much needed distracting), always being incredibly supportive, and lending a hand whenever I needed it.

Last but not least, I extend a massive thank you to my immediate family for believing in me and being there when I needed you, especially during the last few months. I am grateful to my parents for instilling in me the value of perseverance and challenging myself, and to my sister for always having my back. A special appreciation goes to my mum, Carmen – while I once mentioned you deserve a medal at the end of my MSc, I now firmly believe you deserve a monument. Thank you for everything.

Statement on the contribution of others

This research is part of the Entrepreneurial Universities Macroalgal Biotechnologies Program, jointly funded by the University of Waikato and the Tertiary Education Commission. This work was produced as part of the collaboration between the University of Waikato and Sea Forest Limited. Funding support, grants and scholarships were provided by Sea Forest Limited (co-sponsorship of PhD), the University of Waikato through the Entrepreneurial Universities Macroalgal Biotechnologies Program, jointly funded by the University of Waikato and the Tertiary Education Commission (Research and Enterprise Study Award), the Waikato Graduate Women Educational Trust, and the University of Waikato Vivienne Cassie Cooper Award.

Principle and editorial guidance were provided by my supervisory team from the University of Waikato: Marie Magnusson (primary supervisor), Rebecca Lawton (secondary supervisor), and Christopher Glasson (secondary supervisor). Additional editorial and technical guidance were provided by Professor Emeritus Rocky de Nys (Sea Forest Limited), Dr Masayuki Tatsumi (Sea Forest Limited), and Dr Roger Huerlimann (Okinawa Institute of Science and Technology). Laboratory assistance was provided by Arianne Brandenburg and Nethmie Jayamasuri. Field work and/or experimental culture maintenance assistance was provided by Holly Robertson, Jacob Nepper-Davidsen, Logan Forsythe, Peter Randrup, Chris Blake, Kim Beaton, Julia Bishop, Arianne Brandenburg and Nethmie Jayamasuri. RNA-sequencing of samples was determined commercially by Novogene (Singapore).

Chapter 2

Alisa Mihaila: investigation, field work, data analysis, visualisation, and writing – original draft, review, and editing.

Marie Magnusson: conceptualisation, design, field work, funding acquisition, supervision, writing – review and editing

Christopher Glasson: conceptualisation, design, supervision, writing – review and editing.

Rebecca Lawton: conceptualisation, design, field work, supervision, writing – review and editing.

Chapter 3

Alisa Mihaila: investigation, data curation, data analysis, visualisation, writing – original draft, review, and editing.

Rebecca Lawton: conceptualisation, design, supervision, writing – review and editing.

Christopher Glasson: conceptualisation, design, supervision, writing – review and editing.

Marie Magnusson: conceptualisation, design, funding acquisition, supervision, writing – review and editing

Chapter 4

Alisa Mihaila: investigation, data curation, data analysis, visualisation, writing – original draft, review, and editing.

Rebecca Lawton: conceptualisation, design, supervision, writing – review and editing.

Christopher Glasson: conceptualisation, design, supervision, writing – review and editing.

Marie Magnusson: conceptualisation, design, funding acquisition, supervision, writing – review and editing.

Chapter 5

Alisa Mihaila: investigation, data curation, data analysis, visualisation, writing – original draft, review, and editing.

Christopher Glasson: conceptualisation, design, supervision, data curation, writing – review and editing.

Rebecca Lawton: conceptualisation, design, supervision, writing - review and editing.

Roger Huerlimann: supervision, writing – review and editing.

Marie Magnusson: conceptualisation, design, funding acquisition, supervision, writing – review and editing.

Table of contents

List of figures

List of tables

List of appendices

Chapter 1

General Introduction

1.1. Introduction

The concentration of atmospheric methane (CH_4) has increased 2.6-fold since the beginning of the industrial era in 1750, reaching ~1875 ppb in 2018 and constituting approximately 18% of global greenhouse gas emissions (IPCC 2007, 2014, ClimateWatch 2022). The high global warming potential (28 times greater per unit of mass compared to carbon dioxide on a 100-year time scale (Boucher et al. 2009, IPCC 2014)) and short atmospheric lifetime of methane (approximately 12 years) make mitigating methane emissions an attractive target for alleviating the impacts of climate change over shorter decadal time scales (Collins 2018). Agricultural practises are the primary source of anthropogenic methane emissions (42%) (ClimateWatch 2022) and agricultural emissions must be reduced by 24 to 47% from the 2010 level by 2050 to meet projected targets from the Paris Climate Agreement (Masson-Delmotte 2018, Arndt et al. 2022). Enteric fermentation – a process where methane is produced through the anaerobic fermentation of feed organic matter (OM) during ruminant digestion (Basarab et al. 2013) – is a major source of agricultural greenhouse gas emissions (Figure 1.1) accounting for 47 and 74% of agricultural methane emissions globally and in New Zealand, respectively (MfE 2020, ClimateWatch 2022). Creating sustainable ruminant production systems by developing strategies to mitigate methane emissions from enteric fermentation is therefore of high priority both globally and in New Zealand (O'Mara 2011, Tubiello et al. 2013, Reisinger et al. 2017, Leahy et al. 2019). New Zealand has a biogenic methane reduction target of 10% by

2030 and 24–47% by 2050 below 2017 levels, and has signed up to the Global Methane Pledge together with over 100 countries to take voluntary actions towards reducing global methane emissions by at least 30% by 2030 below 2020 levels (Climate Change Comission 2023). However, New Zealand's current climate policies and actions have been rated as "highly insufficient" (Climate Action Tracker 2023). The implementation and rapid advancement of the agricultural emissions pricing system, in combination with the availability of practical and effective agricultural methane mitigation strategies to New Zealand farmers, will be crucial for meeting these targets (Climate Change Comission 2023).

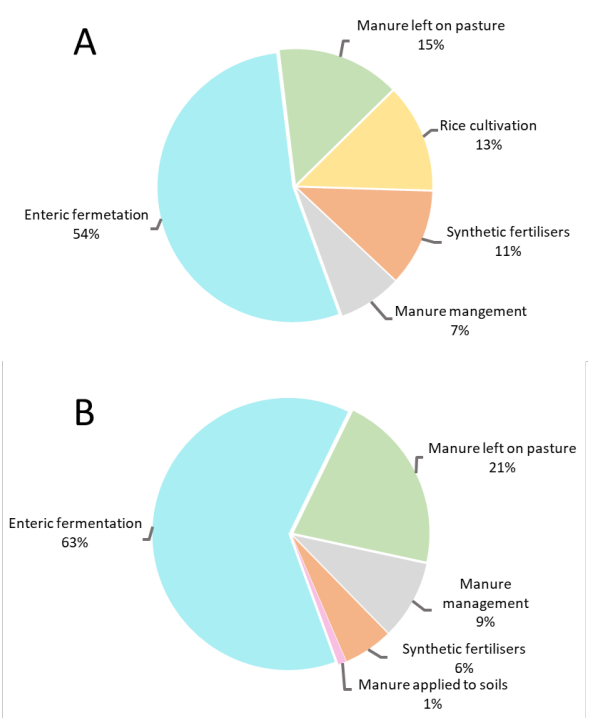

Figure 1.1 Top five sources of total GHG emissions from the agriculture sector globally (A) and in New Zealand (B). Data sourced from Ministry for the Environment (2020) and Climate Watch (2022).

Strategies for mitigating enteric methane emissions include legislation (Key and Tallard 2012), selective breeding (Basarab et al. 2013), antibiotics (e.g. Monensin) (Grainger et al. 2008), nutritional strategies (Beauchemin et al. 2008, Hristov et al. 2013), feed additives (Hristov et al. 2013, Durmic et al. 2014, Machado et al. 2014, Bayat et al. 2018, DSM 2019,

Melgar et al. 2020), and vaccines (Williams et al. 2009, Wedlock et al. 2010) (Table 1.1). Cattle can be selectively bred to have lower residual feed intakes due to the inheritance of better feed conversion efficiencies, thereby lowering enteric methane production (Johnson et al. 2019). Nutritional strategies involve the manipulation of food composition, specifically crude protein, energy (fiber), fat, and water-soluble vitamins and minerals, to improve feed conversion efficiency (McGrath et al. 2018). While several feed additives contain nutrients, feed additives differ from nutritional strategies in that they are not fed to meet a ruminant's nutritional requirements, rather, their purpose is to alter ruminal or post-ruminal metabolism (Hutjens 1991, McGrath et al. 2018). Feed additives, in particular seaweed secondary metabolites, are among the most effective and immediate of these mitigation strategies and are the focus of this thesis.

Table 1.1 Strategies for mitigating enteric CH_4 emissions, their expectedreduction: low (0–10%), moderate (10–40%), and high (>40%) and their expected time to implementation: short-term (current or within 1–5 yrs), mid-term (trials in place, within 5–10 yrs), long-term (research and development stage, >10 yrs).

Mitigation strategy	Expected global CH_4 reduction	Expected time to implementation	Notes	Source
Legislation				
Emissions tax	Low	Short-term	Can be imposed directly on CH_4 emissions or on livestock commodities.	1, 2
Selective breeding				
Low RFI*	Moderate	Long-term	Ruminants with low RFI would consume less dry matter and have improved feed conversion efficiencies.	3, 4
Nutritional strategies				
Replacing fibre with lipids	Moderate	Mid-term	Reduction based on 6–8% increase in lipid concentration. Has also shown to increase milk production by 6.4%.	5, 6
Improving forage quality	Moderate	Mid-term	E.g., Increasing the proportion of legumes/replacing grass silage with maize silage, but may indirectly increase GHG emissions.	6, 7, 8
Feed additives				
Fats/oils	Moderate	Mid-term	Notably medium chain C8–C14 fatty acids. E.g., rapeseed, safflower, and linseed oil.	9, 10
Seaweed secondary metabolites	High	Short – mid-term	E.g., Brown algal phlorotannins and red algal halogenated low molecular weight metabolites.	11, 12, 13
Essential oils	Low – high	Mid – long-term	E.g., *Maleleuca ericifolia* and *Malelauca teretifolia.*	14, 15
NOP-3	Moderate	Short-term	Blocks the activity of the nickel enzyme methyl coenzyme M reductase. Applications for registration approved by EPA in NZ.	16, 17
Antibiotics				
Monensin	Low	Considered unviable	Inhibits the activity of select rumen microbes (gram-positive over gram-negative) associated with rumen fermentation. Deemed unviable due to public health authority concern.	15, 18, 19
Vaccines				

Sheep immunisation	Low	Long-term	Intended to induce an immune response causing a significant supply of salivary-produced methanogen-targeting antibodies.	20, 21

Source: Adapted from Mihaila (2020)

**RFI: Residual feed intake, NOP-3: 3-Nitrooxypropanol*

Sources: [1]Key and Tallard (2012); [2]Narassimhan et al. (2018); [3]de Haas et al. (2011); [4]Pickering et al. (2015); [5]Caro et al. (2016); [6]Knapp et al. (2014); [7]Hammond et al. (2013); [8]Hart et al. (2015); [9]Bayat et al. (2018); [10]Chijioke and Rudinow (2018); [11]Roque et al. (2021); [12]Kinley et al. (2016); [13]Mayberry et al. (2019); [14]Gerber et al. (2013); [15]Martin et al. (2010); [16]Melgar et al. (2020); [17]Jayanegara et al. (2018); [18]Clark et al. (2011); [19]Odongo et al. (2007); [20]Wright et al. (2004); [21]IPCC (2018)

1.1. Seaweed

Seaweeds are macroscopic, photosynthetic, polyphyletic, multicellular marine organisms that typically inhabit coastal waters (Lobban and Harrison 1994, Anis et al. 2017). Approximately 9,000 species of seaweed are broadly classified into three main phyla, Rhodophyta (red seaweeds), Ochrophyta (brown seaweeds), and Chlorophyta (green seaweeds), but ongoing revisions of classification and nomenclature mean this number is approximate (Bolton 2020). These are grouped based on differences in their pigmentation, composition of cell wall and energy storage compounds, and ultrastructural features. In New Zealand 919 species of seaweed have been identified to date, including 594, 183, and 142 taxa in the Rhodophyta, Ochrophyta, and Chlorophyta phyla, respectively (Khan et al. 2009). Seaweeds have been utilised as a source of food, industrial materials, and in botanical and therapeutic applications for over a millennium (Dillehay et al. 2008, Khan et al. 2009). Since the 1950s, seaweed cultivation has become an important global aquaculture practice (Buschmann et al. 2017).

1.1.1. Seaweed aquaculture

Seaweed aquaculture has been one of the fastest growing food production sectors globally since 1990, reaching 35.1 million tons and a commercial value of $US 16.5 billion in 2022 (Chopin and Tacon 2021, FAO 2022). Along with seaweed aquaculture, seaweed biomass can be sourced from wild harvest and by beach-cast collection, however, these methods are not commonly used and seaweed aquaculture accounts for nearly all global seaweed production (97%) (Buschmann et al. 2017, FAO 2022). Asian countries account for 97% of global seaweed aquaculture production, with China as the leading producer (58%)

followed by Indonesia (27%) and the Republic of Korea (5%) (FAO 2022). Major farmed seaweed species include *Laminaria japonica* (35.5%), *Eucheuma* spp. and *Kappaphycus* spp. (Eucheumatoids) (28.2%), *Gracilaria* spp. (14.8%), *Undaria pinnatifida* (8%), and *Porphyra* spp. (6.3%), which together account for over 90% of global seaweed aquaculture production (Buschmann and Camus 2019, FAO 2020). The majority of seaweeds are produced for human food applications (80%), either directly for human consumption (48%) or for the use of extracted hydrocolloids (alginates, agars, and carrageenans) in processed foods (32%) (Buschmann et al. 2017, FAO 2022, FAO and WHO 2022). Seaweed is also used for medicinal and pharmaceutical products, textile and paper printing, and agricultural applications (as components of animal feed or biostimulants for plant growth) (accounting for 20% collectively). Over recent decades, research has increasingly focused on the use of seaweeds in animal feed additives due to their production of secondary metabolites (Machado et al. 2016a, Maia et al. 2016, FAO 2018a, b, Vijn et al. 2020, Min et al. 2021).

1.1.2. Seaweed secondary metabolites

Seaweeds produce a plethora of secondary metabolites with high bioactivity that enable them to cope with the ecological pressures associated with living in the marine environment, such as high levels of herbivory, and exposure to pathogens and epibionts (Lubchenco and Gaines 1981, Sudatti et al. 2018, Zerrifi et al. 2018). Secondary metabolites differ from primary metabolites in that they are not involved in the intrinsic function of an organism (i.e., growth and reproduction), but instead have important ecological functions. Green seaweeds have the lowest abundance of secondary metabolites, with fewer than 300 identified compounds, while over 1,140 and 1,500 compounds have been identified in brown and red seaweed, respectively (Amsler 2008). Most of the secondary metabolites

produced by green seaweeds are terpenoids, most commonly sesquiterpenoids and diterpenoids produced primarily by members of the order Bryopsidales (Blunt et al. 2007). Phlorotannins, a class of phloroglucinol-based polyphenolic secondary metabolites, are unique to brown seaweed and consist of an extremely diverse group of molecules with high biological activity (Burtin 2003, Wijesekara et al. 2010, Pérez et al. 2016, Liu et al. 2018). Over 90% of the secondary metabolites produced by red seaweeds are halogenated compounds consisting of several chemical classes, including indoles, terpenes, polyketides, acetogens, phenols, and volatile halogenated hydrocarbons, i.e., hydrocarbon molecules where at least one carbon is replaced by a fluorine (F), chlorine (Cl), bromine (Br), or iodine (I) atom (Butler and Carter-Franklin 2004, Butler and Sandy 2009).

Halogenated compounds are often reactive and have high bioactivity (Holdt and Kraan 2011). Extensive research has been conducted on these compounds for various biomedical and biotechnological applications (Blunt et al. 2009, Abad et al. 2011, Holdt and Kraan 2011, Yu et al. 2014), with numerous studies highlighting their potential as naturally sourced halogenated compounds with antimicrobial activity in pharmaceutical and food applications (Ito and Hori 1989, Cabrita et al. 2010, Holdt and Kraan 2011). For example, the bromophenol 3,3′,5,5′-tetrabromo-2,2′,4,4′-tetrahydroxydiphenylmethane isolated from the red alga *Odonthalia corymbifera* demonstrated significant *in vitro* antifungal activity against *Candida albicans,* the most prevalent cause of fungal infections in humans, as well as other common human pathogenic fungi including *Aspergillus fumigatus* and *Trichophyton rubrum* (Oh et al. 2008). The brominated diterpene 10-acetoxyangasiol isolated from *Laurencia* spp. exhibited strong *in vitro* antimicrobial activity against clinical human pathogenic bacteria, including *Staphylococcus aureus, Staphylococcus* sp*., Salmonella* sp*., and Streptococcus pyogenes* (Vairappan et al. 2008).

Halogenated compounds from seaweed can also be utilised as antimicrobial agents for preventing and curing diseases and managing parasitic infections in aquaculture (Bansemir et al. 2006). These could be applied either in addition or as an alternative to conventional medication in the aquaculture industry (Bansemir et al. 2006, Vatsos and Rebours 2015). For example, water-soluble components of *Asparagopsis taxiformis* were highly active against *Neobenedenia* sp., a commercially important ectoparasite of marine aquaria and aquaculture fish (Hutson et al. 2012). When administered to the seawater of hatchery-reared juvenile barramundi (*Lates calcarifer*) at dosage rates of 1 mL of extract per 100 mL of seawater, *Neobenedenia* sp. hatching success was reduced by 96% compared to the control (Hutson et al. 2012). Similarly, white shrimp (*Litopenaeus vannamei*) fed diets containing compounds isolated from *Gracilaria tenuistipitata* at concentrations of ≤1.0 g per kg of feed exhibited increased immunity, as evidenced by enhancements in immune parameters such as phenoloxidase and lysozyme activities. Furthermore, white shrimp also showed greater resistance against bacterial (*Vibrio alginolyticus*) and viral (white spot syndrome virus) infections during challenge tests (Sirirustananun et al. 2011). The inclusion of *A. taxiformis*, *Ulva fasciata,* and *Dictyota intermedia* in fish feed pellets at 3% (by weight) also significantly boosted several innate immune parameters of the rabbit fish *Siganus fuscescens* (Thépot et al. 2021). Seaweed secondary metabolites also offer a potential solution for mitigating enteric methane emissions, which is discussed in more detail below.

1.1.3. Seaweed secondary metabolites as antimethanogens

Seaweed secondary metabolites have the potential to alter the rumen microbial ecosystem to inhibit methanogenesis and could provide a natural solution to mitigating

enteric methane emissions (Duarte et al. 2017, Morais et al. 2020). Various species of red, green, and brown seaweed, as well as several species of freshwater macroalgae, have been assessed for their capacity to reduce enteric methane production (Machado et al. 2014, Kinley et al. 2016, Maia et al. 2016, Molina-Alcaide et al. 2017, Abbott et al. 2020), with over 20 species of seaweed demonstrating significant *in vitro* antimethanogenic effects (Table 1.2). Of note was the brown seaweed *Dictyota bartayresii*, which decreased enteric methane production during *in vitro* trials by 92.2% at a dose of 16.7% OM, but also caused a large reduction in the production of volatile fatty acids (VFAs), which act as the main direct source of ruminant energy (Machado et al. 2014). Moreover, *in vitro* trials with the red seaweeds *Gigartina* sp. and *Gracilaria vermiculophylla* and the green seaweed *Ulva* sp. found that these seaweeds decreased enteric methane production by 44%, 59%, and 55%, respectively, when included at a dose of 25% OM (Maia et al. 2016). While fermentation efficiency was not compromised with the inclusion of these seaweeds, the high dose required to achieve the reported antimethanogenic effects would make it challenging to cultivate enough seaweed biomass to implement any of these species as feed additives over large-scale production systems.

The red alga *Asparagopsis* is the top performing seaweed for naturally mitigating enteric methane emissions, producing halogenated compounds known to inhibit methanogenesis (McConnell and Fenical 1977, Denman et al. 2007, Tomkins et al. 2009). Experiments assessing the effect of *Asparagopsis* on rumen fermentation, both *in vitro* and *in vivo*, demonstrate that this species exhibits a potent antimethanogenic effect (≥98% reduction of methane) at exceptionally low doses ranging between 0.2–2% OM, without causing harmful effects on fermentation (Machado et al. 2014, Kinley et al. 2016, Li et al. 2016, Roque et al. 2019a, Roque et al. 2019b, Kinley et al. 2020, Roque et al.

2021). Implementing *Asparagopsis* as an antimethanogenic feed additive is therefore more feasible compared to other species of seaweed in terms of meeting the biomass requirements for commercialisation.

Table 1.2 Summary of marine seaweeds and freshwater macroalgae with anti-methanogenic effects *in vitro* and *in vivo.* ** indicates *in vivo* study. DOM = degradation of organic matter, FE = fermentation efficiency, FDE = feed efficiency, TGP = total gas production, VFA = volatile fatty acids, DMI = dry matter intake, n.e. = no effect, n.m. = not measured.

Seaweed	Dose (% OM)	CH_4 reduction (↓) vs. control	Other effects	Source
Red seaweed				
Asparagopsis spp.*	0.1, 0.2**	40% at 0.1; 90% at 0.2	n.e. VFA or DMI; ↑ productivity	1
	1, 2	>99%	n.e. TGP or DOM	2
	16.7	>99%	↓TGP	3
	2, 6, 10	>99%	↓TGP; ↓VFA	4
	0.07, 0.125, 0.25, 0.5, 1, 2, 5, 10, 16.7	n.e. at ≤0.5; 85% at 1; >99% at ≥2	↓TGP at ≥1; ↓DOM ≥10; ↓ VFA at ≥ 0.5	5
	0.5, 1, 2, 5, 10	>99% at ≥2	↓TGP at ≥2; n.e. DOM at ≤5; n.e. VFA at ≤2	6
	0.5**	60%	↑FDE; ↓ milk fat yield	7
	2	99%	↓TGP; VFA n.m.	8
	5	95%	↓TGP; n.e. VFA	9
	0.5, 1**	26% at 0.5; 67% at 1	↑productivity; TGP & VFA n.m.	10
	5	74%	n.m.	11
	0.25, 0.5**	69.8% at 0.25; 80% at 0.5	↑FE; ↓DMI	12
Bonnemaisonia hamifera	2, 6, 10	n.e. at 2; >95% at 6 & 10	↓TGP; ↓VFA at 6 & 10	4
	2.5, 5, 7.5	12.3%	↓TGP; n.e. VFA	13
Chondrus crispus	0.5	12%	n.e. DOM or VFA	12
Delisia compressa	2, 6, 10	n.e. at 2; 16 – 40% at 6 & 10	↓TGP; ↓VFA at 6 & 10	4
Euptilota formisissima	2, 6, 10	n.e. at 2; 40 – 50% at 6 & 10	↓TGP; ↓VFA at 6 & 10	4
Furcellaria sp.	0.5	10%	n.e. VFA or DOM	14

Gigartina sp.	25	36%	↓TGP; n.e. VFA or FE	15
Gracilaria sp.	2, 4, 6, 8	49% at 2; n.e. at other doses	↓TGP at 2; ↑DOM at 6 & 8	16
Gracilaria vermiculophylla	25	39%	↓TGP; n.e. VFA or FE	15
Hypnea pannosa	16.7	43%	↓TGP & DOM; n.e. VFA	3
Laurencia filiformis	16.7	40%	↓TGP, DOM, & VFA	3
Vidalia colensoi	2, 6, 10	n.e. at 2; 13% at 6 & 10	↓TGP; ↓VFA at 6 & 10	4
Green seaweed				
Chaetomorpha linum	16.7	40%	↓TGP & DOM; n.e. VFA	3
Cladophora patentiramea	16.7	66%	↓TGP, DOM, & VFA	3
Ulva sp.	16.7	50%	↓TGP & DOM; n.e. VFA	3
Ulva ohnoi	16.7	45%	↓TGP & DOM; n.e. VFA	3
Ulva sp.	25	26%	↓TGP; n.e. VFA or FE	14
Brown seaweed				
Ascophyllum nodosum	11.1	15%	↓TGP & VFA	17
Colpomenia sinuosa	16.7	49%	↓TGP, DOM, & VFA	3
Cystoseira trinodis	16.7	45%	↓TGP, DOM, & VFA	3
Dictyota bartayresii	16.7	92%	↓TGP, DOM, & VFA	3
Ecklonia radiata	2, 6, 10	n.e. at 2, 9 – 21% at 6 & 10	↓TGP at 6 & 10; ↓VFA at 10	4
Hormophysa triquetra	16.7	44%	n.e. TGP or DOM; ↓VFA	3
Padina australis	16.7	50%	↓TGP, DOM, & VFA,	3
Sargassum flavicans	16.7	34%	n.e. TGP or VFA; ↓DOM	3
Zonaria farlowii	5	11%	n.m.	11
Freshwater algae				
Oedogonium sp.	10, 16.7, 25, 50, 75, 100	20% at 50; 50% at ≥75; 61.1% at 100	↓TGP, DOM, & VFA at ≥50	5
	16.7	30%	↓TGP; ↑VFA; n.e. DOM	3

**Asparagopsis taxiformis and Asparagopsis armata*

Sources: [1]Kinley et al. (2020); [2]Chagas et al. (2019); [3]Machado et al. (2014); [4]Mihaila (2020); [5]Machado et al. (2016b); [6]Kinley et al. (2016); [7]Krizsan et al. (2023); [8]Machado et al. (2018); [9]Roque et al. (2019a); [10]Roque et al. (2019b); [11]Brooke et al. (2020); [12]Roque et al. (2021) ;[13]Guinguina et al. (2023); [14]Kinley and Fredeen (2015); [15]Maia et al. (2016); [16]Prayitno et al. (2019); [17]Wang et al. (2008)

1.2. Asparagopsis

The genus *Asparagopsis* belongs to the red algal family Bonnemaisoniaceae (Bonnemaisoniales). Two species from this genus can be found in New Zealand: *Asparagopsis taxiformis*, which occurs in the Kermadec Islands, and *Asparagopsis armata*, which is distributed throughout the rest of New Zealand (Bonin and Hawkes 1987). The life cycle of *Asparagopsis* is heteromorphic, consisting of a haploid, plumose gametophyte, a microscopic carposporophyte, and a diploid, filamentous tetrasporophyte (Figure 1.2) (Chapter 3/Mihaila et al. (2023a)). *Asparagopsis* is rich in halogenated compounds, with over 100 low molecular weight halomethanes, haloacetones, and haloacetates identified within this genus (McConnell and Fenical 1977). The brominated halomethane bromoform ($CHBr_3$) is the most abundant of these compounds, ranging from 0.6 to 4.3% of the total biomass in *Asparagopsis* (dry weight (DW)) (Paul et al. 2006, Machado et al. 2016a). Other major halogenated compounds in *Asparagopsis* include dibromochloromethane ($CHBr_2Cl$), dibromoacetic acid ($C_2H_2Br_2O_2$), and bromochloroacetic acid ($C_2H_2BrClO_2$), which are present in considerably lower quantities.

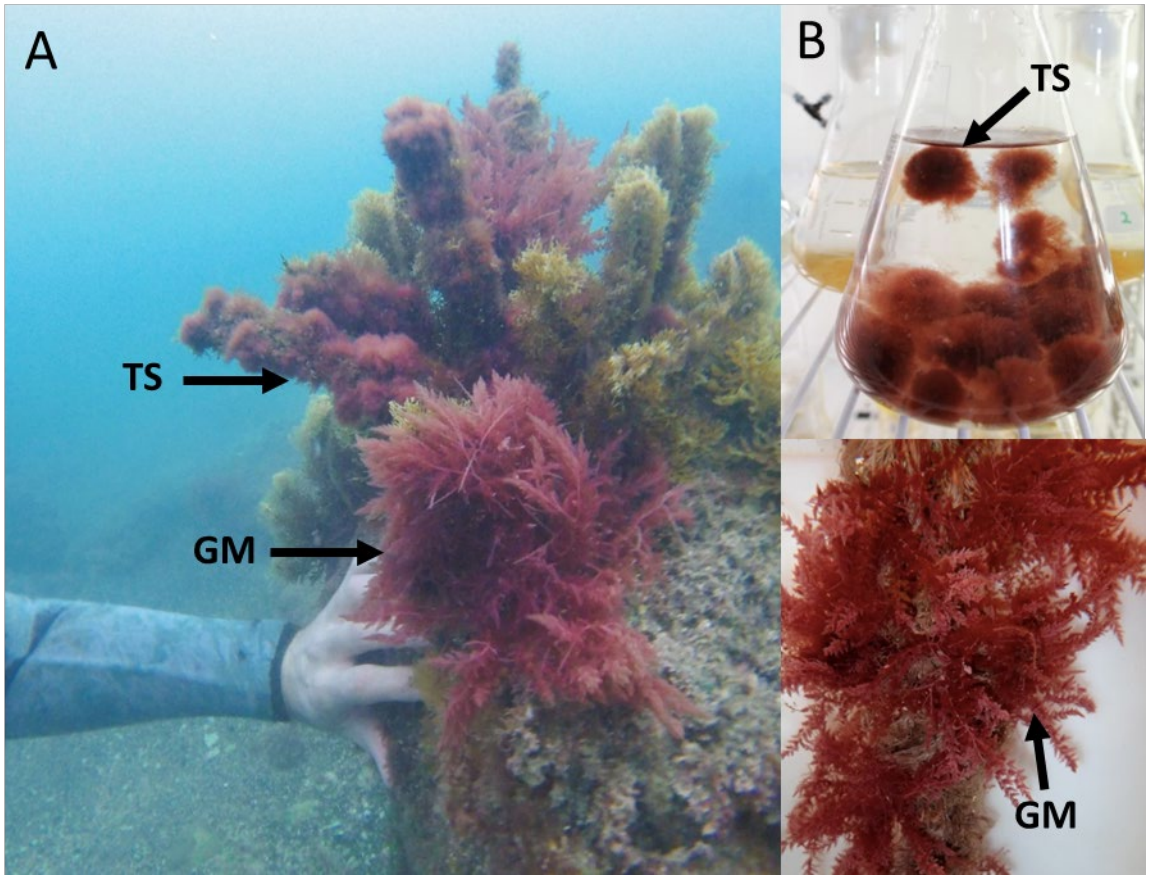

Figure 1.2 Growth habit of *Asparagopsis armata*: (A) tetrasporophyte (TS) and gametophyte (GM) in its natural habitat, (B) TS in culture, and (C) GM in culture.

The antimethanogenic effect of this species was first demonstrated in an *in vitro* study where *Asparagopsis taxiformis* reduced the production of enteric methane by 98.9% at a dose of 16.7% OM (Machado et al. 2014). Subsequent *in vitro* and *in vivo* studies on *A. taxiformis* and *A. armata* within the last ten years confirmed that similar effects (>90% reduction in methane) can be achieved at inclusion rates ranging between 0.2–2% OM (Machado et al. 2014, Kinley et al. 2016, Li et al. 2016, Roque et al. 2019a, Roque et al. 2019b, Kinley et al. 2020, Roque et al. 2021, Krizsan et al. 2023) (Table 1.2), and that this dose minimised any adverse effects on fermentation (i.e., the degradability of OM and

production of VFAs) that were associated with higher doses of *Asparagopsis* (Kinley et al. 2016).

The effectiveness of *Asparagopsis* depends on the concentration of its primary bioactive compound, bromoform ($CHBr_3$) (Machado et al. 2016a), which varies in concentration due to genetic components, in response to environmental conditions (Mata et al. 2017), and as a result of post-harvest processing (Vucko et al. 2017, Magnusson et al. 2020). Bromoform inhibits methanogenesis by inhibiting methyl transfer in methanogenesis through competitive binding with coenzyme M methyltransferase (Wood et al. 1968). It also blocks the activity of methyl coenzyme M reductase, which catalyses the final and rate limiting step of methanogenesis (Krone et al. 1989), summarized in Glasson et al. (2022). The antimethanogenic effect of bromoform induces a shift in the rumen microbial community composition and reduces the relative abundance of methanogens without completely eradicating them (Machado et al. 2018, Roque et al. 2019a). This is important for maintaining a balance between methane mitigation and animal health (Glasson et al. 2022).

1.2.1. Asparagopsis aquaculture

Wide-scale adoption of *Asparagopsis* as an antimethanogenic feed additive requires a reliable supply of large quantities of biomass (Table 1.3) that can only be supplied through aquaculture production. The gametophyte phase of *A. armata* can be cultivated in the sea through vegetative propagation, provided that gametophyte fragments possess barbs and frond tissue to enable attachment to a substratum and regrowth once attached (Wright et al. 2022). Farming of *A. armata* first began in France in the mid 1990's in collaboration with the cosmetic company Algues et Mer to produce Ysaline 100, a mixture of bioactive

secondary metabolites used for anti-dandruff, anti-wrinkle, and anti-acne treatments (Moigne 1998, Werner et al. 2004). Each year, wild-harvested gametophytes were collected, fragmented, and attached to specialised ropes via barbs for ocean outplanting. The first harvest was carried out approximately two months after seeding the culture ropes and was followed by a second harvest approximately two months later. The growth cycle occurred during the European winter–spring period, as the growth rate of *A. armata* would decline at the start of summer and the bioactivity of the substances extracted from the seaweed would be lost (Werner et al. 2004, Kraan and Barrington 2005). The farm occupied an area of 2 ha and produced 8 tons of FW biomass per annum (Kraan and Barrington 2005). Cultivation trials of *A. armata* were also carried out in Ireland and took place in a 1 ha farm in 1998; however, the amount of biomass harvested was not reported. The cultivation methods applied in France were modified (particularly in regards to the timing and duration of the growth period) to suit local Irish conditions, although there is no full description of the original cultivation methods or how they were modified (Werner et al. 2004). Today, these farms are no longer operating.

Table 1.3 Estimated quantity of *Asparagopsis* (DW, whole seaweed, i.e., including ash) required to treat 50% of the New Zealand cattle herd.

Cattle type	Seaweed dose (% OM)	Seaweed biomass (DM) required/day	
		Per year/head	Per year/50% of herd
Dairy	0.2	2.7 kg	8,677 tonnes
	1	13.4 kg	43,406 tonnes
	2	26.8 kg	86,811 tonnes
Beef	0.2	1.6 kg	2,895 tonnes
	1	8.1 kg	14,482 tonnes
	2	16.1 kg	28,965 tonnes

[1]*Calculations are based on feed intakes of 16.1 and 9.7 total kg DM eaten per day (kg/DM/day/head) and herds of 6.5 and 3.6 million cattle for dairy and beef herds, respectively (dairynz.co.nz; Beef+LambNZ (2017); stats.govt.nz (2017 data))*

Alternatively, gametophytes of *Asparagopsis* can be farmed through closed-life cycle production. This method involves artificially inducing the mass production of tetraspores (tetrasporogenesis) from tetrasporophyte cultures under hatchery conditions. Subsequently, the released tetraspores are seeded onto a substrate, and the germinated gametophytes are maintained under nursery conditions until they are ready for ocean outplanting. The ability to induce reproduction in tetrasporophytes on demand enables year-round production of gametophytes, minimises the dependence on field collections, and ensures cultures with little or no contamination. Neither partial (described above) nor complete closed-life cycle cultivation – where produced and released tetraspores develop into gametophytes, which in turn mature to release carpospores that develop into tetrasporophytes – have been established due to difficulties in stimulating life-history transitions and maintaining gametophyte survival in culture. Nevertheless, these methods are critical for enabling potential strain selection and selective breeding, which necessitate the selective crossing of sires and dams.

The tetrasporophyte stage of *Asparagopsis* can be cultivated in land-based culture systems. This method was successfully established in Portugal to produce biomass for supplying potentially interested aquaculture, agriculture, cosmetic, and pharmaceutical industries. The cultured biomass was supplied with effluent from a commercial fish farm and weekly average biomass yields of 70 and 100 g DW m^{-2} day^{-1} were produced at 100 µmol L^{-1} h^{-1} (weekly average total ammonia nitrogen flux) in December (winter) and May (spring), respectively (Mata et al. 2006, Schuenhoff et al. 2006, Mata et al. 2010).

Renewed interest in *Asparagopsis* aquaculture has emerged with the discovery of this species as a highly effective inhibitor of enteric methane production. As a result, several start-up companies worldwide have been established to develop commercial farming of *Asparagopsis*. However, methods for cultivating *Asparagopsis* are nascent, and a lack of fundamental knowledge regarding the reproductive biology of this species and cultivation requirements for certain life stages has limited several aspects of commercial production. A critical first step towards informing the development of cultivation methodologies for *A. armata* is to obtain an understanding of its reproductive phenology (i.e., the seasonal timing of a species' life cycle). This is described in more detail in the following section.

1.2.2. Reproductive phenology

Seaweeds often have complex biphasic or triphasic reproductive cycles that are controlled by a combination of endogenous and environmental factors related to seasonal change, such as temperature, light, and photoperiod (Lüning and Dieck 1989, Lüning et al. 2008, de Bettignies et al. 2018). A review summarising the influence of temperature on the reproductive phenology of seaweeds reported that gametogenesis and sporogenesis are

mediated by temperature for approximately 70% of assessed temperate seaweed species (*n* = 71) (de Bettignies et al. 2018). In several members of the Antarctic Desmarestiales (Phaeophyceae), the development of gametangia, fertilisation, and the early germination of sporophytes take place in winter, when irradiance levels are <5 µmol photons m^{-2} s^{-1} and the temperature is below 5 °C (Wiencke and Clayton 1990, Wiencke et al. 1996), while the growth of sporophytes occurs once the photoperiod increases in late winter–spring (Wiencke et al. 1991).

Shifts in reproductive phenology in response to climate change have become an increasingly common phenomenon for a range of organisms across different kingdoms over the past few decades, particularly due to the advancement in the seasonal timing of spring temperatures (Parmesan 2006, Burrows et al. 2011, Poloczanska et al. 2013). Leaf and insect emergence, leaf unfolding, flowering, and spawning events are occurring earlier in the year than they have over the historical past (Fitter et al. 1995, Menzel and Fabian 1999, Gordo and Sanz 2005, Reusch 2014). An analysis of a phenological network data set including 542 plant species throughout 21 European countries demonstrated that 78% of all leaf emergence, flowering, and fruiting records had advanced (30% significantly) over a 29-year period (1971–2000) (Menzel et al. 2006). The peak spawning event of the bivalve *Macoma balthica* in the Wadden Sea (northern Europe) occurs eight days earlier in the year than it did 28 years ago as a result of a 1 °C rise in temperature (Philippart et al. 2003). Gonad development of the limpet *Patella depressa* in south-west coast of Britain has advanced by an average of average of 10.2 days per decade over the last 80 years (Moore et al. 2011).

Unlike land plants and aquatic organisms, shifts in the reproductive timing of marine seaweeds are not well-documented in the literature (Richardson and Poloczanska 2008, Wernberg et al. 2012). Instead, the majority of climate change-related seaweed studies and

long-term data series describe shifts in the distribution and abundance of seaweed populations (Lima et al. 2007, Reusch 2014, Martins et al. 2019), particularly with regards to the tropicalisation of temperate marine species (Vergés et al. 2014, Vergés et al. 2016, Vergés et al. 2019). The reproductive phenology of seaweeds is often finely tuned to changes in their environment (Brawley and Johnson 1992, Molenaar et al. 1996, Mohring et al. 2013); therefore, it can be expected that increases in temperature due to climate change have caused shifts in the onset of reproductive events in seaweeds.

Knowledge regarding the reproductive phenology of seaweeds is critical for developing large-scale seaweed cultivation. The timing of reproductive events combined with their associated environmental conditions form a baseline for multiple components of seaweed aquaculture, such as knowing when to carry out wild collections (both for research and farming purposes), outplanting, and harvesting. It also helps determine which conditions are optimal for maximising production or inducing/preventing the occurrence of reproductive events, which will be critical for hatchery and nursery development.

1.2.3. Hatchery and nursery cultivation

Hatchery and nursery systems are integral components in the cultivation of seaweeds propagated through spore production. Their effective development and refinement rely upon thorough comprehension of environmental influences on fundamental biological processes, such as reproduction, development, and growth (Charrier et al. 2017, Kim et al. 2017). Moreover, understanding the biochemical and genetic factors governing important aquaculture traits, such as growth rates, reproductive success, or the production of target bioactive compounds, is important for enhancing these systems and driving

technological advancement (Robinson et al. 2013, Charrier et al. 2017, Liu et al. 2022). Physiological studies have been instrumental in establishing hatchery and nursery protocols to tightly control seaweed life cycles (Pang and Lüning 2006, Zhou et al. 2013, Vesty et al. 2015, Peteiro et al. 2019, Boderskov et al. 2021b). However, there remains a lack of understanding regarding both the external environmental factors and internal regulatory mechanisms that affect developmental biology in *Asparagopsis* from a production standpoint. This lack of knowledge impedes the implementation of hatchery and nursery systems for this species, as well as improvements in aquaculture practices.

1.3. Significance of topic and thesis aims

The objective of this thesis was to provide a foundation for implementing the closed-life cycle aquaculture of *A. armata.* This involved addressing several fundamental knowledge gaps associated with reproductive phenology, the cultivation requirements for optimal hatchery and nursery production, and the molecular and biochemical mechanisms involved in reproduction.

Chapter 2: Detailed knowledge of the reproductive phenology of seaweeds is an integral part of aquaculture development and is critical for understanding how climate change will impact these organisms. Understanding the current life history events of *A. armata* in New Zealand and correlating these events with environmental parameters is necessary for determining when biomass samples will need to be collected for carrying out reproductive culture experiments, for developing the cultivation methodologies for nursery production, the timing of outplanting, harvesting, and broodstock collection, and for triggering or avoiding reproductive events in land-based cultivation. The average sea surface

temperature along the northeast coast of the North Island, New Zealand (Leigh Marine Reserve) was 1–2 °C higher from 2020 onwards compared to the early 1980's, when the reproductive phenology of *A. armata* was previously assessed at this location (Bonin and Hawkes 1987). This change in temperature may have caused a shift in the reproductive phenology of *A. armata* over this period. The aim of chapter 2 was therefore to provide an up-to-date assessment of the phenology of *A. armata* in New Zealand to help in detecting shifts in reproductive phenology and facilitate the development of *A. armata* aquaculture in New Zealand.

Chapter 3: Seaweed aquaculture requires a high degree of control over the environmental factors regulating reproductive processes. However, knowledge of the external factors controlling reproduction in tetrasporophytes of *A. armata* is limited and no method containing sufficient detail to enable hatchery development has been published. The aim of chapter 3 was therefore to investigate the effect of fundamental environmental factors on tetrasporogenesis in *A. armata* and provide a detailed method for obtaining a high and reliable supply of tetraspores to facilitate hatchery development.

Chapter 4: Maximising the development and growth of the early life stages of seaweeds is essential for successful nursery production. This can be achieved through the manipulation of environmental factors and the optimal nursery conditions must be established on a species-specific basis. To date, the optimal conditions for cultivating the early life stages of *A. armata* have not been investigated. The aim of chapter 4 was therefore to determine the effect of environmental factors on the development and growth of juvenile gametophytes of *A. armata* to identify critical parameters for maximising production during the nursery phase.

Chapter 5: Our understanding of the biochemical and molecular regulators of reproduction in *A. armata* is still in its infancy, exacerbated by the overall scarcity of knowledge surrounding internal reproductive regulation in seaweeds. Enhancing our comprehension of the metabolomic and genomic aspects of fundamental reproduction processes is crucial for bridging this gap in knowledge. This is especially true for *A. armata*, as this information will be instrumental in refining aquaculture practices in the future. The aim of chapter 5 was therefore to examine metabolomic and transcriptomic dynamics of *A. armata* during tetrasporogenesis, serving as a first step towards understanding the intricate biochemical pathways and genetic mechanisms underpinning this process.

Chapter 2

The reproductive phenology of *Asparagopsis armata* in New Zealand – potential shifts 40 years later

---

This chapter has been published in Algal Research as:

Mihaila, A. A., M. Magnusson, C. R. K. Glasson, and R. J. Lawton. 2023b. The reproductive phenology of *Asparagopsis armata* in New Zealand – potential shifts 35 years later. Algal Research 76:103318 (Appendix 12).

2.1. Abstract

The reproductive phenology (the timing of key reproductive events) of seaweeds is largely controlled by environmental factors related to seasonal change, particularly temperature. Therefore, it can be expected that climate change-induced increases in sea temperature can cause shifts in the reproductive phenology of seaweeds, although this has been difficult to detect due to the lack of baseline data for reproduction. We investigated the seasonal occurrence and reproductive phenology of the emerging aquaculture-target species *Asparagopsis armata* on the North Island of New Zealand from 2021–2022, which was previously assessed 40 years ago (1978–1981) when temperatures were on average 1.5 °C cooler. Seasonality in reproduction was assessed via the presence of tetrasporangia, tetraspore release and germination rate, presence of cystocarps, cystocarp density and cystocarp opening. Tetrasporophytes occurred year-round with tetrasporangia present from March–September (austral autumn–spring), with populations most fertile from May–July (austral autumn–winter). Tetraspore release peaked in June 2021 and September 2022, but

was otherwise low during our sampling. Gametophytes were present from August–November (austral winter–spring) with cystocarps present from September (austral spring), which was delayed in comparison to the 1978–1981 assessment. Viable carpospores were also only released under controlled conditions during September, as opposed to during all reproductive months in the 1978–1981assessment. Discolouration was a common occurrence in natural populations during 2022 that translated into poor reproductive output and high mortality under controlled conditions, which could be explained by prolonged heat stress throughout 2022. This study presents the first temporally longitudinal analysis of potential climate driven shifts in reproductive phenology of a seaweed and provides a quantitative baseline for detecting changes in reproductive phenology in the future.

2.2. Introduction

Shifts in reproductive phenology (the seasonal timing of key reproductive events) have become one of the most prevalent biological responses to climate change in many taxonomically diverse organisms over recent decades (Menzel et al. 2006, Parmesan 2006, Cleland et al. 2007, Vitasse et al. 2022), including woody plants (Menzel and Dose 2005, Aono and Kazui 2008, Ge et al. 2015), frogs (Gibbs and Breisch 2001), birds (Gordo et al. 2005), phytoplankton (Parmesan 2007, Beaugrand 2009), and bony fish (Poloczanska et al. 2013, Rogers and Dougherty 2019). Despite faster warming on land, shifts in the onset of seasonal transitions are generally greater in the ocean, especially with regard to the advancement of spring temperatures (Burrows et al. 2011). Nevertheless, studies assessing climate-induced shifts in the reproductive phenology of marine species are lacking compared to terrestrial species (Richardson and Poloczanska 2008, Wernberg et al. 2012), and most phenological shifts in marine ecosystems have been reported for fish (Asch 2015, Rogers and Dougherty 2019) or invertebrates (Moore et al. 2011, Richards 2012, Philippart et al. 2014, Slesinger et al. 2021). To date, no studies have investigated the effects of climate change on the reproductive phenology of seaweeds, and this is largely due to a lack of suitable baselines and time series against which change can be detected (Wernberg et al. 2012, Poloczanska et al. 2013, de Bettignies et al. 2018). Instead, the majority of climate change-related seaweed studies and long-term data series describe shifts in the distribution and abundance of seaweed populations (Lima et al. 2007, Reusch 2014, Martins et al. 2019). Improving our knowledge of the reproductive phenology of seaweeds is crucial for understanding how climate change will affect this important group of organisms.

Understanding the reproductive phenology of seaweeds is also fundamental for the development of sustainable seaweed aquaculture (Searles 1980, Charrier et al. 2017, de Bettignies et al. 2018). Such knowledge can form the basis for developing multiple components of seaweed aquaculture, such as knowing when to conduct outplanting and harvesting, identifying peaks and patterns in reproduction to enable targeted wild-collections of broodstock, and determining the optimal culture conditions for seaweed maturation and reproduction to develop hatchery and nursery cultivation technologies (Charrier et al. 2017, Fernand et al. 2017, Liu et al. 2017, Kim et al. 2019, Leal et al. 2021). Identifying how the seasonal timing of reproductive events varies with prevailing environmental conditions also enables the design of management strategies for climate resilient aquaculture (Charrier et al. 2017).

Red seaweeds of the genus *Asparagopsis* are of emerging commercial importance due the discovery of their bioactive compounds, notably bromoform, as highly effective mitigators of enteric methane production in ruminants (Machado et al. 2016a, Kinley et al. 2020, Kinley et al. 2021, Roque et al. 2021, Glasson et al. 2022, Ridoutt et al. 2022). While advancements have been made in techniques for cultivating these species (Mata et al. 2006, Mata et al. 2012, Torres et al. 2021, Wright et al. 2022, Mihaila et al. 2023a), critical knowledge gaps remain around their reproductive ecology (Zhu et al. 2021, Zanolla et al. 2022). The life cycle of *Asparagopsis* is heteromorphic and triphasic, alternating between a filamentous tetrasporophyte, a plumose gametophyte, and a microscopic carposporophyte (Bonin and Hawkes 1987). Reproductive culture studies for *Asparagopsis* have primarily focused on the tetrasporophyte stage, with temperature and photoperiod identified as critical factors for controlling tetrasporogenesis and the subsequent release of tetraspores (Oza 1977, Bonin and Hawkes 1987, Guiry and Dawes 1992, Mihaila et al. 2023a). Culture

studies of other life stages of *A. armata* have received considerably less attention and are therefore not as well understood.

The reproductive phenology of *A. armata* in New Zealand has only been assessed in a single study conducted from 1978 to 1981 (Bonin and Hawkes 1987) at Leigh Marine Reserve along the northeast coast of the North Island. During this time, it was reported that immature gametophytes were present in early August (austral winter), and that spermatangia bearing male gametophytes and cystocarp bearing female gametophytes were present from the end of August until mid-December (austral winter to early summer) (Bonin and Hawkes 1987). Tetrasporophytes were reported as abundant year-round, with peak abundance occurring during winter, and tetrasporangia present from March until September (austral autumn to spring). Reproductive outputs, however, were not quantified. While average sea surface temperatures (SSTs) along the northeast coast of the North Island have not increased over the last 50 years (Shears and Bowen 2017), long-term records suggest shifts in seasonality and interannual variability, particularly influenced by marine heat waves (Cook et al. 2022). Data from 2020 onwards also shows that SSTs were 1–2 °C higher than in the early 1980s (Sea Temperature Info 2022, National Institute of of Water and Atmospheric Research [NIWA] 2022a). Given the strong relationship between temperature and reproduction in *A. armata* (Oza 1977, Bonin and Hawkes 1987, Guiry and Dawes 1992, Mihaila et al. 2023a), it is likely that the reproductive phenology of *A. armata* has shifted over the last 40 years. This notion is supported by personal observations in the field, such as the presence of cystocarpic females in early august approximately three weeks earlier than described in Bonin and Hawkes (1987) (A. Mihaila, Unpublished results, 2020).

The present study was therefore conducted to provide an up-to-date assessment of the reproductive phenology of *A. armata* with the aims of (1) detecting potential shifts in

seaweed phenology, (2) serving as a baseline for detecting future shifts in seaweed phenology, and (3) facilitating the development of *A. armata* aquaculture in New Zealand. We quantified fecundity and reproductive viability of *A. armata* gametophytes and tetrasporophytes within the North Island of New Zealand over a 16-month period. To our knowledge, this is the first repeated assessment of the reproductive phenology of a seaweed, providing the first longitudinal analysis of potential climate driven shifts in the timing of reproductive events for seaweed.

2.3. Materials and methods

2.3.1. Sample collection

Wild *A. armata* was sampled from rocky reefs (2–5 m depth) at Mathesons Bay, Leigh (36.31°S, 174.80°E) located on the North Island of New Zealand. Mathesons Bay is a small beach located within the Auckland region of New Zealand and is relatively sheltered by a natural rock wall and a small islet (Mathesons Bay Island). Samples were collected approximately 200 m from the shoreline within 10 m of the islet. This site was selected because it was previously assessed by Bonin and Hawkes (1987), and it is easily accessible with *A. armata* reportedly present year-round. Geographical features were used to establish a permanent sampling area at the site (approximately 100 m^2). Sampling was initially set to be carried out approximately monthly from March 2021–March 2022, with collections spaced at least three weeks apart, taking into account tides, weather, and logistical constraints. However, due to COVID-19 restrictions during August 2021–December 2021, sampling was only able to be carried out from March 2021–July 2021. Approximately monthly sampling was therefore repeated the following year from January 2022–December 2022 to enable sampling across a full calendar year and to assess for between-year variation in reproductive seasonality. In 2021, samples were collected on March 19th, April 9th, May 14th, June 18th, and July 21st. In 2022, samples were collected on Jan 21st, April 3rd, May 13th, June 28th, August 24th, Sept 28th, October 27th, November 22nd, and December 22nd.

When tetrasporophytes (Figure 2.1A) were present within the sampling area, 20 individuals (whole pom poms) were haphazardly collected using tweezers and transported in a single 2 L bucket filled with seawater collected at the site to the laboratory. When cystocarpic gametophytes (Figure 2.1B) were present within the sampling area, 10

cystocarpic individuals (whole individual with a single holdfast and not connected to another individual) were haphazardly collected by hand and transported in separate 2 L buckets filled with seawater collected at the site to the laboratory. If present, five non-cystocarpic individuals were also sampled and brought back to the laboratory to determine whether spermatangia were present, as these are only visible by microscopy. Both gametophytes and tetrasporophytes were sampled at least 1 m apart. All buckets containing the samples were transported in an electric cooler maintained at the ambient water temperature of the site until processing. All samples were processed within 24 h of collection.

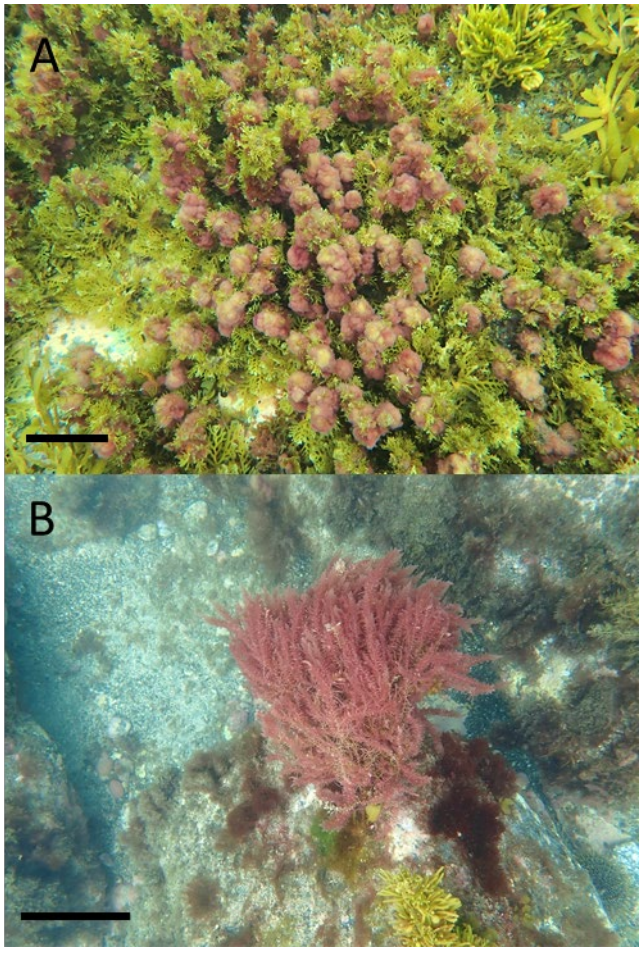

Figure 2.1 *Asparagopsis armata* at Mathesons Bay; (A) tetrasporophyte 'pom poms' growing epiphytically on *Carpophyllum plumosum*, (B) cystocarpic female gametophyte. Scale bars = 5 cm (A) and 10 cm (B).

2.3.2. Tetrasporophyte processing

The collected tetrasporophytes were rinsed in autoclaved filtered seawater (AFSW) and epiphytes were removed using tweezers. Tetrasporophytes were transferred into individual Petri dishes (90 x 20 mm, LabServ, LBS60016) filled with 50 mL AFSW with nutrients added at a concentration of F/8 (3.5 mg N L^{-1} and 0.3 mg P L^{-1}, Varicon Aqua, Cell-Hi F2P). To quantify the proportion of reproductive individuals, tetrasporophytes were cut into 5–6 mm length filaments using dissecting scissors and visually inspected using a stereomicroscope (Olympus SZX2-ILLTQ) to determine the presence/absence of mature (i.e., all four spores formed) and/or immature (i.e., only one or two spores formed) tetrasporangia in each tetrasporophyte (*n* = 20) (Figures 2.2A and 2.2B). The visual condition of each individual (e.g., whether thallus was discoloured) was also recorded. If tetrasporangia were present, subsamples of 5–12 filaments each containing 1–3 tetrasporangia from half (*n* = 10) of the dishes were randomly selected under the stereomicroscope by stirring the filaments inside the dish and selecting the first filaments with visible tetrasporangia. These were then transferred via pipette into new Petri dishes (60 x 14 mm, LabServ, LBS60060) filled with 15 mL AFSW, keeping filaments from each replicate tetrasporophyte in a separate dish. This resulted in 10 dishes each containing 5–12 filaments and within them a total of 8–12 tetrasporangia from each tetrasporophyte. The total number of tetraspores present inside the filaments for each dish was recorded, and both immature and mature tetrasporangia were included as immature tetrasporangia can mature and release within 48 h of exposure to these conditions (Chapter 3/Mihaila et al. (2023a)). If less than 10 out of the 20 tetrasporophytes contained tetrasporangia then the sample size was reduced accordingly. Dishes containing the filaments with tetrasporangia were then transferred to an environmental control cabinet (Panasonic, MLR-352) set at 15

°C and 10–15 µmol photons m^{-2} s^{-1} with a photoperiod of 8 h L:16 h D. These conditions have previously been shown to induce tetraspore release (Chapter 3/Mihaila et al. (2023a)). After 48 h, tetraspore release was quantified by removing the filaments from the dishes and counting the total number of tetraspores at the bottom of each dish using a stereomicroscope, as mature tetraspores are released within 48 h of exposure to the conditions described above (Chapter 3/Mihaila et al. (2023a)) (Figure 2.2C). The percentage of tetraspores released was then calculated by dividing the total number of tetraspores released by the total number of tetraspores initially present inside the filaments for each dish (as described previously). The water in the dishes was then replaced with fresh nutrient enriched AFSW (F/8), and these were then returned to the cabinet and maintained under the same conditions described above. After 24 h, germination was quantified by counting the total number of germinated tetraspores at the bottom of each dish using a stereomicroscope, as the first division of the germinating tetraspore is evident within 24 h of release (Chapter 3/Mihaila et al. (2023a)) (Figure 2.2D). The germination rate (%) was then calculated by dividing the total number of germinated tetraspores by the total number of tetraspores released for each dish (as described previously).

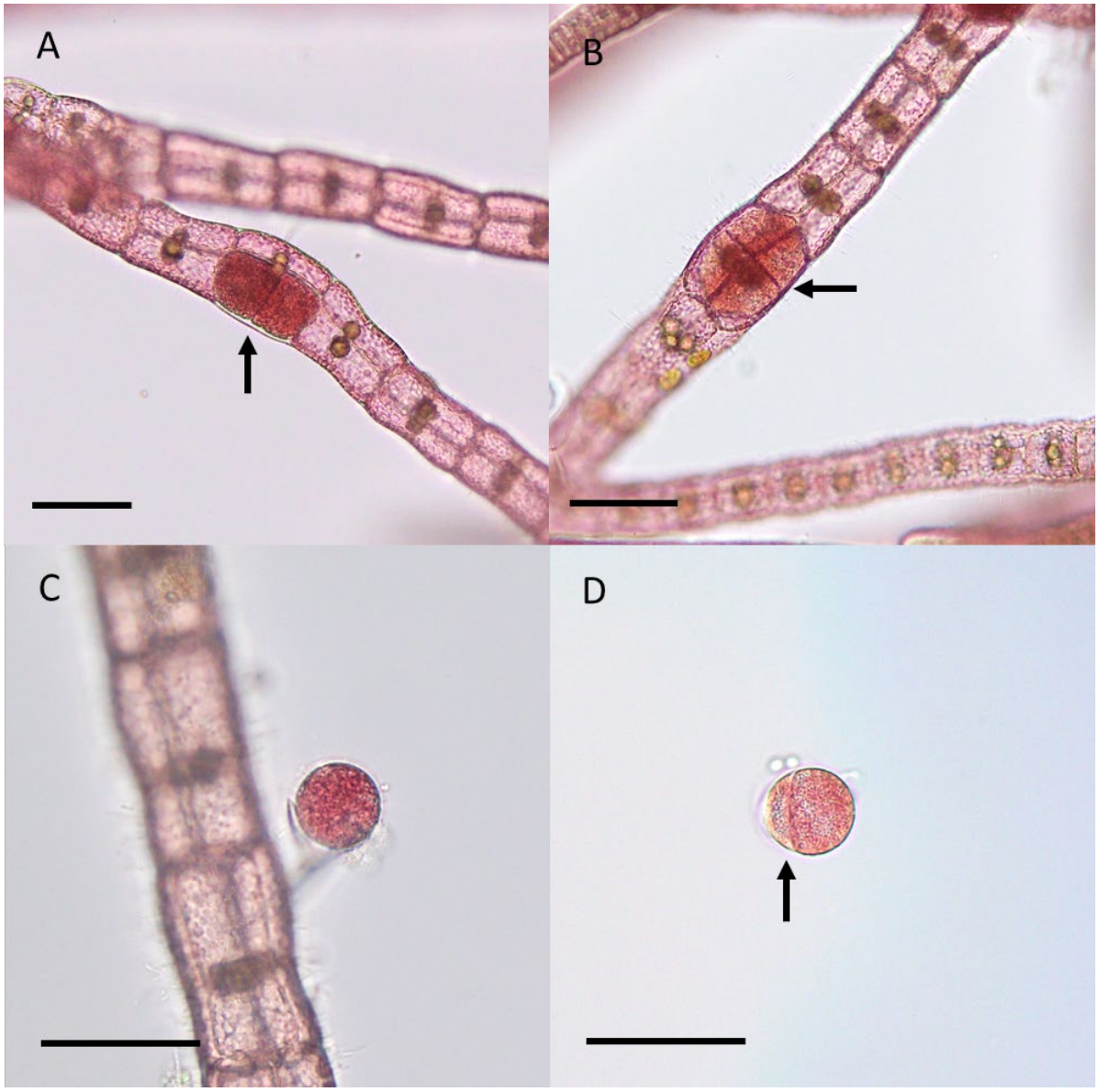

Figure 2.2 Reproductive structures of tetrasporophytes of *A. armata*; (A) immature tetrasporangia (i.e., with two spores formed (arrowhead)), (B) mature tetrasporangia (i.e., with four spores formed (arrowhead)), (C) newly released tetraspore (zero days old), (D) first division of a germinating tetraspore (arrowhead, one day old). Scalebar = 25 µm.

2.3.3. Gametophyte processing

The collected gametophytes were rinsed in AFSW to remove any small animals, epiphytes were removed using tweezers, and the visual condition of each individual (e.g., whether thallus was discoloured) was recorded. One whole branch containing cystocarps (Figure 2.3A) was sampled from each cystocarpic gametophyte and these were transferred

into individual crystallisation dishes (90 x 50 mm, Pyrex, 3140-90) filled with 150 mL AFSW with nutrients added at F/8. Only branches originating from the base of each gametophyte were sampled to ensure that the location of the branch within the plant did not affect results. Non-cystocarpic gametophytes were inspected for the presence of spermatangia (Figure 2.3B) by examining three branches selected from the lower, middle, and upper region of each individual under a stereomicroscope. No further processing/analysis was undertaken for these samples. To quantify cystocarp density, the total number of cystocarps on each cystocarpic branch was counted using a stereomicroscope and the total length of the branch was measured (n = 10). The number of cystocarps per linear cm was then calculated using this data. Some cystocarps had evidence of prior release of carpospores in the wild (indicated by the opening of the cystocarp (formation of ostiole)). Therefore, the number of unopened and opened cystocarps was also recorded for each branch (Figures 2.3A and 2.3C). Dishes containing the branches were then placed in an environmental control cabinet (Panasonic, MLR-352) set at 18 °C and 20–25 µmol photons m^{-2} s^{-1} with a photoperiod of 12 h L:12 h D. These conditions have previously resulted in carpospore release (A. Mihaila, Unpublished results, 2020) and are similar to the spring conditions at the collection site when carpospores have previously been reported to release (Bonin and Hawkes 1987). After 48 h, cystocarp opening was quantified by counting the total number of newly opened cystocarps per branch, as mature carpospores are released through the ostiole within 48 h of exposure to the conditions described above (Figure 2.3D). Branches were removed from the dishes and the presence/absence of released carpospores at the bottom of each dish was also recorded. The water in the dishes was then replaced with fresh nutrient enriched AFSW (F/8) and dishes containing the carpospores were then returned to the cabinet and maintained under the same conditions described above. After a

further 48 h, the presence/absence of germinated carpospores at the bottom of each dish was recorded as a measure of viability using an inverted microscope (Olympus CKX53), as the first division of the germinating carpospore is evident within 48 h of release (Figure 2.3E).

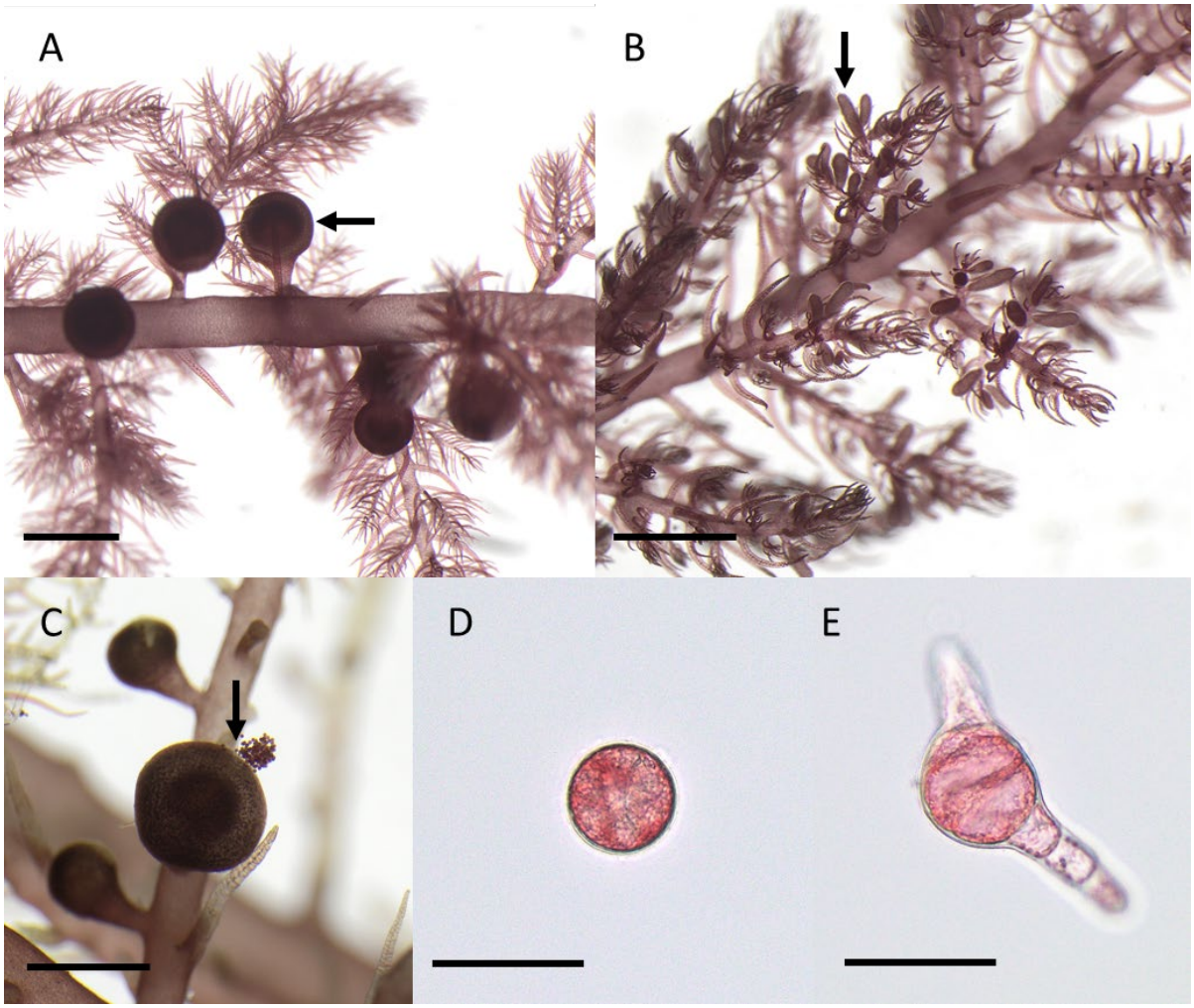

Figure 2.3 Reproductive structures of gametophytes of *A. armata*; (A) cystocarps (arrowhead) on female gametophytes, (B) spermatangia (arrowhead) on male gametophytes, (C) carposporophytes releasing carpospores (arrowhead) through the ostiole, (D) released carpospore (zero days old), (E) germinated carpospore (three days old). Scale bars = 1mm (A)–(C) and 50 µm (D)–(E).

2.3.4. Environmental data

The following variables were selected to analyse for relationships between reproductive measures of *A. armata* and environmental factors: (a) sea surface temperature (SST), (b) photoperiod (light: dark hours), (c) total bright sunshine hours (BSH), (d) salinity (ppt), and (e) nutrient concentration (total nitrogen (TN) and total phosphorus (TP), mg L^{-1}). Monthly averages of sea surface temperature, photoperiod and total values for BSH were obtained from long-term data records at nearby Goat Island (SST and photoperiod) (Sunrise and sunset 2020, Sea Temperature Info 2022) and North Shore, Auckland (BSH) (NIWA, 2022a, 2022b). Monthly averages of salinity and monthly spot measurements of TN and TP were sourced from long-term environmental monitoring datasets at Goat Island (Auckland Council 2023). All data were obtained from sources as a single value for each month and so are reported in this format without any error estimates.

2.3.5. Statistical analyses

Statistical analyses were carried out in PRIMER ver.7 (Primer-E., UK) and R-Studio ver. 4.3.0 and legibility of figures was improved in Adobe Illustrator. A two-factor permutational analysis of variance (PERMANOVA) was used to determine the effect of "Year" and "Month" on tetraspore release (% of tetraspores released per dish) and germination rate (% of released tetraspores that had germinated per dish). A one-factor PERMANOVA was used to determine the effect of "Month" on cystocarp density (cm^{-1}) and cystocarp opening. Data analysed for cystocarp opening included the combined total of cystocarps that had opened before and after exposure to controlled conditions to compare the total number of opened cystocarps during each month. PERMANOVAs were run using

Euclidean distance resemblance matrices, 9,999 unrestricted permutations of raw data, and Type III sum of squares (Anderson et al. 2008). Pair-wise *a posteriori* comparisons were carried out in PRIMER using PERMANVOA if a significant difference ($P \leq 0.05$) was detected. Relationships between reproductive measures (% reproductive tetrasporophytes, tetraspore release, cystocarp density and cystocarp opening) and environmental factors (temperature, photoperiod, total BSH, salinity, TN and TP) were analysed using Pearson correlation coefficients and linear regression models in R-studio, and correlations were visualised using the ggcorrplot package. All data is reported as mean ± standard error (SE); n = 10 to 20.

2.4. Results

2.4.1 Tetrasporophytes

Tetrasporophytes of *A. armata* were present year-round at Mathesons Bay and tetrasporangia were present from March–September (Figure 2.4A). The proportion of reproductive individuals (i.e., containing immature or mature tetrasporangia) ranged from 35–55% during March–April across 2021 and 2022 and peaked from May–July with tetrasporangia present in almost 100% of individuals during these months in both years (Figure 4A). During 2022, the proportion of reproductive individuals decreased from 70% in August to 40% in September (Figure 4A).

There was a significant interactive effect of month and year on tetraspore release (Table 2.1). During 2021, tetraspore release significantly increased from 20 ± 9% in May to a peak of 75 ± 21% in June (P = 0.017) and all released tetraspores successfully germinated (Figures 2.4B and 2.4C). In contrast, there was no significant change in tetraspore release from May to June during 2022 and both tetraspore release and germination rate were

significantly lower in June 2022 compared to June 2021 by approximately 50 and 20%, respectively (P <0.001) (Figures 2.4B and 2.4C). No tetraspores were released in July 2021, despite 100% of individuals bearing tetrasporangia upon collection (Figures 2.4A and 2.4B). During 2022, tetraspore release was highest in September with 65 ± 16% of tetraspores released and 73 ± 14% of these germinated (Figures 2.4B and 4C).

Most individuals (80–100%) collected during March and April in both years were poorly pigmented upon collection and only contained immature tetrasporangia (Appendix 1) that did not release tetraspores and became completely discoloured and died within 24 h. All individuals collected during May and June in 2021 were well-pigmented and appeared healthy, whereas 30–50% of individuals collected during these months in 2022 were poorly pigmented and died within 24 h of collection. This also occurred in over half of the individuals collected during August and September in 2022.

Table 2.1 Results of Permutational Analysis of Variance (PERMANOVA) determining the effect of "Year" and "Month" on tetraspore release and germination rate (%). F-statistics (F) and the significance level (P) with significant effects in bold are reported.

		Tetraspore release		Germination rate	
Source	*df*	*F*	*P*	*F*	*P*
Year	1	**4.40**	**0.041**	3.20	0.0843
Month	3	**3.91**	**0.015**	1.63	0.1869
Year x Month	1	**9.92**	**0.003**	3.27	0.077
Residuals	54				

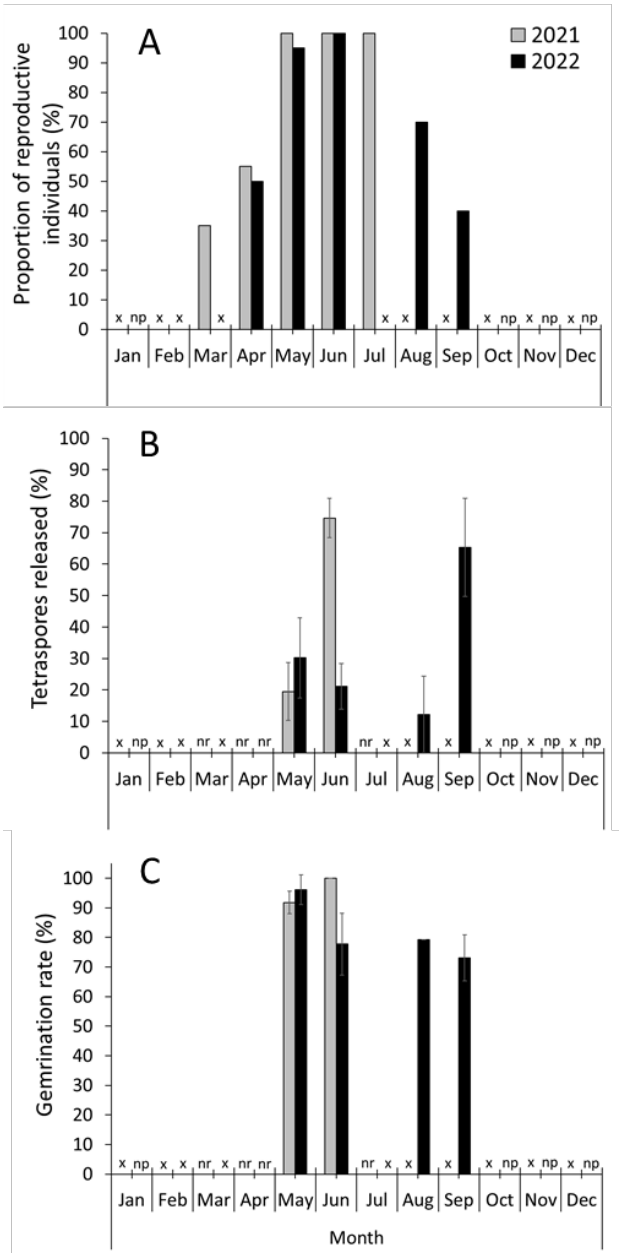

Figure 2.4 Reproductive phenology of tetrasporophytes of *A. armata* in natural populations at Mathesons Bay in 2021 and 2022; (A) Proportion of reproductive individuals (*n* = 20), (B) Mean (± SE) tetraspore release (%) from reproductive individuals (*n* = 10), (C) Mean (± SE) germination rate (%) of released tetraspores (*n* = 10). x indicates months when sampling was unable to be conducted, np indicates months when individuals were not reproductive, and nr indicates months when tetraspores were not released from reproductive individuals.

2.4.2 Gametophytes

Gametophytes of *A. armata* were present from August–November in 2022 at Mathesons Bay and cystocarps were present from September–November (Figure 2.5, Table 2.2). There was little to no evidence of prior release of carpospores from cystocarps in September, however, most individuals (70–80%) had a low number of cystocarps with evidence of prior release of carpospores in October and November (Figure 2.6). Cystocarp

density significantly increased from approximately five cystocarps cm^{-1} in September to approximately seven cystocarps cm^{-1} in October (P = 0.043, Figure 2.5). In contrast, cystocarp density significantly decreased from October to November by approximately 50% (P <0.001).

Cystocarp opening was low in September and October with fewer than five newly opened cystocarps out of a total of 43, and 67 unopened cystocarps per branch during September and October respectively (Figure 2.6). There were no newly opened cystocarps in November (Figure 2.6). All individuals with newly opened cystocarps in September released viable carpospores that germinated into tetrasporophytes. Although the number of carpospores released per cystocarp and their germination rate were not explicitly quantified, it was clear that each opened cystocarp released hundreds of carpospores that had settled and germinated directly underneath each opened cystocarp. In contrast, individuals with newly opened cystocarps in October did not release viable carpospores; rather, the entire contents of each dish (thallus, cystocarps, and carpospores) became completely discoloured and died within 24 h (Appendix 2). This also occurred in all individuals collected during November. Individuals collected during October and November were also poorly pigmented upon collection. Spermatangia were present in 60% and 40% of the extra individuals brought back to the laboratory at the end of August and September, respectively (Figure 2.5). No spermatangia were present in the remaining months.

Table 2.2 Results of Permutational Analysis of Variance (PERMANOVA) determining the effect of "Month" on cystocarp density (cm^{-1}) and cystocarp opening. F-statistics (F) and the significance level (*P*) with significant effects in bold are reported.

		Cystocarp density		Cystocarp opening	
Source	*df*	*F*	*P*	*F*	*P*
Month	2	12.26	**<0.001**	3.42	**0.028**
Residuals	27				

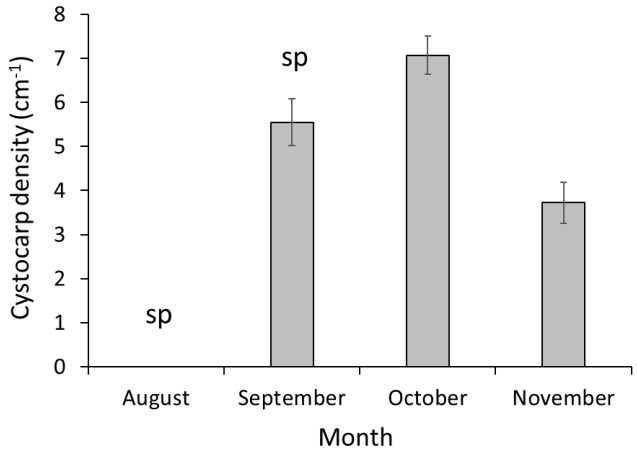

Figure 2.5 Mean (± SE) cystocarp density (cm^{-1}) in *A. armata* gametophytes in natural populations at Mathesons Bay during 2022 (*n* = 10); sp indicates months where spermatangia were present. Only months when gametophytes were present are shown in the graph.

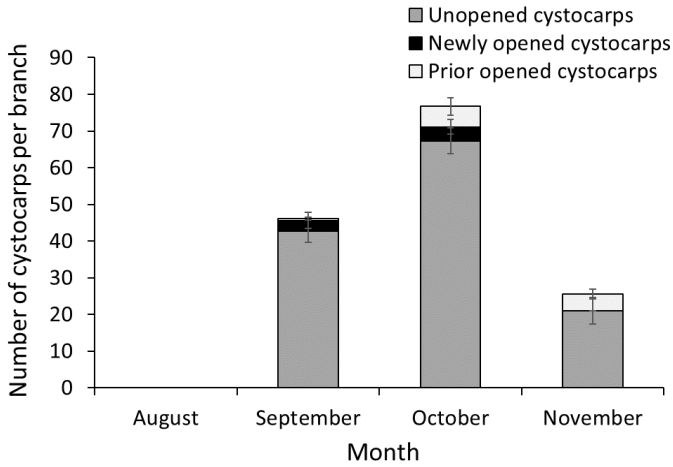

Figure 2.6 Mean (± SE) number of unopened cystocarps (prior to exposure to controlled conditions), newly opened cystocarps (i.e., opened 48 h after exposure), and prior opened cystocarps (i.e., opened upon collection) per branch in *A. armata* gametophytes in natural populations at Mathesons Bay during 2022 (*n* = 10). Only months when gametophytes were present are shown.

2.4.3. Environmental data and correlations with reproductive measures

The mean SST across all months was relatively similar during 2020 and 2021, however, the mean SST was consistently higher during January–May 2022 than during

January–May 2021 by approximately 1.0 °C and was on average 0.6 °C higher in 2022 compared to 2021 across all months (Figure 2.7A). The longest photoperiods occurred during summer with a maximum of 14 h L:10 h D in December while the shortest photoperiods occurred in winter with a minimum of 9 h L:15 h D in June (Figure 2.7A). Total BSH were highest in summer and lowest during winter across both years, however, there were notable differences between years (Figure 2.7B). Monthly BSH were higher in 2022 than 2021 during January, March, and September, whereas monthly BSH were lower in 2022 than 2021 during February, July, and December (Figure 2.7B). There were minor differences in salinity across all months between 2021 and 2022 (Figure 2.7C), with the exception of a consistently lower period of salinity from August–October 2022 averaging at 33.8 ppt compared to 34.7 ppt across all remaining months (Figure 2.7C).

Concentrations of TN and TP were relatively stable throughout 2021 and from April–September 2022, averaging 0.1 mg N L^{-1} and 0.01 mg P L^{-1} (Figure 2.8A). In contrast, concentrations of TN and TP were over three times greater during October 2022 reaching 0.25 mg N L^{-1} and 0.04 mg P L^{-1} (Figures 2.8A and 2.8B), and concentrations of TN were over two times greater during February–March 2022 reaching an average of 0.2 mg N L^{-1}. No data is available for salinity and nutrient concentration from September–October and December during 2021 due to COVID-19 restrictions.

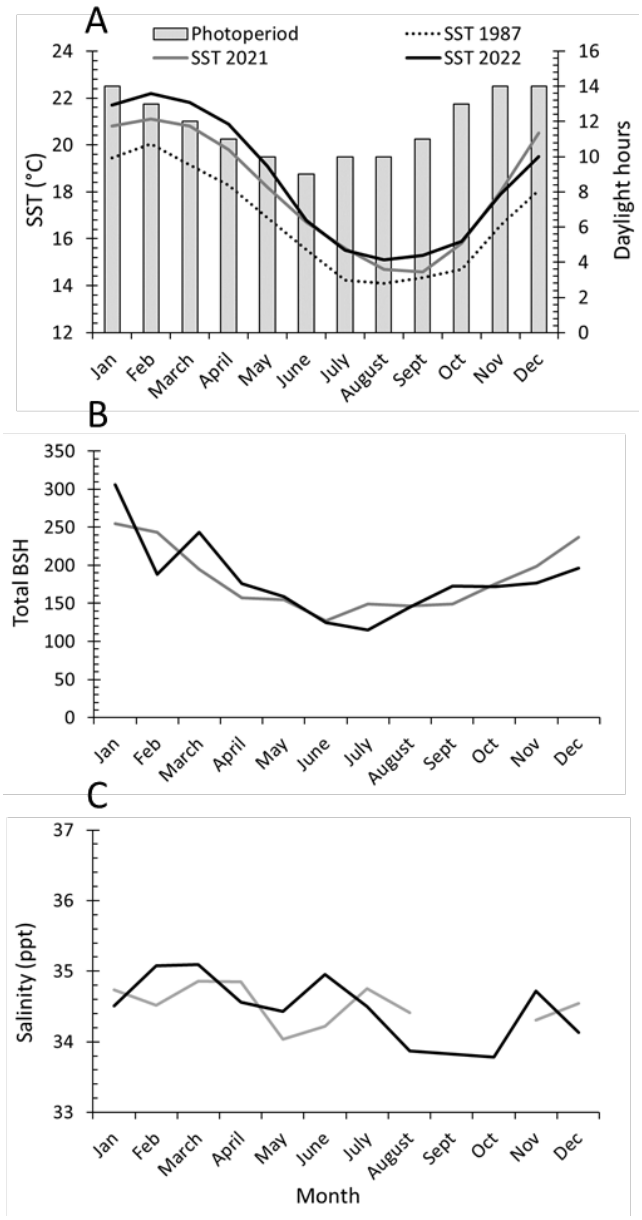

Figure 2.7 (A) Mean monthly sea surface temperature (SST, °C) and daylight hours (photoperiod) at Goat Island, Leigh, (B) Total monthly bright sunshine hours (BSH) at North Shore, Auckland (73 km from Goat Island) and (C) Mean monthly salinity (ppt) at Goat Island, Leigh, New Zealand. Light grey line indicates data from 2021 and black line indicates data from 2022 in (B) and (C).

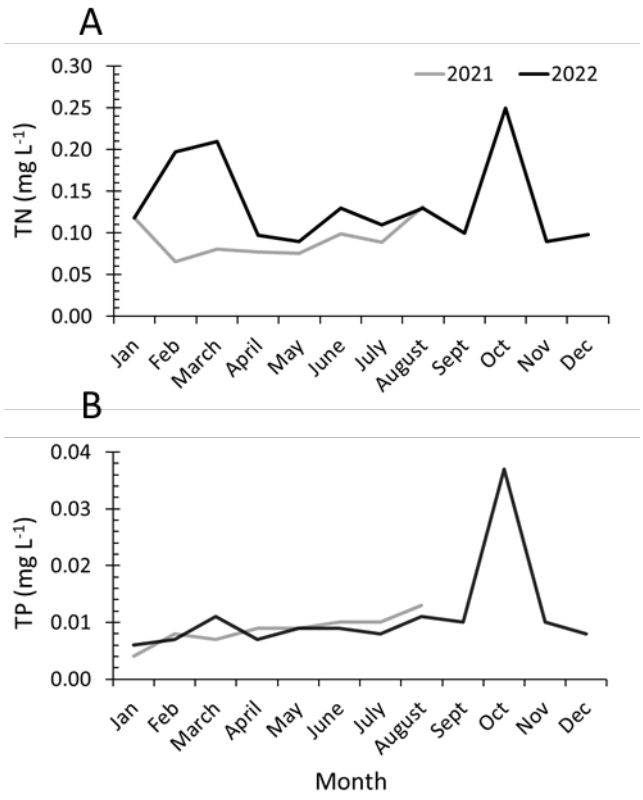

Figure 2.8 Monthly spot measurements of (A) total nitrogen (TN) and (B) total phosphorous (TP) at Goat Island, Leigh, New Zealand.

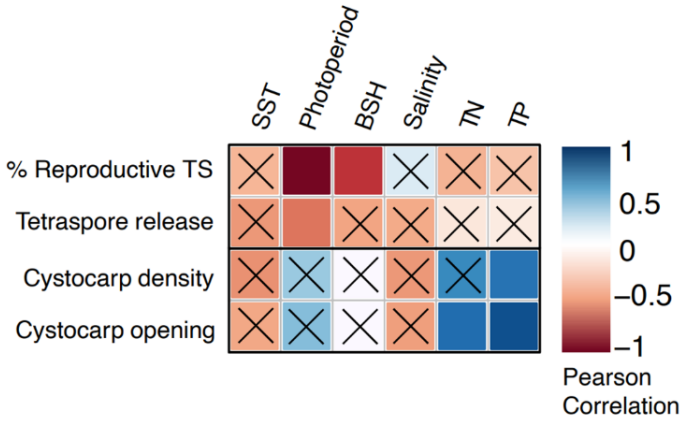

Figure 2.9 Correlation matrix between reproductive measures of *A. armata* (*n* = 10–20) and environmental factors at the collection site calculated by Pearson correlation coefficient (r). TS = tetrasporophyte, TN = total nitrogen, TP = total phosphorous. Red/orange boxes indicate a negative correlation and blue boxes indicate a positive correlation. X marks non-significant based on linear regression models ($P \leq 0.05$).

The proportion of reproductive tetrasporophytes was significantly negatively correlated with photoperiod (linear regression: F(1,13) = 131.87, P = <0.001, R^2 = 0.92, n = 20) and total BSH (linear regression: F(1, 13) = 13.27, P = 0.003, R^2 = 0.53, n = 20) (Figure 2.9). Tetraspore release was also significantly negatively correlated with photoperiod,

although the correlation was weak (linear regression: $F(1,13) = 4.83$, $P = 0.048$, $R^2 = 0.29$, $n = 10$). In contrast, cystocarp density was significantly positively correlated with TP (linear regression: $F(1,8) = 8.27$, $P = 0.024$, $R^2 = 0.54$) and cystocarp opening was significantly positively correlated with TN and TP (highest correlation: TP, linear regression: $F(1,8) = 23.39$, $P = 0.002$, $R^2 = 0.77$).

2.5. Discussion

This study presents the first temporally longitudinal analysis of potential climate driven shifts in the reproductive phenology of a seaweed, and our findings provide a detailed baseline for detecting changes in reproductive phenology in the future. While the timing of when tetraspores were present in natural populations of *A. armata* did not appear to have shifted since 1978–1981 (Bonin and Hawkes 1987), there was a clear difference in the release of tetraspores between June 2021 and June 2022 (austral winter) (Figure 2.10). Notably, the period of when cystocarps were present was reduced in this study compared to 40 years ago (Bonin and Hawkes 1987), and viable carpospores were only released under controlled laboratory conditions during September (Figure 2.10).

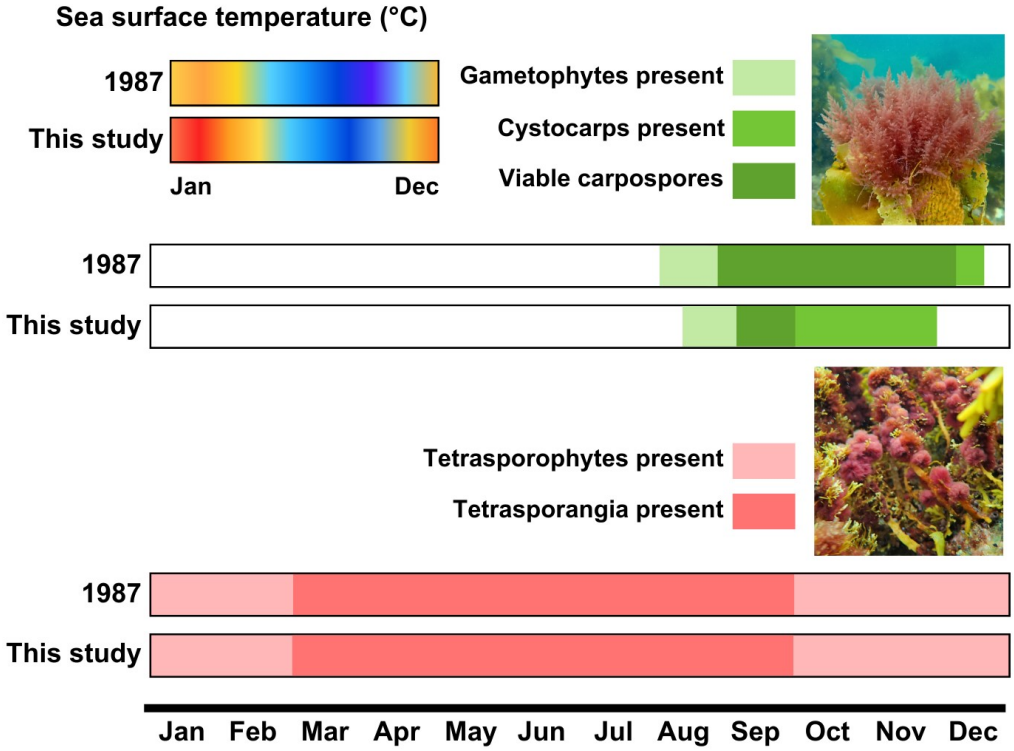

Figure 2.10 Reproductive phenology of *Asparagopsis armata* at Mathesons Bay in the current study (2021–2022) compared to Bonin and Hawkes (1987). Gradients represent the average sea surface temperature throughout 2021–2022 and 1978–1981; red colours represent high temperatures (20–22 °C), orange – yellow colours represent moderate temperatures (18–19 °C), and blue colours represent low temperatures (14–17 °C).

2.5.1. Tetrasporophytes

Our findings demonstrate that the formation and release of tetraspores is a continuous process in wild populations in northern New Zealand initiated under long photoperiods (12 h L:12 h D) and warm temperatures (21 °C) prevalent at the study site in March (austral autumn). However, in contrast to these findings, tetrasporogenesis was only induced in controlled laboratory studies using samples isolated both from wild populations and released carpospores under short photoperiods (8 h L:16 h D–10 h L:14 h D) (Oza 1977, Guiry and Dawes 1992, Mihaila et al. 2023a). This divergence in results could be due to the time of year when samples in laboratory studies were collected from wild populations as

this occurred outside of when tetrasporogenesis was naturally occurring. The induction of tetrasporogenesis in samples under controlled conditions may have also been influenced by their previous environmental history. Tetraspores present during March–April in the field in this study were mostly immature and not released when individuals were brought back to the laboratory during either 2021 or 2022, indicating that tetraspores produced during these months either require more time and/or different conditions to mature and release, or that they do not reach this stage altogether. Tetrasporophytes were most fertile from May–July when temperatures were moderate–cold (15–19 °C), photoperiods were short (9 h L: 15 h D–10 h L:14 h D), and total BSH were low (150–120 h). Moreover, the proportion of reproductive individuals and tetraspore release were mostly strongly correlated with photoperiod, reinforcing that this, rather than temperature, is the predominant factor controlling tetrasporogenesis in *A. armata* (Oza 1977, Guiry and Dawes 1992, Mihaila et al. 2023a).

Tetraspore release under controlled conditions was generally low at the times of our sampling except for two separate peaks occurring at the start of winter in 2021 and the start of spring in 2022. Unfortunately, we were unable to determine whether a second peak in tetraspore release in 2021 occurred in spring due to COVID-19 travel restrictions. Regardless, our results demonstrate that wild collection is not likely to be a reliable source of tetraspores for aquaculture purposes within this region of New Zealand. Instead, we recommend that tetraspores are acquired through induction under controlled laboratory (hatchery) conditions, as previous work has demonstrated that tetrasporogenesis can be consistently induced throughout the year in cultured broodstock to obtain large numbers of tetraspores (>10 million tetraspores per 100 g FW of tetrasporophyte biomass over a 15-day

period) (Chapter 3/Mihaila et al. (2023a)). This method would therefore be suitable for obtaining a reliable and sustainable supply of tetraspores for seeding.

Previous work using domesticated tetrasporophytes originating from Mathesons Bay showed a bimodal pattern in sporulation with two peaks from the onset of reproduction, along with a 28-fold increase in the release of tetraspores at 18 °C compared to 15 °C under an 8 h L:16 h D photoperiod (Chapter 3/Mihaila et al. (2023a)). In the current study, all measures of reproduction and viability were high in June during 2021 when the temperature and photoperiod were closest to these values. However, despite the presence of what appeared to be mature tetrasporangia in all individuals in June the following year, tetraspore release was low and viability was also notably reduced. We were unable to determine the driver behind the marked difference in reproductive phenology between 2021 and 2022 in this study, although it is possible that this represents small-scale interannual variation. Without comparable baseline data for tetraspore release and germination, it is not possible to determine whether patterns in these processes have shifted over the last 40 years, highlighting the importance of a quantitative baseline for detecting phenological change (Wernberg et al. 2012, Poloczanska et al. 2013). Future repeats of this study and/or longer-term studies are critical to account for short-term variation in reproduction and/or seasonal conditions that can occur between years (Hoffmann 1987, Viejo et al. 2011, Howells et al. 2017).

2.5.2. Gametophytes

Gametophyte abundance in natural populations of *A. armata* at Mathesons Bay was highly seasonal with individuals only present from late August–late November (austral winter–spring). While spermatangia-bearing males were identified from August–September,

cystocarpic gametophytes were only present from September–November, which was delayed and shorter in duration compared to the last phenological assessment in 1978–1981 (cystocarps present from August–December) (Bonin and Hawkes, 1987). This was unexpected based on our previous observations where an advancement in the formation of cystocarps (present from early-August) was observed in 2020 (A. Mihaila, Unpublished results, 2020) compared to 1978–1981 (present from late-August, (Bonin and Hawkes 1987)). Temperature, usually in combination with light, has been found to regulate precursory reproductive processes (e.g., gametogenesis and fertilisation) in gametophytes of many species of the brown seaweed *Laminaria* (Lüning and Neushul 1978, Lüning 1980, Lüning and Dieck 1989) and some species of red seaweeds, such as *Cystoclonium purpureum* (Molenaar et al. 1996) and *Pyropia yezoensis* (Kakinuma et al. 2006). For *Asparagopsis*, knowledge is lacking on the environmental regulation of reproductive processes in gametophytes as controlled culture experiments have largely been inconclusive, often resulting in the unexplained mortality of individuals (Mickelson 2013, Batista 2020). A reproductive phenology assessment of the sister species *A. taxiformis* in a population located in southern Spain reported that reproduction in gametophytes was independent of environmental conditions (Zanolla et al. 2017). A moderate significant correlation was identified between cystocarp density and TP in the present study. Moderate correlations between cystocarp density and SST and salinity were also found, although these were not significant. In combination, these results suggest that one or more of these environmental factors are important for controlling reproduction in gametophytes of *A. armata* in New Zealand, and therefore provide a starting point for manipulative controlled experiments to confirm the main drivers of reproduction.

Already opened cystocarps were present in the collected gametophytes throughout the entire reproductive season (September–November, austral spring) indicating, together with the previous assessment in 1978–1981, that carpospore release is a continuous process in *A. armata* (Bonin and Hawkes 1987). Continuous patterns of carpospore release for periods of up to 58 days have been observed from carposporophytes of several species of red seaweed, including *Bostrychia moritziana, Pterosiphonia pennata*, *Kappaphycus alvarezii*, and *Murrayella periclados* under controlled conditions (Azanza and Aliaza 1999, West and McBride 1999). We cannot directly compare our findings to these results due to the fact that we were unable to adequately assess carpospore release here as seemingly mature cystocarps collected during October–November failed to release carpospores under controlled conditions. This was despite a clear unimodal pattern in cystocarp density peaking during October. In the last assessment in 1978–1981, viable carpospores were released from late August–early December, although the extent of release was not quantified (Bonin and Hawkes 1987). Conversely, viable carpospores were only released from a low proportion of cystocarps during September in this study, suggesting that the period when individuals are reproductively viable may have decreased since 1978–1981. It is also important to consider, however, that our observed patterns could have been driven by unknown environmental factors that negatively impacted reproduction (West and McBride 1999, Niwa and Harada 2013, Zubia et al. 2014) (see Section 2.5.3). General patterns in cystocarp opening and carpospore release still ultimately remain unclear for *A. armata* and this could be resolved with repeated and more frequent sampling.

2.5.3. Discoloration and environmental variables

Tetrasporophytes and gametophytes were often poorly pigmented during our sampling in 2022, and in all cases these individuals failed to release viable spores and became completely discoloured and died within 24 h of initial inspection. Discoloration in seaweeds can indicate either a lack of resource(s), usually nutrient depletion, and/or exposure to adverse conditions, such as temperature or light stress (Niwa and Harada 2013, Zubia et al. 2014, Endo et al. 2017, Kreusch et al. 2019). Both situations have been associated with reduced survival and/or reproductive success in red seaweeds (West and McBride 1999, Choi et al. 2006). Large peaks in TN during February–April (austral summer–autumn) and October in 2022, potentially as a result of increased run-off from higher rainfall, suggest that nutrient depletion was not a cause of discoloration in this study. On the other hand, SST's were consistently higher during all months in 2022 compared to 2021, particularly during summer and autumn when they repeatedly exceeded 21 °C. Given the direct influence of temperature on the survival, reproduction, and recruitment of seaweeds and reported negative effects of heat waves on these processes (Lee and Brinkhuis 1986, Lüning and Yarish 1990, Bartsch et al. 2013, Kreusch et al. 2019), it is likely that heat stress negatively impacted the survival and/or reproductive success of individuals during our study. Increasing temperature can inhibit the production of phycobiliproteins and prolonged exposure can cause thalli to bleach and disintegrate (Graiff et al. 2015, Kumar et al. 2020). Long term exposure to heat stress (timescale of weeks) may also impair or cause irreversible damage to metabolic processes (Eggert 2012). Manipulative temperature tolerance experiments would provide a starting point for understanding the effect of elevated temperatures on reproductive processes in *A. armata*. Such studies would also assist in the development of management strategies for climate resilient aquaculture of *Asparagopsis*,

which will be especially important given the predicted increases in the frequency and intensity of marine heatwaves (Allen 2018) that could pose a challenge to gametophyte outplanting. Longer-term regular quantitative monitoring will be critical to gaining a better understanding of how our identified patterns compare with more general trends in reproductive phenology that encompass both warmer (including heat waves) and cooler temperatures.

2.6. Conclusion

The timing of when tetraspores were present in *A. armata* was not different in our study compared to the last phenological assessment in 1978–1981, although we did identify changes in when peak tetraspore release occurred between 2021 and 2022. In contrast, the timing of when cystocarps were present was delayed and shorter in duration in our study compared to the 1978–1981assessment, and the period of when viable carpospores were released under controlled conditions was greatly reduced. While there were clear patterns in the occurrence of tetraspores and cystocarps during 2022, reproductive output and viability under controlled conditions was generally low for both life stages. Based on our observed patterns, along with the high rates of initial discoloration and subsequent mortality throughout 2022, we hypothesize that aspects of reproduction in *A. armata* were compromised as a result of heat stress during this year. The effect of prolonged high temperatures on reproduction and survival in *A. armata* requires further investigation and will be an important consideration in managing the aquaculture of this species. This study provides an up-to-date, quantitative assessment of the reproductive phenology of a species of increasing commercial importance and supplies a baseline from which to further measure

how increases in temperature due to climate change will affect the timing of reproductive events in seaweeds.

Chapter 3

Early hatchery protocols for tetrasporogenesis of the antimethanogenic seaweed *Asparagopsis armata*

This chapter has been published in Journal of Applied Phycology as:

Mihaila, A. A., R. J. Lawton, C. R. K. Glasson, and M. Magnusson. 2023a. Early hatchery protocols for tetrasporogenesis of the antimethanogenic seaweed *Asparagopsis armata*. Journal of Applied Phycology 35:2323-2335 (Appendix 12).

3.1. Abstract

Asparagopsis armata is an emerging aquaculture-target species due to its application as an antimethanogenic feed ingredient in ruminants, yet information on *A. armata* reproduction and cultivation is currently lacking. We therefore quantified the effects of temperature, irradiance, nutrients, and photoperiod, and addition of plant growth regulators (PGRs; indole-3-acetic acid, abscisic acid, 1-aminocyclopropane-1-carboxylic acid) on tetrasporogenesis in domesticated *A. armata* that had been maintained under controlled conditions (18 °C, 12h light:12h dark photoperiod) for 18 months prior to experimentation. Tetrasporogenesis was only induced at 5 and 15 µmol photons m^{-2} s^{-1} under an 8h light:16h dark photoperiod with 3.5 mg nitrogen L^{-1} and tetraspore release was 28-fold greater at 18 °C compared to 15 °C after 28 days of exposure. After 29 days, tetraspore release and germination rate both declined. All PGR treatments prevented tetrasporogenesis. This study is the first to provide the detail and framework necessary to enable *A. armata* hatchery development. We conclude that tetrasporogenesis was most likely induced in response to a

significant reduction in photoperiod rather than as a result of replicating seasonal environmental conditions, and that temperature played a key role in determining reproductive output. With overall higher tetraspore release and a consistent germination rate of >90%, we recommend exposing tetrasporophyte biomass to 18 °C, 15 µmol photons m^{-2} s^{-1} and 3.5 mg nitrogen L^{-1} under an 8 h L:16 h D photoperiod for up to 29 days to obtain a reliable supply of tetraspores for seeding onto ropes for transfer to the hatchery phase.

3.2. Introduction

The red seaweeds *Asparagopsis armata* and *Asparagopsis taxiformis* are potent inhibitors of enteric methane due to their production and storage of the bioactive secondary metabolite bromoform (Kinley et al. 2016, Li et al. 2016, Machado et al. 2016a, Machado et al. 2018, Kinley et al. 2020, Roque et al. 2021). As a result, there is high interest to commercially cultivate these seaweeds at scale to supply the beef and dairy industries with biomass for inclusion in anti-methanogenic feeds (Duarte et al. 2017). However, before wide-scale adoption of *Asparagopsis* becomes possible, further research is required to develop techniques for large-scale commercialisation, product application technologies, and management strategies to ensure the long-term safety and efficacy of *Asparagopsis* in animal production systems (Vijn et al. 2020, Pandey et al. 2021, Glasson et al. 2022).

The commercialisation of *Asparagopsis* requires a continuous supply of high quality biomass that will need to be provided through efficient and sustainable aquaculture (Vijn et al. 2020). As such, there are three approaches that can be used to farm *Asparagopsis,* namely: a) land-based aquaculture of the tetrasporophyte in tanks (Mata et al. 2010), b) mariculture of wild-harvest gametophyte by seeding ropes for grow-out (Kraan and

Barrington 2005, Wright et al. 2022), and c) closed life-cycle cultivation of gametophytes from tetraspores for mariculture on ropes (Figure 3.1). Closed-life cycle cultivation is a desirable method as it enables the year-round production of gametophytes via the induced reproduction of tetrasporophytes, although the complex life cycle of *Asparagopsis* (Figure 3.1) makes it challenging to close all the stages of the life cycle under aquaculture. This approach will also enable future strain selection and selective breeding for the production of high quality *Asparagopsis* containing high content of bromoform (the primary bioactive component in *Asparagopsis* (Machado et al. 2016a, Glasson et al. 2022), thereby reducing the dosage of *Asparagopsis* required to achieve an optimal mitigation effect (Li et al. 2016, Charrier et al. 2017, Roque et al. 2019b, Kinley et al. 2020, Roque et al. 2021).

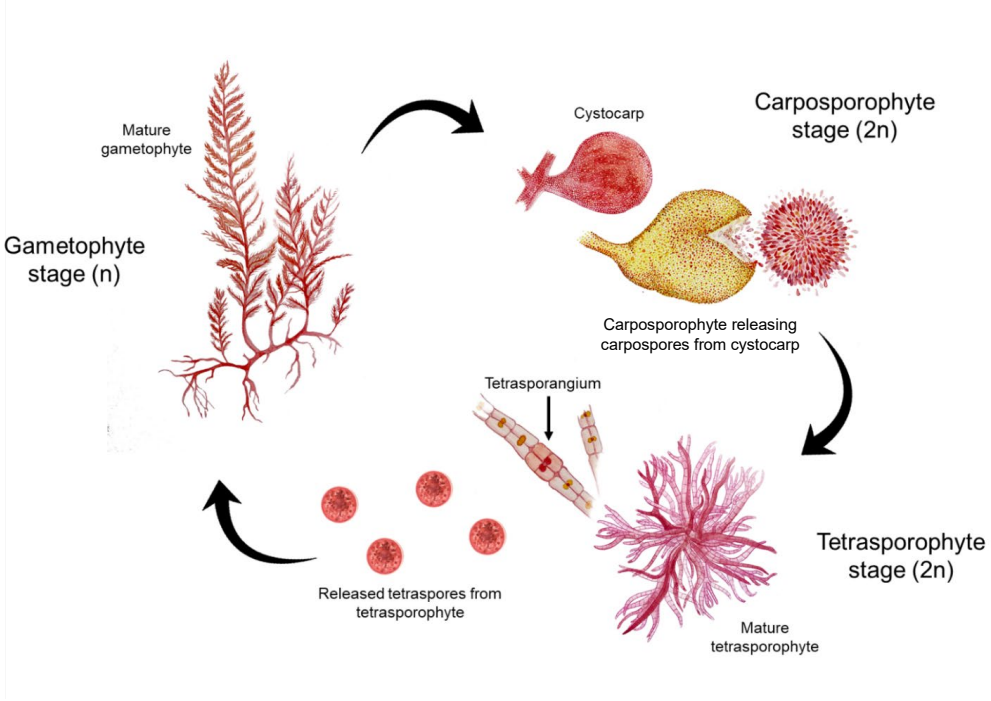

Figure 3.1 Schematic diagram of the life cycle of *Asparagopsis armata*
Asparagopsis armata has a triphasic life cycle, alternating between a terete gametophyte (n), a microscopic carposporophyte (2n), and filamentous tetrasporophyte (2n) phase. Gametophytes are dioecious, with males producing spermatangia and females producing carpogonia. After fertilisation, the carposporophytes develop on the female thallus. Carposporophytes produce carposporangia, which release carpospores that germinate into tetrasporophytes. Tetrasporophytes (also referred to as individual 'pom poms') develop tetrasporangia, which release tetraspores that germinate into gametophytes (Bonin & Hawkes, 1987). Original pencil drawings, assembly and edits in Adobe Photoshop and Illustrator by Maro Guy. Drawings are not to scale.

Successful seaweed aquaculture requires a high degree of control over the external factors regulating seaweed reproduction, such as irradiance, temperature, photoperiod, pH, and nutrient concentration (García-Jiménez and Robaina 2015, Charrier et al. 2017, Liu et al. 2017). Identifying the optimum conditions to induce tetrasporogenesis (i.e., the mass formation of tetrasporangia) and the release, settlement, and germination of subsequent tetraspores into juvenile gametophytes are pivotal steps in establishing closed-life cycle aquaculture of *Asparagopsis* as it will enable the development of commercial hatcheries for generating sufficient and sustainable biomass supply to meet future demands (Jun Pang and

Lüning 2004, Charrier et al. 2017). Temperature, photoperiod, and nutrient concentration are critical factors for inducing tetrasporogenesis in *Asparagopsis,* and tetrasporogenesis has only been induced under short photoperiods (Oza 1977, Bonin and Hawkes 1987, Guiry and Dawes 1992). For example, when cultured at 17 °C, the critical photoperiod for inducing tetrasporogenesis in Irish and Australian strains of *A. armata* tetrasporophytes ranged between 8 h L:16 h D (Light:Dark)–9 h L:15 h D (Guiry and Dawes 1992). Similarly, tetrasporogenesis occurred when cultured at 15 °C under low nutrient concentrations (i.e. nitrate/phosphate deficient) and at photoperiods ranging between 6 h L:18 h D–8 h L:16 h D in French strains of *A. armata* (Oza 1977). However, no method with sufficient detail surrounding the timing and practical setup for inducing tetrasporogenesis or optimising the release, settlement and germination of tetraspores has been published.

There is accumulating evidence that the application of plant growth regulators (PGRs) can provide benefits for aquaculture by accelerating and/or enhancing seaweed reproduction (Sacramento et al. 2007, Stirk and Van Staden 2014, Pilar et al. 2016, Garcia-Jimenez and Robaina 2017, Liu et al. 2017). For example, the exogenous application of methyl jasmonate (100 µM) to *Grateloupia imbricata* reduced the cystocarp maturation period to 48 h compared to the typical >3-week period and increased the number of cystocarps 7.5-fold compared to controls (Pilar et al. 2016). Multiple studies have also detected increases in the production of indole-3-acetic acid (IAA), abscisic acid (ABA), and 1-aminocyclopropane-1-carboxylic acid (ACC) in fertile thalli compared to infertile thalli in several species of seaweed (Nimura and Mizuta 2002, Kai et al. 2006, García-Jiménez and Robaina 2012, 2015, Uji et al. 2020), indicating that these PGRs may play a role in regulating seaweed reproduction. There is significant potential for PGRs to improve the efficiency of *A. armata* grown in hatcheries by reducing the induction period for tetrasporogenesis, which

would drastically improve the production of tetraspores over the same time scale, resulting in reduced overall costs of hatchery production (Watson and Dring 2011, Taelman et al. 2015).

The aim of this study was therefore to identify the optimal cultivation under controlled laboratory conditions for inducing and controlling tetrasporogenesis in the anti-methanogenic red seaweed *A. armata* in New Zealand. This will provide a baseline method for obtaining a reliable supply of *A. armata* tetraspores to facilitate the development of sustainable *A. armata* aquaculture. The specific objectives of this study were to: (1) determine the effect of temperature, irradiance, nutrient concentration, and photoperiod on the induction of tetrasporogenesis under controlled laboratory conditions; (2) quantify the number of tetraspores released and germination rate of released tetraspores under successful inducing conditions; (3) determine the effect of selected PGRs on tetrasporogenesis with the target of accelerating tetrasporogenesis; and (4) regulate the induction of tetrasporogenesis (i.e. "switching" reproduction off and on) under controlled laboratory conditions.

3.3. Materials and methods

3.3.1. Sample collection and tetrasporophyte production

Cystocarpic *A. armata* (approximately 20 individuals) were haphazardly collected from natural populations (Ministry for Primary Industries Special Permit number 742) at 2–3 m depth by snorkelling in Matheson Bay, Leigh, New Zealand (36.31°S, 174.80°E) in August 2020. Samples were transported in buckets filled with seawater collected at the site to the laboratory. The collected specimens were transferred to nutrient enriched (3.5 mg nitrogen

(N) L^{-1} and 0.3 mg phosphorus (P) L^{-1} (F/8), Varicon Aqua, Cell-Hi F2P) filtered seawater upon arrival to the laboratory and maintained in a temperature and light controlled room (18 °C, ~15 µmol photos m^{-2} s^{-1}, 12 h L:12 h D; spring/autumn conditions at Matheson Bay). Within a week, carpospores were released that had germinated into tetrasporophytes. Tetrasporophytes were scraped from the bottom of the bucket where they had settled and transferred into a new 2 L white plastic bucket filled with autoclaved-filtered seawater (AFSW) with nutrients were added at F/8. Germanium dioxide (GeO_2) was added at a concentration of 2.5 mL L^{-1} to inhibit diatom growth. Tetrasporophytes were scaled up and maintained over an 18-month period under the same conditions described above with weekly water changes and were well acclimated to pre-experimental culture conditions. This biomass was used in the four succeeding experiments:

(1) Induction of tetrasporogenesis

(2) Enhancing tetrasporogenesis

(3) Use of plant growth regulators

(4) Controlling repeated cycles of tetrasporogenesis

3.3.2. Experimental overview

The present study was divided into four experiments:

In experiment one (induction of tetrasporogenesis, Figure 3.2A), *A. armata* tetrasporophyte filaments were exposed to different combinations of temperature, irradiance, and nutrient concentration to determine the effect of these environmental drivers on the induction of tetrasporogenesis under controlled laboratory conditions. Several treatment combinations resulted in the induction of tetrasporogenesis during

experiment one, but only at 15 °C (i.e. no treatments that included 11 or 13 °C resulted in tetrasporogenesis); therefore, in experiment two (enhancing tetrasporogenesis, Figure 3.2B), the conditions were further refined by including photoperiod and adding a higher temperature treatment. Here, the number of released and settled tetraspores (hereafter referred to as released tetraspores) and the germination rate of released tetraspores were quantified under each set of conditions to identify an optimal set of conditions for inducing tetrasporogenesis. In experiment three (use of plant growth regulators), tetrasporophyte filaments exposed to the optimal set of conditions for inducing tetrasporogenesis were treated with selected PGRs at a range of concentrations to assess their effect on the induction of tetrasporogenesis with a target of shortening the required hatchery period. In experiment four (controlling repeated cycles of tetrasporogenesis), filaments were switched between the optimal set of conditions for inducing tetrasporogenesis and a set of conditions targeted at ceasing tetrasporogenesis to assess whether tetrasporogenesis can be ceased and restarted in the same biomass or if biomass is 'spent' following mass-production of tetraspores. Water changes were carried out weekly during all experiments.

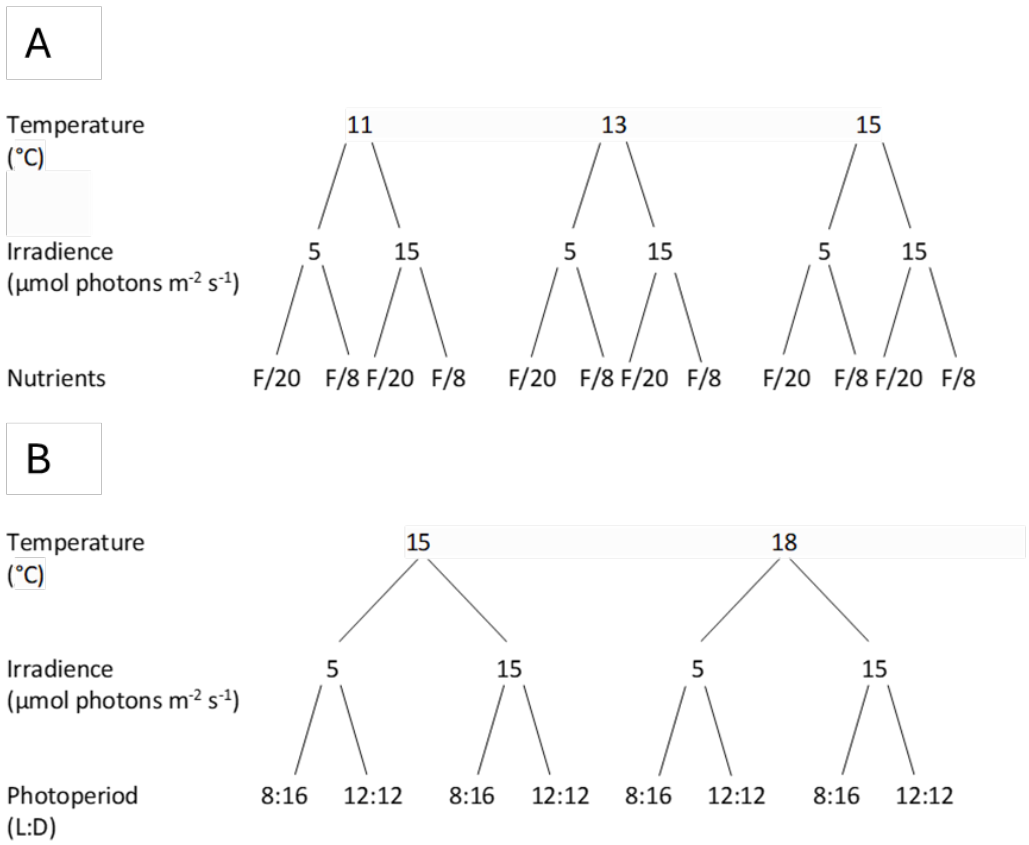

Figure 3.2 (A) Experimental design for experiment one testing the effect of temperature, irradiance, and nutrient media (F/8 = 3.5 mg N L^{-1} and 0.3 mg P L^{-1}, F/20 = 1.4 mg N L^{-1} and 0.1 mg P L^{-1}) on the induction of tetrasporogenesis (*n* = 3). Photoperiod (L:D) was maintained at 8 h L :16 h D throughout the experiment. (B) Experimental design for experiment two testing the effect of temperature, irradiance, and photoperiod on the induction of tetrasporogenesis with the aim of enhancing tetrasporogenesis (*n* = 5).

3.3.3. Experiment one: induction of tetrasporogenesis

Twenty individual tetrasporophytes from the stock cultures were cut into 3–4 mm length filaments using dissecting scissors to obtain a homogenous mass of cuttings. Subsamples of approximately 40–50 filaments (~10 mg fresh weight (FW)) per replicate were transferred into individual Petri dishes (90 x 20 mm, LabServ, LBS60016) filled with 50 mL of AFSW with nutrients (Varicon Aqua, Cell-Hi F2P) added at concentrations of F/8 (3.5 mg N L^{-1} and 0.3 mg P L^{-1}) and F/20 (1.4 mg N L^{-1} and 0.1 mg P L^{-1}). Dishes were placed in environmental control cabinets (Panasonic, MLR-352) set at 11 °C, 13 °C, and 15 °C and light

setting 1 (LS1) with a photoperiod of 8 h L:16 h D based on previously published papers (Oza 1977, Guiry and Dawes 1992). All dishes were placed at the back of the light source where light measurements (LI-COR, LI-1500) confirmed an average irradiance of 15 µmol photons m^{-2} s^{-1}. The 5 µmol photons m^{-2} s^{-1} treatment was achieved by covering dishes with a white plastic tray. This resulted in 12 treatment combinations in a fully factorial design (*n* = 3 for each treatment, Figure 3.2A). Treatments were maintained under experimental conditions for 42 days. All treatments were visually inspected weekly for the presence of tetrasporangia by examining 30 filaments from each dish under a stereomicroscope (Olympus SZX2-ILLTQ), and the presence/absence of tetrasporangia for each treatment was recorded.

3.3.4. Experiment two: enhancing tetrasporogenesis

Tetrasporangia were only formed at 15 °C with F/8 treatments exposed to both 5 and 15 µmol photons m^{-2} s^{-1} during the experiment one. Therefore, we used these conditions as the baseline for experiment two, which was a factorial experiment investigating the effect of temperature (15 and 18 °C), irradiance (5 and 15 µmol photons m^{-2} s^{-1}), and photoperiod (8 h L: 16 h D and 12 h L: 12 h D), with F/8, resulting in eight treatment combinations (*n* = 5 for each treatment, Figure 3.2B). A homogenous mass of tetrasporophyte filaments was prepared and subsamples were transferred into Petri dishes as described in experiment one (Section 3.3.3). Nutrients (Varicon Aqua, Cell-Hi F2P) were added at F/8. Dishes were placed in environmental control cabinets (Panasonic, MLR-352) set at temperatures of 15 and 18 °C and LS1 with photoperiods of 12 h L:12 h D and 8 h L:16

h D. Irradiances of 5 and 15 µmol photons m^{-2} s^{-1} were achieved as described in experiment one. The experiment was carried out in two parts, described below.

For part one of the experiment (day 0–27), all treatments were maintained under experimental conditions for 27 days. These conditions were based on temperature, light and nutrient conditions that led to the successful induction of tetrasporogenesis after 21 days during experiment one. Here, the objective was to determine which treatment combination produced the highest number of released tetraspores over the shortest period of time and with the highest germination rate of the released tetraspores. After 7 days, treatments were visually inspected daily for the presence/absence of tetrasporangia by examining 30 filaments from each dish under a stereomicroscope and the presence/absence of tetrasporangia for each treatment was recorded. For treatments in which tetrasporogenesis was successfully induced, the number of tetraspores released and germination rate of released tetraspores were quantified daily by counting the total number of newly released (ungerminated) and germinated tetraspores settled at the bottom of each dish using a stereomicroscope, as the first division of the germinating tetraspore is evident after 24 h (Figure 3.3). The biomass was kept in the same dish throughout this part of the experiment.

For part two of the experiment (day 28–52), only the most successful treatment combination was selected for continuation. This combination was identified as the one in which filaments produced the highest number of released tetraspores over the shortest period of time and with the best germination rate of released tetraspores after 27 days. Here, the aim was to determine the peak time period for tetraspore release and the cut-off point for tetrasporogenesis under these conditions. Due to the high total number of tetraspores released per day (>500 day^{-1} per dish) during part one of the experiment, the

method for quantifying tetraspore release and germination rate was adjusted as follows: each day, the entire contents (biomass and water) of each dish were transferred into a new dish and tetraspore release was quantified by counting the number of released tetraspores at the bottom of each original dish. New nutrient medium was added back into the original dishes which were transferred back to their respective culture cabinets. Germination rate was then quantified by counting the number of germinated tetraspores in each original dish three days post-release. The most successful treatment was maintained under experimental conditions for a total of 52 days.

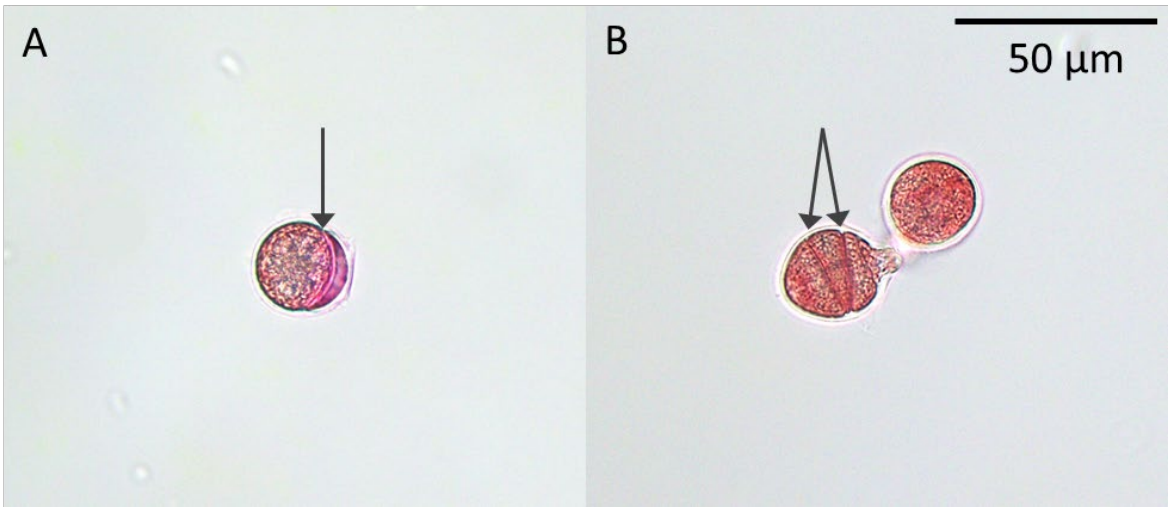

Figure 3.3 (A) First division of a germinating tetraspore (<24h of release). Arrow indicates the first division. (B) Released tetraspore (right) and second division of a germinating tetraspore (left) (<48h of release). Arrows indicate the first and second division. Scale is the same for both images.

3.3.5. Experiment three: use of plant growth regulators

A homogenous mass of tetrasporophyte filaments was prepared and subsamples were transferred into Petri dishes as described in experiment one. Three PGRs: indole-3-acetic acid (IAA), abscisic acid (ABA), and 1-aminocyclopropane-1-carboxylic acid (ACC), were applied at three concentrations: 0.1 µM, 1.0 µM, and 10 µM (*n* = 3 for each

treatment). A control with no PGRs added was also included (*n* = 3). PGR stock solutions were prepared using reverse osmosis (RO) treated water at concentrations of 17.5 mg 100 mL^{-1}, 10.1 mg 100 mL^{-1}, and 26.43 mg mL^{-1} for IAA, ABA, and ACC, respectively. IAA and ABA were dissolved in ethanol (EtOH) and dimethyl sulfoxide (DMSO), respectively, as carriers due to their low solubility in water. Solvent controls were previously tested with no effect detected and were therefore not included in the run. PGR stock solutions were added to each dish according to the three treatment concentrations and topped up to 50 mL with AFSW and nutrients added at F/8. Dishes were placed in an environmental control cabinet (Panasonic, MLR-352) set at 18 °C, 15 µmol photons m^{-2} s^{-1} (LS1), and an 8 h L:16 h D photoperiod. All treatments were visually inspected every second day for the presence of tetrasporangia by examining 30 filaments from each dish under a stereomicroscope and the presence/absence of tetrasporangia for each treatment was recorded. Water changes were carried out with PGRs added as described above. As the aim of this experiment was to determine whether tetrasporogenesis can be accelerated to shorten the required hatchery period, the experiment was run for a total of 14 days based on the successful induction of tetrasporogenesis after 14 days under these conditions during experiment two.

3.3.6. Experiment four: controlling repeated cycles of tetrasporogenesis

A pilot experiment using excess reproductive tissue grown under the optimal conditions for inducing tetrasporogenesis (i.e., 18 °C, 15 µmol photons m^{-2} s^{-1}, 8 h L: 16 h D, F/8) in experiment two was conducted to identify conditions to cease tetrasporogenesis. On day 30 and 42 of experiment two, approximately 3–4 filaments from each replicate Petri dish were combined and transferred into separate Petri dishes (90 x 20 mm) filled to 50 mL

with AFSW and incubated under conditions selected to inhibit tetrasporogenesis (*n* = 1, Figure 3.4A). The filaments transferred on day 30 were grown at 18 °C, 15 µmol photons m^{-2} s^{-1}, 12 h L: 12 h D, and with nutrients added at F/8, whereas the filaments transferred on day 42 were exposed to 20 °C, 5 µmol photons m^{-2} s^{-1}, 15 h L:9 h D, and with nutrients added at F/4 (7.0 mg N L^{-1}). All treatments were visually inspected every 2–3 days for the presence of tetrasporangia by examining all filaments from each dish under a stereomicroscope and the presence/absence of tetrasporangia for each treatment was recorded. Both treatments were maintained under experimental conditions for 16 days, or until tetrasporogenesis had ceased. Since tetrasporangia only ceased in 20 °C, 5 µmol photons m^{-2} s^{-1}, 15 h L:9 h D, F/4 treatments (non-inducing conditions), these conditions were tested with new stock culture biomass as described below to confirm their effects on tetrasporogenesis.

A homogenous mass of tetrasporophyte filaments was prepared and subsamples were transferred into Petri dishes as described in experiment one (Section 3.3.3). Nutrients were added at F/8 and dishes were placed in an environmental control cabinet (Panasonic, MLR-352) set at 18 °C, 15 µmol photons m^{-2} s^{-1} (LS1), and a photoperiod of 8 h L:16 h D (inducing conditions, *n* = 5, Figure 3.4B). Dishes were visually inspected to confirm the presence of tetrasporangia after 14 days as described in experiment three. Treatments were maintained under inducing conditions for a further 16 days, and then visually inspected to confirm tetrasporogenesis was still occurring. Cabinet settings were then changed to 20 °C and 5 µmol photons m^{-2} s^{-1}, and a photoperiod of 15 h L:9 h D, and the nutrient concentration was increased to F/4 (non-inducing conditions). Treatments were visually inspected every second day for the presence/absence of tetrasporangia as described previously and were maintained under these experimental conditions for 14 days, or until

tetrasporogenesis had ceased. Once tetrasporangia were no longer present inside filaments, cabinet settings were changed back to inducing conditions and treatments were visually inspected weekly for the presence of tetrasporangia. Treatments were maintained under inducing conditions for 21 days, or until tetrasporangia were formed, at which point the experiment ended.

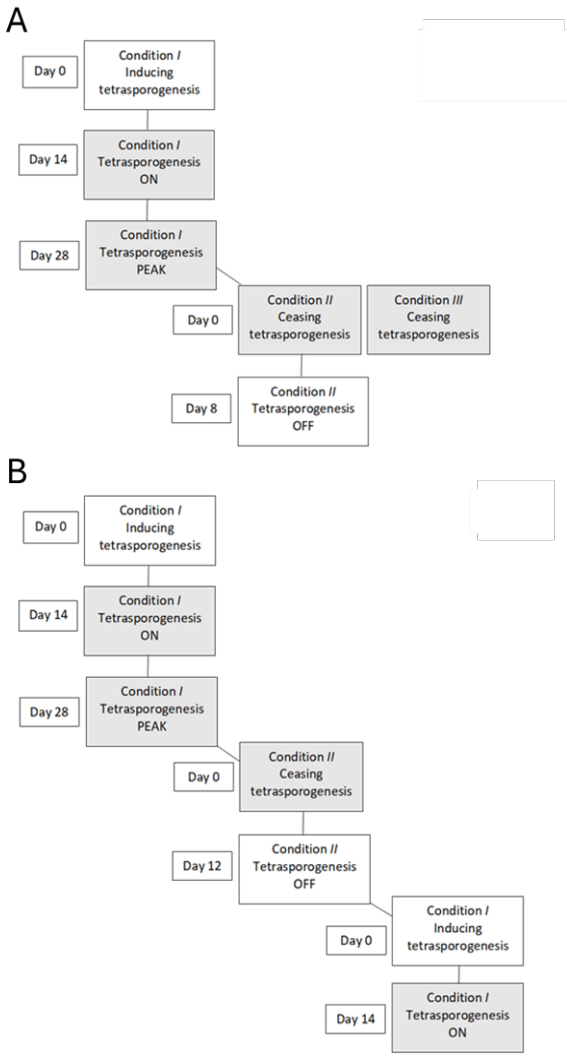

Figure 3.4 Experimental flow for (A) pilot trial and (B) experimental flow for experiment four where tetrasporophytes were exposed to different sets of conditions targeted at either inducing (condition *I*; 18 °C, 15 µmol photons m^{-2} s^{-1}, 8 h L: 16 h D, F/8 (3.5 mg N L^{-1}), ceasing (condition *II*; 20 °C, 5 µmol photons m^{-2} s^{-1}, 15 h L:9 H D, F/4 (7.0 mg N L^{-1}) and condition *III*; 18 °C, 15 µmol photons m^{-2} s^{-1}, 12 h L: 12 h D, F/8), or re-starting (condition I) tetrasporogenesis. Days indicate the time under each set of conditions. Box colour indicates whether biomass was reproductive (grey) or non-reproductive (white) during each stage of the experiment.

3.3.7. Statistical analysis

Three-factor permutational analysis of variance (PERMANOVA) was used to compare the effect of temperature, light, and photoperiod (fixed factors) on the number of

tetraspores released day^{-1}. As tetrasporogenesis is a prolonged process, analyses on tetraspore release were carried out using data that had been averaged across day 14–20 (week 3) and day 21–27 (week 4) for each treatment; data for time period were analysed separately to identify the best treatment combination at each time period, rather than to detect significant differences over time. PERMANOVAs were run using Euclidean distance resemblance matrices, 9,999 unrestricted permutations of raw data, and Type III sum of squares (Anderson et al. 2008). Pair-wise *a posteriori* comparisons were carried out using PERMANVOA if a significant difference ($P \leq 0.01$) was detected. Eta-squared (%) $\eta^2 = SS_{factor} / SS_{total} \times 100$; with SS_{factor} being the sum of squares of a particular factor and SS_{total} being the total sum of squares, was calculated to determine the proportion of the total variation in the number of tetraspores released that was associated with each factor (temperature, light, and photoperiod) (Richardson 2011). Formal statistical analyses were not carried out for germination rate because including all replicates shows a decline in germination rate on days where some replicates had no released tetraspores. Consequently, only including replicates where tetraspores were released would result in an unbalanced design with low statistical power due to a low number of replicates. All statistical analyses were conducted using PRIMER ver.7 (Primer-E., UK). All data is reported as mean ± standard error (SE); $n = 3$ for experiments one and three, $n = 5$ for experiments two and four.

3.4. Results

3.4.1. Experiment one: induction of tetrasporogenesis

Tetrasporangia were formed only in 15 °C and F/8 treatments exposed to either 5 (2/3 replicates) or 15 µmol photons m^{-2} s^{-1} (3/3 replicates) and were first visible from day 21

of the experiment (Table 3.1). Tetrasporangia continued to form on day 28 and 35, and by day 28, both treatments had released tetraspores that had successfully settled and germinated into juvenile gametophytes (Table 3.1). No tetrasporangia were formed on day 42. No tetrasporangia were formed in 11 °C and 13 °C or F/20 treatments exposed to either irradiance at any point during the experiment.

Treatment	Day					
	7	14	21	28	35	42
11 T 15 L F/8	-	-	-	-	-	-
11 T 5 L F/8	-	-	-	-	-	-
11 T 15 L F/20	-	-	-	-	-	-
11 T 5 L F/20	-	-	-	-	-	-
13 T 15 L F/8	-	-	-	-	-	-
13 T 5 L F/8	-	-	-	-	-	-
13 T 15 L F/20	-	-	-	-	-	-
13 T 5 L F/20	-	-	-	-	-	-
15 T 15 L F/8	-	-	+	+	+	-
15 T 5 L F/8	-	-	+	+	+	-
15 T 15 L F/20	-	-	-	-	-	-
15 T 5 L F/20	-	-	-	-	-	-

Table 3.1 Presence/absence (+/-) of tetrasporangia, over a 42-day period (experiment one: induction of tetrasporogenesis) (*n* = 3). Treatment names correspond to the given temperature (T, °C), light (L, µmol photons m^{-2} s^{-1}), and nutrient conditions for each treatment.

3.4.2. Experiment two: enhancing tetrasporogenesis

Tetrasporangia were formed only in 18 and 15 °C treatments exposed to 15 µmol photons m^{-2} s^{-1} and an 8 h L:16 h D photoperiod and first began to form on day 14 and 17 of the experiment, respectively. The number of tetraspores released per day (tetraspores day^{-1}) differed significantly among temperature treatments, but the effects were not consistent among photoperiod or light treatments (Table 3.2). Tetraspore release was 9-fold and 28-fold greater for 18 °C treatments compared to 15 °C treatments during day 14–20 and day 21–27 of the experiment, respectively (P = 0.007, Figure 3.5). Tetraspore release was higher during day 21–27 of the experiment for both temperature treatments, with an average of

541 ± 136 (18 °C) and 20 ± 7 (15 °C) tetraspores day^{-1} during day 21–27 compared to an average of 56 ± 34 (18 °C) and 6 ± 5 (15 °C) tetraspores day^{-1} during day 14–20, and there were generally large variations in tetraspore release occurring between replicates of the same treatment (Figure 3.5). Approximately 14% of the variation in tetraspore release was due to the interaction between light and photoperiod (L x L:D), as well as light and photoperiod as individual factors, whereas approximately 10% of the variation was due the remaining interactions (T x L, T x L:D, T x L x L:D) and temperature as an individual factor (Table 3.2). The germination rate of released tetraspores during day 20–14 and day 21–27 ranged between 94 ± 6–97 ± 3% for both treatments (Figure 3.6). No tetrasporangia were formed in treatments exposed to 5 µmol photons m^{-2} s^{-1} or a 12 h L:12 h D photoperiod.

Table 3.2 Results of permutational analysis of variance (PERMANOVA) testing the effect of temperature (T), light (L), and photoperiod (L:D) on tetraspore release (day^{-1}) (*n* = 5) 14–20 days and 21–27 days after initial exposure to different treatments (experiment two: enhancing tetrasporogenesis). F-statistics (F), the significance level (*P*) with significant effects in bold, and the eta-squared value (η^2, % of variance) as a measure of effect size are reported.

		Day 14–20			Day 21–27		
Source	*df*	*F*	*P*	η2	*F*	*P*	η2
T	1	**12.82**	**<0.001**	9.1	**29.65**	**<0.001**	11.7
L	1	**19.29**	**<0.001**	13.7	**34.25**	**<0.001**	13.5
L:D	1	**19.29**	**<0.001**	13.7	**34.25**	**<0.001**	13.5
T x L	1	**12.82**	**<0.001**	9.1	**29.65**	**<0.001**	11.7
T x L:D	1	**12.82**	**<0.001**	9.1	**29.65**	**<0.001**	11.7
L x L:D	1	**19.29**	**<0.001**	13.7	**34.25**	**<0.001**	13.5
T x L x L:D	1	**12.82**	**<0.001**	9.1	**29.65**	**<0.001**	11.7
Residuals	32						

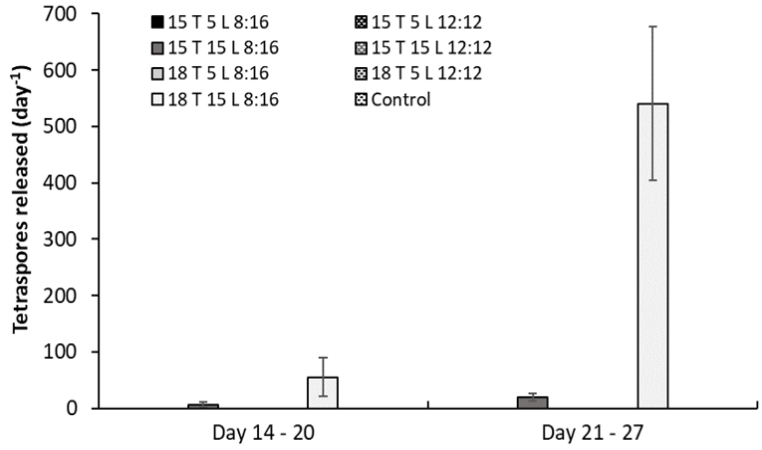

Figure 3.5 Mean (± SE) tetraspore release (day^{-1}) 14–20 days and 21–27 days after initial exposure to different treatments (experiment two: enhancing tetrasporogenesis) (*n* = 5). Treatment names correspond to the given temperature (T, °C), light (L, µmol photons m^{-2} s^{-1}), and photoperiod (L:D, h) conditions for each treatment. Pre-experimental culture conditions (18 T; 15 L; 12L: 12D) were used as a control.

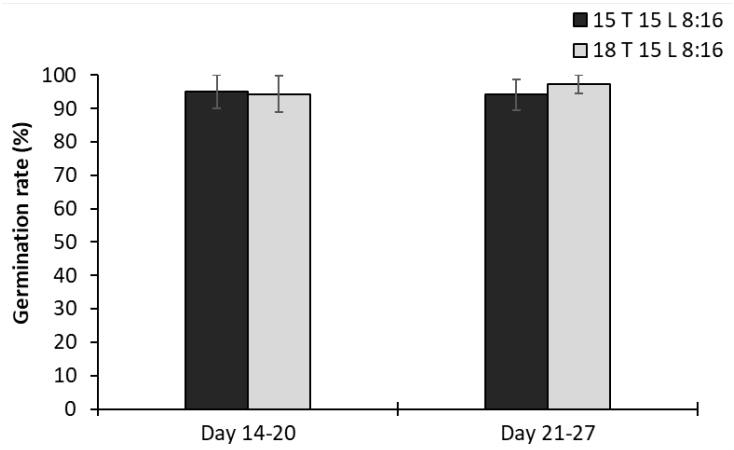

Figure 3.6 Mean (± SE) germination rate (%) of released tetraspores (i.e. tetraspores germinated within 24 h of release) 14–20 days and 21–27 days after initial exposure to different treatments (experiment two: enhancing tetrasporogenesis) (*n* = 5). Treatment names correspond to the given temperature (T, °C), light (L, µmol photons m^{-2} s^{-1}), and photoperiod (L:D, h) conditions for each treatment.

Tetrasporophyte filaments exposed to 18 °C, 15 µmol photons m^{-2} s^{-1}, and an 8 h L:16 h D photoperiod produced the highest number of released tetraspores during day 14–20 and day 21–27 while maintaining a germination rate of >90%; therefore, these filaments

were kept under the same treatment conditions for a further 25 days to continue assessing tetraspore release and germination rate. There were two peaks in tetraspore release under these conditions throughout the whole experimental period (Figure 3.7A). The peaks occurred from day 27–29 (peak one) and day 49–50 (peak two) and were similar in size, with averages of 859 ± 173 and 757 ± 128 tetraspores day^{-1} respectively, with large variations in tetraspore release occurring between replicates of the same treatment (Figure 3.7A). In contrast, the germination rate of released tetraspores was notably higher during peak one with an average of 92 ± 4% across peak one, compared to an average of 44 ± 8% across peak two, and was overall more consistent between samples of the same treatment (Figure 3.7B). Tetrasporangia continued to form at the end of the experiment (day 52).

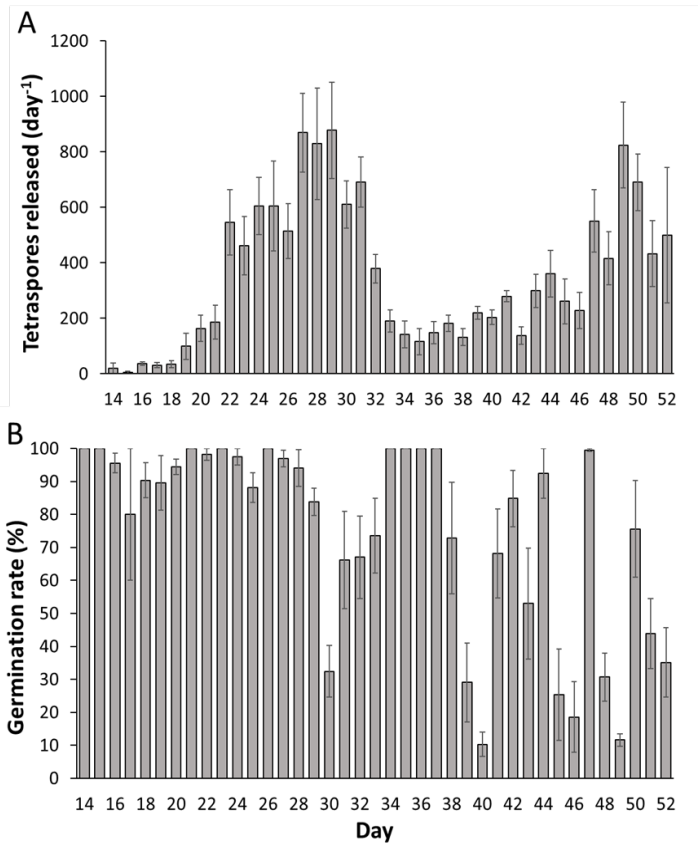

Figure 3.7 Mean (± SE) (A) tetraspore release (day^{-1} per dish) and (B) germination rate (%) of released tetraspores (i.e., tetraspores germinated within 24 h of release from 18 °C, 15 µmol photons m^{-2} s^{-1}, and 8 h L:16 h D treatments from the onset of tetraspore release (day 14) over a 52-day period (experiment two: enhancing tetrasporogenesis) (*n* = 5).

3.4.3. Experiment three: use of plant growth regulators

Tetrasporangia were not observed in the seaweeds treated with PGRs after 14 days. As observed previously in the enhancing tetrasporogenesis experiment, tetrasporangia were formed in the 18 °C, 15 µmol photons m^{-2} s^{-1}, and 8 h L:16 h D (control conditions with no PGRs added) treatment (3/3 replicates) after 14 days.

3.4.4. Experiment four: controlling repeated cycles of tetrasporogenesis

In pilot trials (*n* = 1), tetrasporangia were present in filaments exposed to inducing conditions (18 °C, 15 µmol photons m^{-2} s^{-1}, 12 h L:12 h D, and F/8) 14 days from the start of tetraspore formation. This was previously demonstrated to be peak tetraspore release before a decline was detected. Once transferred to non-inducing conditions (20 °C, 5 µmol photons m^{-2} s^{-1}, 15 h L:9 h D, and F/4), tetrasporogenesis ceased after 8 days.

In the replicated experiment (*n* = 5), tetrasporangia were present in filaments exposed to inducing conditions after 14 days from the start of tetraspore formation. After 12 days of exposure to non-inducing conditions, tetrasporangia were no longer present in filaments. After 14 days of exposure back to inducing conditions, tetrasporangia were present again in filaments. These results were consistent in all five replicates.

3.5. Discussion

In this study, we successfully induced tetrasporogenesis and the release and germination of tetraspores in domesticated *A. armata* tetrasporophyte that had been acclimated at 18 °C, ~15 µmol photos m^{-2} s^{-1}, and 12 h L:12 h D for 18 months prior to experimentation. Reproductive processes in seaweeds are typically controlled by one or

more environmental factors (Liu et al. 2017, de Bettignies et al. 2018) which can be manipulated to induce and optimise reproduction under controlled laboratory conditions for aquaculture purposes (Charrier et al. 2017). Previous studies assessing the effects of environmental factors on tetrasporogenesis in *A. armata* (Oza 1977, Guiry and Dawes 1992) were carried out from an ecological standpoint, rather than with the purpose of informing and developing farming techniques, and thus lack the detail necessary for applying these methods at the scale required for commercial aquaculture. This study presents a quantitative analysis of the effects of temperature, irradiance, nutrient concentration, and photoperiod on the induction of tetrasporogenesis in *A. armata* tetrasporophytes and provides a foundational method for obtaining a high and reliable supply of tetraspores that can be upscaled to facilitate commercial hatchery development. There were clear interactive effects of light and photoperiod on tetrasporogenesis, and manipulating temperature was key to optimising this process. Based on our findings, the proposed method for optimising the production of tetraspores and their germination into juvenile gametophytes to maximise the number of tetraspores for seeding onto ropes for mass-scale seaweed cultivation is to expose tetrasporophytes to 18 °C, 15 µmol photons m^{-2} s^{-1} and F/8 (3.5 mg N L^{-1}) under an 8 h L:16 h D photoperiod for up to 29 days.

Our findings demonstrate that a specific combination of temperature, irradiance, photoperiod, and nutrients is required to induce tetrasporogenesis in *A. armata*. A photoperiod of 8 h L:16 h D was critical for inducing tetrasporogenesis in our New Zealand strain of *A. armata*, but only at temperatures of 15 and 18 °C and a nutrient concentration of F/8 (3.5 mg N L^{-1}). This was similar to previous studies where tetrasporogenesis was only induced under short photoperiods in combination with relatively narrow temperature bands that differed between strains (Oza 1977, Lüning and Dieck 1989, Guiry and Dawes 1992)

(Table 3.3). The optimal conditions that induced tetrasporogenesis in our New Zealand strain, as well as several previously assessed strains (Oza 1977, Guiry and Dawes 1992), coincided with the spring/autumn temperature and natural winter photoperiod at the collection locations for these strains (Tables 3.3 and 3.4). These temperature and photoperiod conditions do not occur simultaneously during any season for the majority of assessed strains (Table 3.3). Furthermore, the inducing photoperiod identified in this study (8 h L:16 h D) does not naturally occur at the collection location of our strain (Table 3.4), suggesting that tetrasporogenesis was induced by stress induction through a significant reduction in photoperiod, rather than by replicating natural reproductive environmental conditions. Moreover, photoperiod was the only factor changed between the conditions that resulted in optimal tetraspore release in experiment two (enhancing tetrasporogenesis) and the maintenance conditions of the stock cultures (18 °C, ~15 µmol photos m^{-2} s^{-1}, 12 h L:12 h D) used to conduct the experiment. This conclusion is also supported by the fact that tetrasporogenesis is first induced in natural populations in March (austral autumn) when the ambient conditions are markedly different from those which induced tetrasporogenesis in this study (Tables 3.3 and 3.4) (Bonin and Hawkes 1987), although such high temperatures were not tested in the current study.

Table 3.3 Results of previous studies testing the effects of temperature and photoperiod on the induction of tetrasporogenesis in *A. armata* tetrasporophytes from different locations. Only successful conditions (i.e. those which resulted in the induction of tetrasporogenesis) are reported. Bracketed letters indicate the season at each location that correspond to the tested temperature and photoperiod conditions.

Author(s)	**Lineage/ Haplotype**[a]	**Strain location**	**Temperature (°C)**[b]	**Photoperiod (L:D)**[c]	**Notes**
Oza 1977	L1A	Brittany, France	15 (AU/SP)	8:16, 6:18 (WI)	Tetrasporogenesis induced under nutrient depletion (1.4 mg N L^{-1})
Guiry and Dawes 1992	L1A	Galway, Ireland	17 (SU)	8:16 (WI)	Tetrasporogenesis induced under nutrient levels >0.21 mg NO^3 L^{-1}
	L1A	Sicily, Italy	17, 19, 21 (AU/SP)	8:16, 9:15 (WI)	No effect of nutrient concentration
	Unknown	Victoria, Australia	13,15,17 (AU/SP)	8:16 (WI)	Low reproduction (<30% of individuals) across all treatments
Bonin and Hawkes 1987	L1B	Leigh, New Zealand	-	-	Culture conditions not described, but tetrasporogenesis reported under 'spring conditions'
Present study	L1B	Leigh, New Zealand	15, 18 (AU–SP)	8:16 (WI)	Tetrasporogenesis induced under increased nutrient levels (3.5 mg N L^{-1}), low reproduction at 15°C

[a]*Based on the mitochondrial cox*2-3 spacer marker *(Dijoux et al. 2014, Preuss et al. 2022)*
[b]*Mean sea surface temperature 2020 (Sea Temperature Info 2022)*
[c]*Mean photoperiod 2020 (Sunrise and sunset 2020, World Data Info 2022)*
SU = summer, AU = autumn, WI = winter, SP = spring

Season	Month	Temperature (°C)[a]	Photoperiod (L:D)[b]
Summer	December	19.1 (18.2–20.3)	14:10
Summer	January	20.1 (18.7–22.4)	14:10
Summer	February	21.9 (21.5–22.8)	13:11
Autumn	March	20.9 (20.0–22.0)	12:12
Autumn	April	19.4 (18.5–20.3)	11:13
Autumn	May	17.6 (16.9–18.7)	10:14
Winter	June	16.5 (15.8–17.0)	9:15
Winter	July	15.3 (14.8–15.8)	10:14
Winter	August	14.5 (14.1–14.9)	10:14
Spring	September	14.6 (14.4–15.0)	11:13
Spring	October	16.0 (14.6–17.8)	13:11
Spring	November	18.0 (17.5–18.5)	14:10

Table 3.4 Environmental conditions at Leigh, Auckland, New Zealand.

[a]*Mean and range sea surface temperature 2020 (Sea Temperature Info 2022)*
[b]*Mean photoperiod 2020 (Sunrise and sunset 2020)*

Tetrasporogenesis was optimal at 18 °C, with both tetraspore release and germination rate significantly higher than at 15 °C, whereas temperatures below 15 °C (11 and 13 °C) did not result in tetrasporogenesis, similar to previous studies (Oza 1977, Lüning and Dieck 1989, Guiry and Dawes 1992). While tetrasporogenesis occurred at 5 µmol photons m^{-2} s^{-1} during experiment one (induction of tetrasporogenesis), there was higher variability between replicates than at 15 µmol photons m^{-2} s^{-1} and tetrasporogenesis did not occur at all at 5 µmol photons m^{-2} s^{-1} during experiment two. Preliminary experiments with higher temperature and light conditions resulted in more bleached and fouled filaments. An irradiance of 15 µmol photons m^{-2} s^{-1} is therefore recommended as the minimum amount of light required for reliable induction. Nutrient depletion (~1.4 mg N L^{-1}) prevented tetrasporogenesis under all conditions tested during experiment one, which contrasts with a previous study reporting the induction of tetrasporogenesis under these same conditions for French strains of *A. armata* (Oza 1977) (Table 3.3). Conversely, nutrient concentration had no effect on the induction of tetrasporogenesis in Italian strains (Guiry and Dawes 1992)

(Table 3.3). Variation in the effects of environmental factors on tetrasporogenesis are expected across geographically isolated strains of seaweed due to the reproductive synchrony of seaweeds with their surrounding environment (Ims 1990, Rule et al. 2013). Moreover, such variation may also occur across geographically separated populations of the same strain, or between co-existing strains as a result of underlying genetic differences (Mata et al. 2017, Jansen et al. 2022). The samples used in the present study were most likely of the L1B lineage, which is part of one of the two lineages (L1B and L2B within two cryptic clades L1 and L2) of *A. armata* found within New Zealand (Preuss et al. 2022). L1B is widespread throughout New Zealand, whereas L2B is currently found only in the south of the North Island to Stewart Island, where it has been found to co-exist with L1B in several locations (Preuss et al. 2022). Future work could look to expose *A. armata* tetrasporophytes from co-occurring L1B and L2B strains, as well as different populations of the L1B strain, to the optimal conditions identified in this study to further understanding of the effects of genetic versus environmental factors on the induction of tetrasporogenesis in *A. armata*.

The method reported in the present study significantly reduced the time required for induction compared to previous studies where tetrasporangia were induced after 5–8 weeks of exposure to experimental conditions (Oza 1977, Guiry and Dawes 1992). This is of critical importance for the viability of seeding at scale, as nursery and hatchery periods typically contribute a substantial proportion of ongoing operational costs (Watson and Dring 2011, Werner and Dring 2011, Taelman et al. 2015). There is also further potential for cost reduction through accelerated and enhanced reproduction with the use of PGRs. For example, sorus formation of the kelp *Laminaria japonica* was accelerated by two weeks with the application of ABA (10 µM) (Nimura and Mizuta 2002), while carpospore release in the red seaweed *Pyropia yezoensis* was significantly enhanced with the application of the

ethylene precursor ACC (50 µM) (Uji et al. 2020). Contrary to these studies, there was no positive effect of PGRs on tetrasporogenesis in this study. One possible explanation for this was that one or more of these PGRs caused a shift in metabolism from reproduction to growth, as evinced by the suppression of sorus formation alongside increased growth in *L. japonica* with the addition of IAA (10 µM) (Kai et al. 2006). However, growth was not quantified here to enable further discussion in this regard. Little is known about the effects of PGRs specifically on tetrasporogenesis, with research concentrated on the effect of ethylene in *Pterocladiella capillecea* where exposure to ethylene (30 min) increased the number of tetrasporangial branches by nearly 200-fold compared to controls (García-Jiménez and Robaina 2012). Omics studies such as internal analyses of seaweed PGR contents from maintenance conditions through to a full reproductive cycle would facilitate the prospective application of PGRs for improving the efficiency of hatchery production.

Most cultivated seaweeds, including kelps and nori (*Porphyra* and *Pyropia*), undergo instant mass spore release where a high number of spores is immediately available for seeding at the onset of spore release (Redmond et al. 2014). Conversely, tetrasporogenesis in *A. armata* is a continuous process with variable sporulation in which there are evident peaks in tetraspore release. The method for seeding tetraspores will need to account for this. The methods reported here are suitable for obtaining a continuous high supply of tetraspores at the scale required for commercial hatchery development. Based on this study where ~10 mg FW of tetrasporophyte biomass was used per dish, an estimated >10 million tetraspores per 100 g FW of tetrasporophyte biomass could be obtained for seeding over a 15-day period from day 14 at the onset of tetrasporogenesis to day 29 at the end of the first peak. However, this method would result in juvenile gametophytes at slightly different stages of development, which may pose challenges if there are marked differences in the

requirements of early-stage hatchery conditions. Another option could be to carry out seeding only at day 27–29 during the first peak, resulting in an estimated 7.6–8.6 million tetraspores per 100 g FW of tetrasporophyte biomass. The second peak in tetraspore release (day 49–50) was lower in both the number and germination rate of released tetraspores, and there was higher variability between replicates compared to the first peak. For these reasons, it is not recommended for seeding to be carried out during the second peak.

For the first time, we showed that tetrasporogenesis can be ceased on demand by exposing tetrasporophytes to an extended photoperiod of 15 h L:9 h D, alongside a decrease in irradiance (5 µmol photons m^{-2} s^{-1}) and increase in temperature (20 °C) and nutrient concentration (7.0 mg N L^{-1}), and then induced again by placing the same tetrasporophytes back under inducing conditions. This would prove useful in situations where tetrasporophyte biomass is limited. The ability to maintain and re-use previously-induced broodstock would also increase management options and be beneficial for research purposes (Jeliani et al. 2018). Additionally, as the second peak in tetrasporogenesis is less reproductive, broodstock may need to recover after being induced for seeding to reduce the risk of contamination that arises from increased time under seeding conditions (Mooney-McAuley et al. 2016). Whether repeatedly inducing tetrasporogenesis in the same biomass affects reproductive output and/or germination rate would need to be addressed in future work to assess whether this is a viable approach. Nevertheless, this work serves as a baseline for the process of undertaking repeated cycles of induced tetrasporogenesis to obtain *A. armata* tetraspores for seeding.

3.6. Conclusion

This study is the first to fundamentally optimise tetrasporogenesis and provide the detail and framework necessary for enabling *A. armata* hatchery development. We provide a baseline method for inducing tetrasporogenesis in *A. armata* and demonstrate that this process can be controlled through the manipulation of specific environmental parameters. Tetrasporogenesis was induced after 14 days when tetrasporophytes were exposed to an 8 h L:16 h D photoperiod with an irradiance of 15 µmol photons m^{-2} s^{-1} and nutrients added at a concentration of 3.5 mg N L^{-1} (F/8). Increasing the temperature from 15 to 18 °C resulted in a mass increase in tetraspore release which peaked after a total of 27–29 days of exposure to inducing conditions. In contrast, exposing tetrasporophytes to 11 and 13 °C under an 8 h L:16 h D photoperiod with lower light intensities and nutrient concentrations did not result in the induction of tetrasporogenesis. We conclude that tetrasporogenesis was most likely induced through stress in the form of a significant reduction in photoperiod rather than as a result of replicating seasonal reproductive environmental conditions, and that temperature plays a key role in determining the reproductive output of *A. armata* tetrasporophytes. These findings will enable further research to optimise the methods for seeding released tetraspores onto ropes, as well as optimising early hatchery and nursery conditions to maximise the development of gametophytes for in-sea outplanting.

Chapter 4

Moderate temperature and water flow increase growth during the nursery phase of *Asparagopsis armata*

This chapter has been published in Algal Research as:

Mihaila, A. A., R. J. Lawton, C. R. K. Glasson, and M. Magnusson. 2024. Moderate temperature and water flow increase growth during the nursery phase of *Asparagopsis armata*. Algal Research 78:103380 (Appendix 12).

4.1. Abstract

The red seaweed Asparagopsis armata is a target species for commercial cultivation. However, to facilitate nursery production, optimal cultivation methods for the early life stages of this species need to be developed. Therefore, this study examined the interactive effects of temperature (15 °C, 18 °C and 21 °C), irradiance (15 and 30 µmol photons m^{-2} s^{-1}) and photoperiod (12 h L:12 h D and 8 h L:16 h D), and nutrient concentration (F/8 and F/4) and water flow (0.6 L min^{-1}) on the development and growth of juvenile gametophytes of *A. armata* across two controlled laboratory experiments. Temperature and water flow had the greatest effect on the length of gametophytes, which was highest at 18 °C and with water flow. Gametophytes developed rapidly and were consistently largest when exposed to a 12 h L:12 h D photoperiod and growth increased when individuals were maintained at 15 µmol photons m^{-2} s^{-1} compared to 30 µmol photons m^{-2} s^{-1} under a 12 h L:12 h D photoperiod. Nutrients did not limit growth at either concentration, although contamination increased with increasing nutrient concentration and irradiance. Water flow is highly recommended

during nursery cultivation of *A. armata* as this resulted in almost double the overall biomass productivity compared to static treatments. This work identifies critical parameters for enhancing development and growth during the early life stages of *A. armata* and provides fundamental information to facilitate system-specific upscaling and enable larger scale nursery production.

4.2. Introduction

Dietary inclusion of *Asparagopsis* (Bonnemaisoniaceae, Rhodophyta) species in ruminant feed is one of the most effective strategies for mitigating enteric methane emissions (Kelly 2020, Morais et al. 2020, Ungerfeld et al. 2022). Given the urgency to implement effective methane mitigation strategies (Gerber et al. 2013), there is a need to generate aquaculture production of these seaweeds at a commercial scale (Zhu et al. 2021, Beauchemin et al. 2022). However, reliable methods for mass cultivation of *Asparagopsis* still require further development for the early life stages (Mayberry et al. 2019, Vijn et al. 2020, Torres et al. 2021, Glasson et al. 2022, Wright et al. 2022). *Asparagopsis* has a triphasic life cycle alternating between a terete gametophyte (n), a microscopic carposporophyte (2n), and a filamentous tetrasporophyte (2n) stage (Bonin and Hawkes 1987). Cultivation of gametophytes by means of inducing the formation and release of tetraspores in tetrasporophytes, subsequent seeding of tetraspores onto lines, and maintenance of gametophyte seedlings under controlled environmental conditions in a nursery for later outplanting on marine farms (i.e., closed life cycle cultivation), is a viable approach for commercial production of red seaweeds (Oliveira et al. 2000, Wang et al. 2020). For *Asparagopsis*, key benefits of this method include the ability to obtain large

numbers of tetraspores for seeding throughout the year (Chapter 3/Mihaila et al. (2023a)), as well as enabling the selection of cultivars with desirable traits (Hwang et al. 2019), such as improved tolerance to environmental stressors (Yan et al. 2010) or high bromoform content, the primary anti-methanogenic compound in *Asparagopsis* (Levy et al. 1990, Paul et al. 2006, Machado et al. 2016a, Glasson et al. 2022).

The induction phase of closed life cycle cultivation involving the mass production and release of viable tetraspores can be achieved year-round by exposing domesticated tetrasporophytes of *A. armata* to 18 °C, 15 µmol photons m^{-2} s^{-1}, and 3.5 mg N L^{-1} under an 8 h L:16 h D (Light:Dark) photoperiod (Chapter 3/Mihaila et al. (2023a)). This method provides a reliable and consistent supply of tetraspores within two weeks (>10 million tetraspores per 100 g FW of tetrasporophyte biomass) for transfer to the nursery phase where germinated gametophyte seedlings are maintained until they are large and resilient enough for outplanting. The manipulation of environmental conditions to maximise the development and growth of gametophytes is essential for achieving successful nursery production of seaweeds and optimum conditions must be established for each target species (Oliveira et al. 2000, Matinfar et al. 2013, Jeliani et al. 2018, Roleda and Hurd 2019). Minimising the time required for gametophyte development is also important for decreasing the costs associated with nursery production, such as ongoing light, water, and nutrient requirements and personnel cost (Camus and Buschmann 2017, Boderskov et al. 2021a). To date, no studies have investigated the effect of environmental factors on the early life stages of *A. armata*, and this is an important research gap to close to enable the commercial production of this species through closed life cycle cultivation (Zhu et al. 2021).

Temperature, irradiance, and photoperiod are fundamental factors controlling growth during the early life stages of seaweeds and should therefore be considered in the

development and optimisation of *Asparagopsis* nursery production. *Asparagopsis armata* is found endemically throughout the Indo-Pacific region (Bonin and Hawkes 1987, Santelices 1989, Mihaila et al. 2023b) and invasively in the northern hemisphere (Guiry and Dawes 1992) and can be observed at depths ranging from 3–25 m (Zanolla et al. 2022), indicating the broad tolerance of this species to environmental conditions. However, natural gametophyte abundance is also highly seasonal with this life stage often only present during certain times throughout the year, such as from late winter to late spring in New Zealand (Bonin and Hawkes 1987, Mihaila et al. 2023b) and late spring to early summer in the Azores Islands (Neto 2000, Neto 2001). On northern New Zealand coasts, immature gametophytes of *A. armata* are present in late winter (Bonin and Hawkes 1987, Mihaila et al. 2023b) during short photoperiods (~10 h L:14 h D photoperiod) and at the lowest temperatures for the area (14–15 °C) (Sunrise and sunset 2020, Sea Temperature Info 2022). These observations suggest that lower temperatures and reduced photoperiod and irradiance will be optimal for nursery cultivation of this life stage.

Nutrient concentration is another key consideration for the development of *A. armata* nursery production (Oliveira et al. 2000, Hurd 2017). The addition of sufficient nutrients is essential for obtaining maximum growth rates under nursery conditions (Roleda and Hurd 2019). However, while higher nutrient concentrations are generally more favourable for growth (Morelissen et al. 2013), over supplementation can become inhibitory or cause high levels of fouling (Amsler and Neushul 1989). This is especially critical to avoid during the early stages of development when individuals are less resilient and more likely to be outcompeted by epiphytic organisms (Vadas et al. 1992, Kerrison et al. 2016). Water flow is also an important driver of seaweed production as it increases nutrient uptake and gas exchange by reducing the thickness of the diffusion boundary layer (Gerard 1982, Hurd

2017, Roleda and Hurd 2019). It is widely acknowledged that seaweed growth increases with water flow when this is applied at moderate levels (Gerard and Mann 1979, Hurd 2000, 2017). Nevertheless, the influence of water flow on the early development of gametophytes of *A. armata* remains unknown.

The present study therefore aimed to identify the optimal conditions for maximising the production of juvenile gametophytes during the nursery phase of *A. armata.* To do this we examined interactive effects of fundamental environmental factors on gametophyte development and growth across two fully crossed laboratory-based experiments, testing (1) the effects of temperature, irradiance, and photoperiod, and (2) the effects of nutrient concentration and water flow. The length and developmental stage of gametophytes was quantified after one, two, and three weeks of exposure to the conditions tested during each experiment. These results provide essential baseline information crucial for larger-scale and system-specific studies, thereby laying the foundation for establishing and optimising nursery production to support the development of *A. armata* aquaculture.

4.3. Materials and methods

4.3.1. Sample collection and induction of tetrasporogenesis

Tetraspores used in the experiments were obtained by inducing tetrasporogenesis in domesticated tetrasporophyte stock cultures as described in (Chapter 3/Mihaila et al. (2023a)). Briefly, tetrasporophytes were scaled up from released carpospores obtained from cystocarpic gametophytes collected by hand from Mathesons Bay, Leigh, New Zealand (36.31°S, 174.80°E) in August 2020. The tetrasporophyte stock cultures were maintained in a temperature and light controlled room (18 °C, ~15 µmol photons m^{-2} s^{-1}, 12 h light:12 h dark (L:D)) with nutrient enriched (3.5 mg nitrogen (N) L^{-1} and 0.3 mg phosphorus (P) L^{-1} (F/8), Varicon Aqua, Cell-Hi F2P) autoclaved filtered seawater (AFSW) that was changed weekly. To induce tetrasporogenesis, ten individual tetrasporophytes from the stock cultures were fragmented into 0.5–0.6 mm length filaments using a homogenizer (Omni, GLH 850) (de Nys et al. 2023). Ten subsamples of approximately 100 filaments per subsample were transferred into individual Petri dishes (90 x 20 mm, LabServ, LBS60016) filled to 50 mL with AFSW with nutrients added at a concentration of F/8. Dishes were placed in an environmental control cabinet (Panasonic, MLR-352) set at 18 °C and 15 µmol photons m^{-2} s^{-1} with a photoperiod of 8 h L: 16 h D (inducing conditions (Chapter 3/Mihaila et al. (2023a)). After 14 days, filaments were visually inspected using a stereomicroscope (Olympus SZX2-ILLTQ) to confirm the presence of tetrasporangia. Dishes were returned back to the cabinet and maintained under inducing conditions for a further seven days to allow for tetrasporogenesis and subsequent tetraspore release to increase (Chapter 3/Mihaila et al. (2023a)). Water changes were carried out weekly.

4.3.2. Experiment one: effect of temperature, irradiance, and photoperiod

To determine the effect of temperature, irradiance, and photoperiod on the development and growth of juvenile gametophytes, previously prepared reproductive tetrasporophyte filaments (Section 4.3.1) were combined and carefully transferred into a plastic tray lined with 60 pre-cleaned (Decon-90 and 10% hydrochloric acid (Kerrison et al. 2016)) microscope slides fully immersed in AFSW. Nutrients were added at a concentration of F/8 and the tray containing the slides and filaments was placed back under inducing conditions. After 36 h, the density of settled tetraspores on the slides was determined by counting the total number of settled tetraspores on each slide. The density was then adjusted to 20 (± 5) spores per slide if needed by gently removing individuals using a disposable pipette. This density was selected to minimise overlapping of gametophyte branches and allow space for accurate growth measurements over a three-week period. Seeded slides were placed into individual Petri dishes (90 x 20 mm) filled to 50 mL with nutrient enriched (F/8) AFSW and transferred into environmental control cabinets set at either 15 °C, 18 °C, or 21 °C with 15 µmol photons m^{-2} s^{-1} and photoperiods of 12 h L:12 h D or 8 h L:16 h D. Dishes were placed at the back and front of the culture cabinets opposite the light source where light measurements (LI-COR, LI-1500) confirmed average irradiances of 15 and 30 µmol photons m^{-2} s^{-1}, respectively. This resulted in 12 different treatment combinations (three temperatures, two photoperiods, two irradiances) in a fully factorial design (*n* = 5 for each treatment combination). Treatments were maintained under experimental conditions for three weeks and water changes were carried out weekly. Each week, the size (total length of all branches, Appendix 3) and stage of curled inward branch development (not-developed (ND), started to develop (SD), or well-developed (WD) curled inward branches, Figure 4.1) of ten randomly selected gametophytes per slide was

quantified using an inverted microscope (Olympus CKX53) and the Olympus CellSens Entry Software (ver. 2.3). In pilot experiments growth rapidly increased once gametophytes reached the stage of WD curled inward branches (Figure 4.1), therefore we chose this feature as a metric for gametophyte development.

Figure 4.1 Different stages of early juvenile gametophyte development: (A) two days post-germination, (B) curled inward branches not-developed (ND) (five days old), (C) curled inward branches started to develop (SD) (seven days old), and (D) curled inward branches well-developed (WD) (nine days old). Gametophytes were cultured at 18 °C, 15 µmol photons m^{-2} s^{-1} and 12 h L:12 h D with nutrients added at F/8. Scale bar (A)–(C) = 100 µm, (D) = 250 µm.

4.3.3. Experiment two: effect of nutrient concentration and water flow

To determine the effect of nutrient concentration (F/8 vs. F/4) and water flow (static vs. flow) on the development and growth of juvenile gametophytes, previously prepared reproductive tetrasporophyte filaments (Section 4.3.1) were combined and carefully transferred into a plastic tray lined with 20 pre-cleaned microscope slides well-immersed in nutrient enriched (F/8) AFSW. Slide seeding and spore density determination and adjustment proceeded as described in Section 4.3.2. For static treatments, half of the seeded slides were placed in the centre of individual 5 L pre-cleaned clear plastic containers (550 mm length (L) x 300 width (W) x 105 height (H)) filled to 3.5 L with AFSW with nutrients added at concentrations of either F/8 (3.5 mg N L^{-1} and 0.3 mg P L^{-1}) or F/4 (7.0 mg N L^{-1} and 0.6 mg P L^{-1}). For flow treatments, the remaining seeded slides were each placed into individual recirculating flow systems to create water current with a total volume of 3.5 L and nutrients added at either F/8 or F/4 (*n* = 5 for each treatment, Appendix 4). In each separate flow system, water was pumped (Aqua One Maxi Powerhead 102) through a pipe (280 mm L x 13 mm diameter (D)) fitted with a stop valve for controlling flow rate and dispersed through a fitted pipe (120 mm L x 5 mm D) that flowed directly into each individual 250 mL pre-cleaned clear plastic container (100 mm L x 65 mm W x 60 mm H). Single drainage holes (6 mm Ø) were drilled into the containers to maintain the water level at 130 mL. Drainage holes were fitted with pipes (280 mm L x 5 mm D) so that outflow water would drain into the sump (3.5 L per system) located underneath to ensure adequate flow-through exchange. The flow rate of each system was measured at 0.6 L min^{-1} (i.e., 4.6 volumes exchanged min^{-1} per treatment container). The static containers and recirculating flow systems were placed in environmental control cabinets set at 18 °C and 15 µmol photons m^{-2} s^{-1} with a photoperiod of 12 h L:12 h D (based on temperature, irradiance and photoperiod conditions

that led to the best development and growth in the previous experiment, Section 4.3.2). Treatments were maintained under experimental conditions for three weeks and water changes were carried out weekly. Each week, the size and stage of curled inward branch development (Figure 4.1) of ten randomly selected gametophytes per slide was quantified as described in Section 4.3.2. However, due to the presence of multiple determinate branches and overlapping of indeterminate branches in gametophytes observed during experiment one, the size measurement of gametophytes was changed to the combined total length of determinate branches only instead of the combined total length of all branches (Appendix 3). As no addition of CO_2 or aeration was included, pH was measured at 8am, 12pm, and 4pm for the last five days of the experiment to assess if photosynthesis driven changes in pH could lead to carbon limitation under the experimental conditions.

4.3.4. Statistical analyses

Three-factor permutational analysis of variance (PERMANOVA) was used to compare the effect of temperature, irradiance, and photoperiod (fixed factors) on the size (length, mm) of gametophytes and proportion (%) of gametophytes with WD curled inward branches after one, two, and three weeks (separate analyses) of exposure to experimental conditions. Two-factor PERMANOVA was used to compare the effect of nutrient concentration and water flow (fixed factors) on the size of gametophytes and proportion (%) of gametophytes with WD curled inward branches after one, two, and three weeks (separate analyses) of exposure to experimental conditions. Data for each week was analysed separately to identify the best treatment combination at each individual time point, rather than measuring differences over time. PERMANOVAs were run using Euclidean distance resemblance matrices, 9,999 unrestricted permutations of raw data, and Type III sum of squares (Anderson et al. 2008). Pair-wise *a posteriori* comparisons were carried out using PERMANVOA if a significant difference ($P \leq 0.05$) was detected. . Eta-squared (%) $\eta^2 = SS_{factor} / SS_{total} \times 100$; with SS_{factor} being the sum of squares of a particular factor and SS_{total} being the total sum of squares, was calculated to determine the proportion of the total variation in the size of gametophytes that was associated with each factor (temperature, irradiance, photoperiod, nutrient concentration, and water flow) (Richardson 2011). All statistical analyses were conducted using PRIMER ver.7 (Primer-E., UK). All data is reported as mean ± standard error (SE); $n = 5$.

4.4. Results

4.4.1. Experiment one: effect of temperature, irradiance, and photoperiod

The total branch length of gametophytes (combined total length of all branches, Appendix 3) ranged from 0.2 ± 0.0 to 0.6 ± 0.2 mm during week one, 1.5 ± 0.2 to 4.7 ± 0.7 mm during week two, and 3.7 ± 0.6 to 14.5 ± 2.1 mm during week three across all treatments (Figures 4.2A and 4.2B). The most important factor explaining the variability in the length of gametophytes during week one was photoperiod (Table 4.1) with the average length of gametophytes in the 12 h L:12 h D treatments (0.5 ± 0.1 mm) being almost double that of gametophytes in the 8 h L:16 h D treatments (0.3 ± 0.0 mm) across all temperatures and irradiances (P <0.001, Figures 4.2A and 4.2B). Temperature also had a significant effect during week one (Table 4.1) with gametophyte lengths approximately 50 and 14% larger in 18 °C treatments compared to 15 °C treatments when cultured under 12 h L:12 h D and 8 h L:16 h D photoperiods, respectively (P = 0.022, Figures 4.2A and 4.2B).

There was a significant interactive effect of temperature and photoperiod on the length of gametophytes during week two (Table 4.1). However, temperature explained almost 50% of the variability in the length of gametophytes during week two and was the strongest driver of variability, followed by photoperiod (Table 4.1). Notably, gametophyte lengths were approximately 90% larger in 18 °C treatments compared to 15 and 21 °C treatments only when cultured under a 12 h L:12 h D photoperiod (P <0.001, Figures 4.2A and 4.2B). Increasing the photoperiod from 8 h L:16 h D to 12 h L:12 h D in 18 °C treatments also resulted in a 2.3-fold increase in gametophyte lengths (P <0.001). There was no effect of irradiance on the length of gametophytes during week one or two.

There was a significant interactive effect between photoperiod, temperature, and irradiance on the length of gametophytes during week three (Table 4.1). The most important factor explaining the variability in the length of gametophytes during week three was temperature explaining nearly 60% of the variance, followed by photoperiod and the interaction between temperature and photoperiod (T x L:D) and temperature and irradiance (Te x Ir) (Table 4.1). Gametophyte lengths in 15 and 18 °C treatments were approximately double those in 21 °C treatments during week three across both photoperiods (P <0.001, Figures 4.2A and 4.2B). Longer day photoperiods also resulted in significantly larger and more variable lengths in 15 and 18 °C treatments (P <0.001), ranging from 8.9 ± 0.7 (15 °C) to 9.8 ± 1.6 mm (18 °C) (30 µmol photons m^{-2} s^{-1}) and 12.2 ± 1.0 (15 °C) to 14.5 ± 2.0 mm (18 °C) (15 µmol photons m^{-2} s^{-1}). Decreasing the irradiance from 30 µmol photons m^{-2} s^{-1} to 15 µmol photons m^{-2} s^{-1} increased gametophyte lengths by approximately 45% across all temperatures but only when cultured under a 12 h L:12 h D photoperiod (P <0.001, Figures 4.2A and 4.2B). There were also visually higher levels of contamination in 30 µmol photons m^{-2} s^{-1} treatments compared to 15 µmol photons m^{-2} s^{-1} treatments across all temperatures and 12 h L:12 h D photoperiods (Appendix 5).

Table 4.1 Results of permutational analysis of variance (PERMANOVA) testing the effect of temperature (Te), irradiance (Ir), and photoperiod (L:D) on the total branch length and proportion (%) of gametophytes with well-developed (WD) curled inward branches after one, two, and three weeks of cultivation under different treatments (experiment one). No analyses were run for proportions of gametophytes with WD branches for week three as all treatments had 100% WD branches. F-statistics (F), the significance level (*P*) with significant effects in bold, and the eta-squared value (η^2, % of variance) as a measure of effect size are reported, *n* = 5.

		Total branch length									**% with WD curled inward branches**					
		Week one			**Week two**			**Week three**			**Week one**			**Week two**		
Source	***df***	***F***	***P***	**η2**	***F***	***P***	**η2**	***F***	***P***	**η2**	***F***	***P***	**η2**	***F***	***P***	**η2**
Te	2	**4.10**	**0.022**	**16.87**	**35.02**	**<0.001**	**45.41**	**81.71**	**<0.001**	**58.65**	1.49	0.235	3.89	2.47	0.095	14.43
Ir	1	1.29	0.261	2.66	2.39	0.129	1.55	**12.81**	**<0.001**	**4.60**	3.05	0.087	4.00	**9.53**	**0.003**	**27.84**
L:D	1	**32.60**	**<0.001**	**67.13**	**54.96**	**<0.001**	**35.63**	**53.88**	**<0.001**	**19.34**	**60.61**	**<0.001**	**79.11**	**5.76**	**0.020**	**16.84**
Te x Ir	2	0.62	0.543	2.55	0.11	0.897	0.14	1.01	0.371	0.73	0.68	0.511	1.78	2.47	0.096	14.43
Te x L:D	2	1.78	0.180	7.33	**11.28**	**<0.001**	**14.62**	**11.01**	**<0.001**	**7.90**	2.25	0.117	5.87	0.82	0.445	9.15
Te x Ir x L:D	1	0.05	0.818	0.11	0.31	0.582	0.20	**19.92**	**<0.001**	**7.15**	0.45	0.505	0.59	**5.76**	**0.020**	**16.82**
Residuals	48															

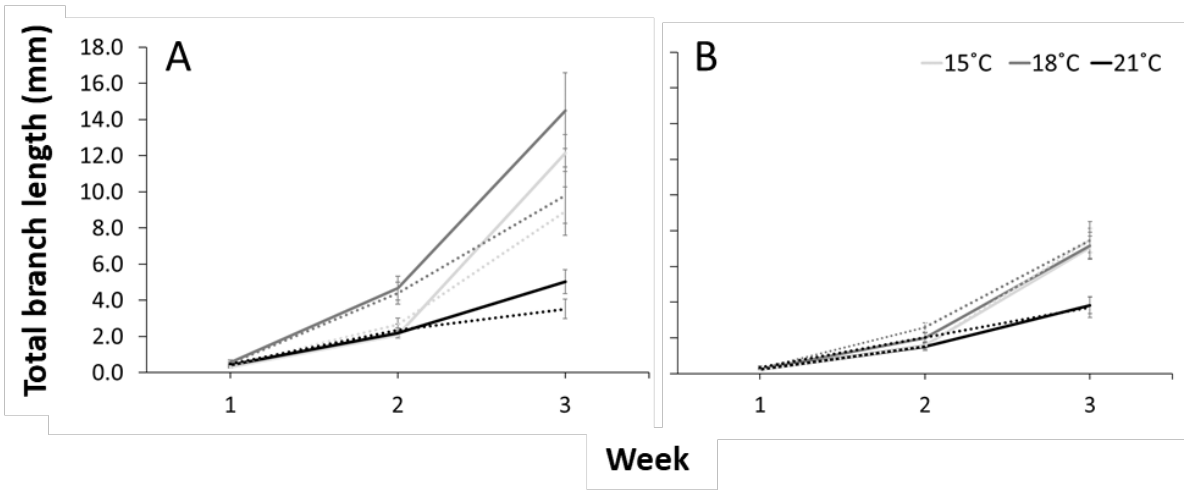

Figure 4.2 Mean (± SE) total branch length (mm) of juvenile gametophytes after one, two, and three weeks of cultivation under three temperature treatments, 15 (filled lines) or 30 µmol photons m^{-2} s^{-1} (dotted lines), and (A) 12 h L:12 h D and (B) 8 h L:16 h D photoperiods (*n* = 5) (experiment one).

The proportion of juvenile gametophytes with WD curled inward branches ranged from 8 ± 1 to 72 ± 2.4% during week one, 92 ± 1 to 100 ± 0% during week two, and by week three all juvenile gametophytes had WD curled inward branches across all treatments (Figures 4.3A and 4.3B). Photoperiod was the most important driver during week one explaining almost 90% of the variability (Table 4.1). Gametophytes were significantly less developed under shorter day photoperiods during week one with higher proportions of gametophytes with curled inward branches either not yet developed or starting to develop (Figures 4.3A and 4.3B). Correspondingly, the proportion of gametophytes with WD curled inward branches were on average 3.6-fold greater in 12 h L:12 h D treatments compared to 8 h L:16 h D treatments during week one (Table 4.1, Figures 4.4A and 4.4B). There was no significant effect of irradiance or temperature during week one, although the 18 °C treatments had the highest proportion of gametophytes with WD curled inward branches averaging at approximately 70% across both irradiances (12 h L:12 h D) (Figures 4.3A and 4.3B). There was a small yet significant interactive effect between photoperiod and irradiance during week two; however, irradiance was the most important driver explaining nearly 30% of the

variation (Table 4.1). Gametophytes were slightly less developed (<7% without WD curled inward branches) in shorter day photoperiod treatments but only when cultured at 15 µmol photons m^{-2} s^{-1} (Figures 4.3A and 4.3B). By week two, there were high proportions (>90%) of gametophytes with WD curled inward branches across all treatments.

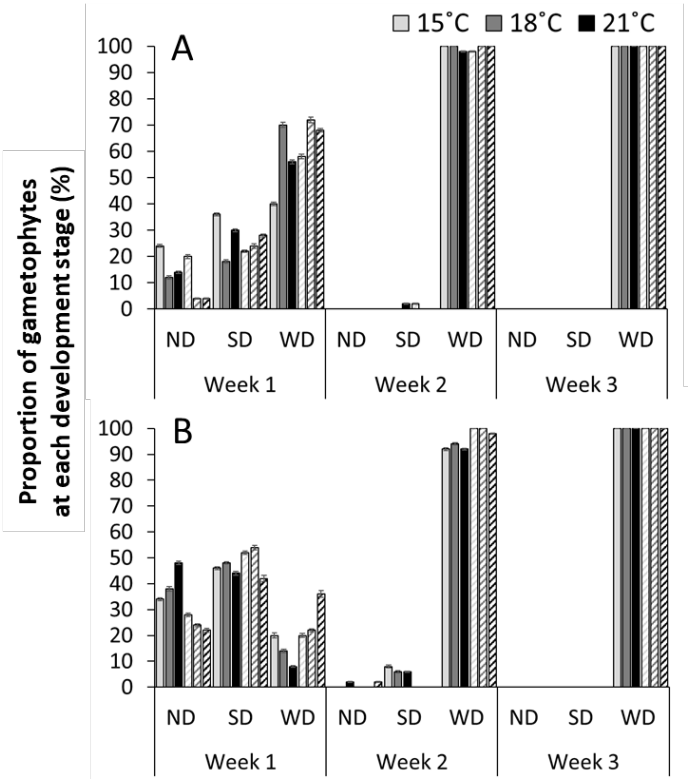

Figure 4.3 Mean (± SE) proportion (%) of juvenile gametophytes that had not-developed (ND), started-developing (SD), or well-developed (WD) curled inward branches after one, two, and three weeks of cultivation under three temperature treatments, 15 (filled bars) and 30 µmol photons m^{-2} s^{-1} (dashed bars, and (A) 12 h L:12 h D and (B) 8 h L:16 h D photoperiods (*n* = 5) (experiment one).

4.4.2. Experiment two: effect of nutrient concentration and water flow

The total branch length of juvenile gametophytes (combined total length of determinate branches only, Appendix 3) ranged from 0.2 ± 0.0 to 0.3 ± 0.0 mm during week one, 1.0 ± 0.1 to 1.5 ± 0.1 mm during week two, and 3.7 ± 0.5 to 6.5 ± 0.6 mm during week three across all treatments (Figure 4.4). There was a significant interactive effect of flow and nutrients on the length of gametophytes during week one and this interaction explained almost 90% of the variability (Table 4.2). During week one, gametophyte lengths in static

treatments were 23% larger than in flow treatments when cultured at F/8 (P = 0.035), whereas lengths were similar across static and flow treatments when cultured at F/4 (Figure 4.4). There was a marked effect of flow on the length of gametophytes during week two and three of the experiment, and flow explained almost 100% of the variation during both of these weeks (Table 4.2). Flow conditions resulted in a 1.5-fold and 1.8-fold increase in gametophyte lengths across both nutrient treatments during week two and three, respectively (P <0.001, Figure 4.4). There were also clear morphological differences between gametophytes cultured under static or flow conditions after three weeks: static-cultured gametophytes typically only comprised a single determinate branch, whereas flow-cultured gametophytes tended to comprise multiple (3–4) determinate branches. In contrast, nutrients had no effect on the length of gametophytes during week two or three. By the end of the experiment, both flow treatments (F/8 and F/4) had the largest gametophyte lengths averaging at 6.4 ± 0.4 mm (Figure 4.4). However, F/4 treatments had notably higher levels of contamination on the slides compared to F/8 treatments and this was observed under both static and flow conditions (Appendix 6), although this did not appear to affect the growth or condition of the algae.

Table 4.2 Results of permutational analysis of variance (PERMANOVA) testing the effect of nutrient concentration and water flow on the total branch length and proportion (%) of gametophytes with well-developed (WD) curled inward branches after one, two, and three weeks of cultivation under different treatments (experiment two). No analyses were run for proportions of gametophytes with WD curled inward branches for week two and three as all treatments had 100% WD branches. F-statistics (F), the significance level (*P*) with significant effects in bold, and the eta-squared value (η^2, % of variance) as a measure of effect size are reported, *n* = 5.

		Total branch length									**% with WD curled inward branches**		
		Week one			**Week two**			**Week three**			**Week one**		
Source	***df***	***F***	***P***	**η2**	***F***	***P***	**η2**	***F***	***P***	**η2**	***F***	***P***	**η2**
Nutrients	1	0.49	0.490	4.08	0.05	0.823	0.10	0.91	0.355	1.33	**4.92**	**0.041**	**23.53**
Flow	1	1.08	0.314	8.81	**52.49**	**<0.001**	**99.81**	**66.71**	**<0.001**	**98.29**	**4.92**	**0.041**	**23.53**
Nutrients x Flow	1	**10.64**	**0.005**	**87.11**	0.05	0.827	0.09	0.25	0.622	0.37	**11.10**	**0.004**	**52.94**
Residuals	16												

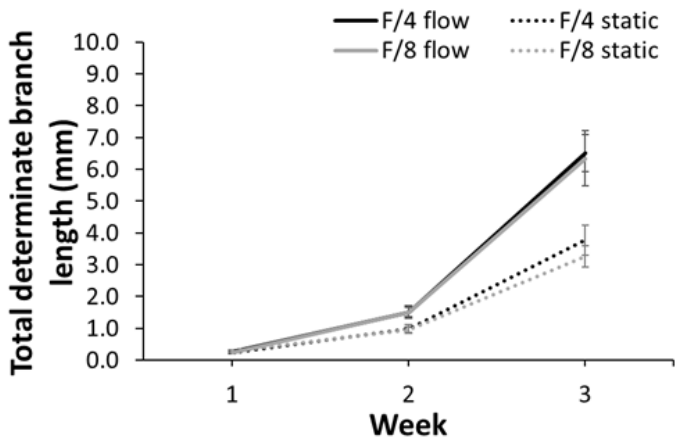

Figure 4.4 Mean (± SE) total determinate branch length (mm) of juvenile gametophytes after one, two, and three weeks of cultivation at high (F/4) and low (F/8) nutrient treatments under flow (filled lines) and static (dotted lines) conditions (*n* = 5) (experiment two).

The proportion of juvenile gametophytes with WD curled inward branches ranged from 42 ± 10 to 82 ± 5% during week one, and by week two all juvenile gametophytes had WD curled inward branches across all treatments (Figure 4.5). There was a significant interactive effect of flow and nutrients on the proportion of juvenile gametophytes with WD curled inward branches during week one and this explained approximately 50% of the variance (Table 4.2). Flow F/4, static F/4, and static F/8 treatments had almost double the proportion of juvenile gametophytes with WD curled inward branches (74–82%) compared to flow F/8 treatments (42%) (P = 0.006, Figure 4.5). Correspondingly, flow F/8 nutrient treatments had higher proportions of juvenile gametophytes with curled inward branches either not yet developed or just starting to develop compared all other treatments during week one (Figure 4.5).

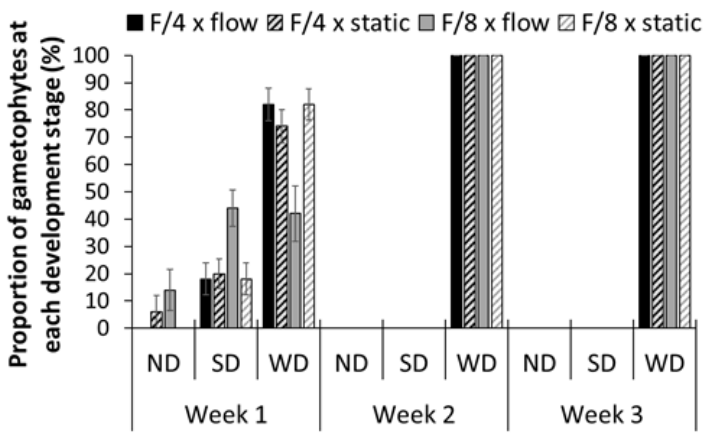

Figure 4.5 Mean (± SE) proportion (%) of juvenile gametophytes with not-developed (ND), started to develop (SD), and well-developed (WD) curled inward branches after one, two, and three weeks of cultivation at high (F/4) and low (F/8) nutrient treatments under flow (filled bars) and static (dashed bars) conditions (*n* = 5) (experiment two).

The pH steadily increased during the last five days of week three (day 17–21) across all treatments (Figure 4.6). The pH was generally higher in flow treatments compared to static treatments. However, by the end of the experiment, flow F/8, flow F/4, and static F/4 treatments all had a similar pH near 8.3. The pH was consistently lowest in static F/8 treatments and was on average 0.2 units lower compared to the other treatments during the last five days.

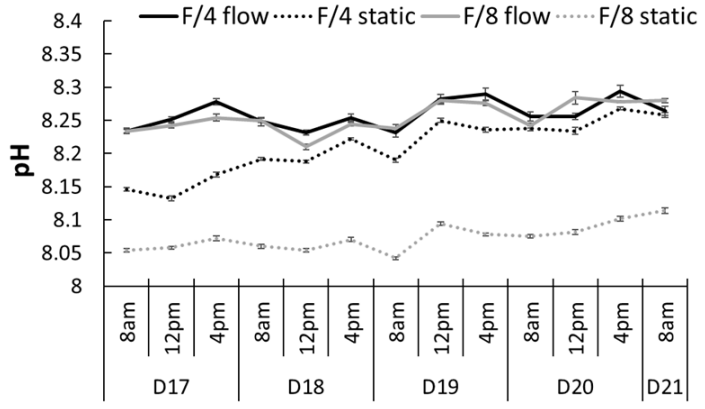

Figure 4.6 pH measurements taken at different time points from F/4 and F/8 nutrient treatments under flow (filled lines) and static (dotted lines) conditions (*n* = 5) during the last five days (day 17–21) of experiment two. No pH data is available for 12pm or 4pm on day 21 as the experiment ended and length and development measurements were carried out on this day.

4.5. Discussion

This study is the first to provide a foundation for understanding the effects of fundamental environmental factors on the development and growth of the early life stages of *A. armata* and identifies conditions for maximising the production of gametophytes during the nursery phase. During experiment one, temperature, photoperiod, and irradiance separately and interactively affected the development and growth of juvenile gametophytes. Photoperiod had the greatest effect on growth during the initial stages of early development (week one), whereas temperature was the strongest driver of growth during the later stages of early development (week two and three). Gametophytes developed rapidly and were consistently largest when cultured at 18 °C under a 12 h L:12 h D photoperiod, with this combination of conditions resulting in over double the length of gametophytes compared to all 8 h L:16 h D treatments during week two and three. Gametophytes also grew well at 15 °C under a 12 h L:12 h D photoperiod, but lengths were 10–20% shorter throughout the experiment compared to 18 °C under the same photoperiod. Seaweed growth typically increases with increasing temperature up to a certain limit depending on the thermal tolerance of the species (Eggert 2012, Singh and Singh 2015). During week one and two, gametophyte lengths in 21 °C treatments were within the range of those in the remaining temperature treatments. However, by week three, both development and growth were greatly reduced in gametophytes cultured at 21 °C across all treatment combinations. These laboratory results are consistent with an in situ phenological study in New Zealand demonstrating possible negative effects of prolonged heat stress (≥21 °C) on survival and reproduction in mature gametophytes (Chapter 2/Mihaila et al. (2023b)). Together, these studies strongly support an upper thermal tolerance of 21 °C in this population of *A. armata*. The average sea surface temperature

along the northeast coast of the North Island (the collection region) repeatedly exceeded 21 °C during austral summer–autumn in 2022 (Sea Temperature Info 2022), with projections indicating general increases in sea surface temperature and marine heatwave occurrence (Oliver et al. 2018). It is therefore recommended that spore induction and subsequent seeding for *A. armata* in this region (Chapter 3/Mihaila et al. (2023a)) are carried out earlier in the year to enable outplanting during austral winter–spring, thereby maximising growth and reducing the risk of in-ocean gametophyte farming in a warming ocean.

Juvenile gametophytes exhibited the highest growth when cultured under the 12 h L:12 h D photoperiod in the current study. This is slightly higher than the ambient photoperiod when juvenile gametophytes are present at the collection site of our strain (10 h L:14 h D–11 h L: 13 h D) (Bonin and Hawkes 1987, Mihaila et al. 2023b). Moreover, the best performing temperature (18 °C) was also above the ambient sea temperature when juvenile gametophytes are present at the collection site (14–15 °C) (Bonin and Hawkes 1987, Mihaila et al. 2023b). Released tetraspores in this study were obtained from tetrasporophytes that had been maintained under 18 °C and 12 h L:12 h D for 18 months, and therefore may have acclimated to optimal growth under these conditions. This result infers that optimal conditions for growth of juvenile gametophytes may correspond to the long-term cultivation conditions of the parental tetrasporophytes. This outcome is worth investigating further since it would make it possible to pre-determine the optimum temperature of gametophytes to correspond with the ambient temperature expected during outplanting, which may improve survival and growth after outplanting. Nevertheless, based on the present findings using laboratory-induced tetraspores from our domesticated tetrasporophyte cultures, 18 °C and 12 h L:12 h D are recommended as the optimal temperature and photoperiod for maximising nursery production of *A. armata*. However,

we acknowledge that optimal temperatures may differ in other strains of *A. armata* depending on the previous environmental history of tetrasporophytes used for nursery production (Hurd et al. 2014). In future, it would be useful to investigate whether nursery-raised gametophytes can be thermally primed by raising the maintenance temperature of tetrasporophyte stock cultures as this would extend the production season and help to future-proof the aquaculture industry against climate change (Wang et al. 2017, Quigley 2018, Jueterbock et al. 2021).

Gametophytes in natural populations of *A. armata* in New Zealand are highly seasonal and have relatively narrow temperature and photoperiod windows corresponding to spring conditions (Bonin and Hawkes 1987, Mihaila et al. 2023b). In terms of irradiance, however, gametophytes exhibit a broad tolerance in nature and are observed at various depths ranging from the upper subtidal to 25 m deep (Shears and Babcock 2007, Zanolla et al. 2022). Therefore, it follows that irradiance was a less significant driver of development and growth during the early life stages of *A. armata* compared to temperature and photoperiod in this study. Nonetheless, irradiance is still an important consideration for nursery development, exerting a significant interactive effect with temperature and photoperiod in the later stages of early development. By week three, gametophytes in lower irradiance treatments (15 µmol photons m^{-2} s^{-1}) were on average 30% larger than those in higher irradiance treatments (30 µmol photons m^{-2} s^{-1}) when cultured at 15 and 18 °C under the optimal photoperiod (12 h L:12 h D). The irradiance favoured by *A. armata* was lower than the recommended irradiances for the early life stages of the red seaweeds *Gracilaria* (20–40 µmol photons m^{-2} s^{-1}) (Redmond et al. 2014) and *Porphyra* (25–50 photons m^{-2} s^{-1}) (Sahoo and Yarish 2005). These differences could have been caused by differing light attenuation, given that the recommendations for *Gracilaria* and *Porphyra* were based on

large-scale nursery production in tanks (Sahoo and Yarish 2005, Redmond et al. 2014), whereas experiment one was conducted in petri dishes. The specific light requirements for the early life stages of gametophytes will ultimately depend on the scale of cultures, but importantly, based on our results, the optimal irradiance for larger-scale cultures of *A. armata* is likely to be at the lower end of the spectrum of what is recommended for other red seaweeds.

Contamination levels need to be considered to ensure successful nursery production as the early life stages of seaweeds are more vulnerable to being outcompeted by fouling organisms (Lüning and Pang 2003, Kim et al. 2017), which would lead to ineffective nursery production. After three weeks in culture, we observed visibly higher levels of contamination in high irradiance treatments compared to low irradiance treatments. Moreover, we have previously observed discoloration of juvenile gametophytes and high levels of contamination under higher irradiances (30–40 µmol photons m^{-2} s^{-1}) during trials conducted in aerated rope-seeded cultures and larger tank-based systems (A. Mihaila, Unpublished results, 2022). Increased contamination under higher irradiances has also been reported in nursery optimisation studies for kelps, including *Saccharina japonica* (Su et al. 2017), *Ecklonia radiata* and *Macrocystis pyrifera* (Visch et al. 2023). Collectively, these findings strongly support culturing the early life stages of *A. armata* at lower irradiances of or near 15 µmol photons m^{-2} s^{-1}, depending on the scale of the cultures, to help reduce contamination levels.

Growth of gametophytes markedly improved under flow conditions during experiment two which is consistent with reported findings for kelps (Camus and Buschmann 2017) and other commercially important red seaweeds, including *Gracilaria* (DeBusk and Ryther 1984, Gonen et al. 1993) and *Kappaphycus* spp. (Glenn and Doty 1992). This was

excepted as water flow is known to improve nutrient uptake through its minimising effect on the diffusion boundary layer where nutrients are exchanged (Hurd 2000, 2017). Gametophytes also developed rapidly across all flow treatments with the exception of relatively slower initial development in flow F/8 treatments during week one, although this did not significantly impact growth later in the experiment. The benefit of water flow only became evident during the second week of culture, suggesting that water flow during the first week of culture may not be necessary for obtaining optimal gametophyte lengths by the end of the nursery period. This possibility is worth investigating as it could lead to a reduction in the use of water flow which in turn would lower the overall cost of nursery production (Redmond et al. 2014, Camus and Buschmann 2017). Moderate flow rates are generally considered optimal for seaweed growth since these promote the breakdown of diffusion boundary layers compared to low flow rates (Hurd 2000, Peteiro and Freire 2011, Hurd et al. 2014), whereas high flow rates can have less or no positive effect on seaweed growth and begin to cause stress rather than promote growth (Gerard and Mann 1979, Peteiro and Freire 2011, Kregting et al. 2016, Roleda and Hurd 2019). For example, the growth rate of *Undaria pinnatifida* seedlings increased with increasing water velocity up to 16.1 cm s^{-1}, beyond which the growth rate declined (Peteiro et al. 2019). Optimal water flow for seaweed growth is species-specific and may also vary between individual systems (e.g., small- and large-scale systems) and with stocking density (Hurd 2000, Stewart and Carpenter 2003, Caines et al. 2014). Therefore, the effect of water flow will need to be further examined for *A. armata.* Our findings, based on a flow rate of 0.6 L min^{-1}, provide a standard against which results from future water flow optimisation studies for *A. armata* can be compared.

Nutrient concentration and water flow often interactively affect seaweed productivity due to the regulating effect of water flow on nutrient uptake (Hurd 2017, Roleda and Hurd 2019). However, gametophytes in high and low nutrient treatments had similar lengths throughout the experiment regardless of whether these were cultured under flow or static conditions. This implies that nutrient concentrations were not limiting in this study, although how this result translates to a larger-scale nursery setting would be determined by the stocking density. Similar to higher irradiances, increases in nutrient concentration can promote the growth of undesirable epiphytes during the nursery phase and this should be avoided or kept to a minimum (Harrison and Hurd 2001, Behera et al. 2022). By week three, both static and flow F/4 treatments had notable levels of contamination on the slides; however, this did not seem to impact the growth of gametophytes. While we undertook significant preventative measures and used clean tetrasporophyte stock cultures during seeding to prevent the development of epiphytic contaminants, we cannot rule out the possibility of fouling originating from when the slides were initially seeded. Higher pH measurements in static F/4 treatments compared to static F/8 treatments may also be partly explained by differences in the level of contamination (i.e., the fouling community was phototrophic rather than heterotrophic). Nutrient concentrations should therefore be limited due to their high cost and the risk of increased fouling, which could impact gametophyte growth at later stages of development after outplanting.

It is important to highlight that while gametophytes cultured under flow and static conditions were similar with respect to the length of the longest branch after three weeks (3.5–4 mm), overall biomass production in flow treatments was well above that in static treatments. This was because static-cultured gametophytes consisted of one or two

determinate branches whereas flow-cultured gametophytes consisted of several determinate branches (Figure S4), and thus were almost twice the combined total branch length of static-cultured gametophytes. The pH during the last five days in culture was also higher in flow treatments due to more biomass photosynthesising. Utilising a flow system can nearly double the biomass production per gametophyte, potentially halving the required nursery time. This could double the number of outplantings within the same timeframe or achieve the same nursery output at half the cost of human resources. Even though gametophytes (with respect to the length of the longest branch) reached outplanting size after two weeks based on the recommended outplanting size of kelps seeded from spores (1–2 mm after 1–2 months) (Redmond et al. 2014, Forbord et al. 2020) and nori (2–3 mm after two months) (Sahoo and Yarish 2005, Redmond et al. 2014), we propose conducting outplanting after three weeks in the nursery when gametophytes have higher biomass and thus increased resistance to grazing and fouling. That being said, outplanting may also be feasible after a two-week nursery period taking into account that flow-cultured gametophytes were already significantly branched and had reached a total determinate branch length of 1.5 mm after two weeks. Importantly, these nursery periods would need to be confirmed with marine farm experiments.

4.6. Conclusion

This study demonstrates that temperature and water flow are critical drivers for successful nursery production of *A. armata*, with the best development and growth of juvenile gametophytes occurring at 18 °C with water flow (0.6 min L^{-1}). A 12 h L:12 h D photoperiod was also identified as important for maximising nursery production, having

improved growth and development compared to an 8 h L:16 h D photoperiod. In addition, our results demonstrate that irradiance and nutrient concentration should be kept at the lower end of the spectrum during the nursery phase of *A. armata* to maximise growth while minimising contamination. Optimal irradiance and nutrient dosing will require system-specific upscaling and should be established according to the nursery setup, starting at low levels. Adaptations of the recommendations provided here will be needed on a case-by-case basis for large-scale systems typical of commercial situations. Our findings provide a fundamental knowledge base for establishing and optimising nursery production to facilitate the development of *A. armata* aquaculture.

Chapter 5

Metabolomic and transcriptomic changes during tetrasporogenesis induction of the red seaweed *Asparagopsis armata*

This chapter is to be submitted for publication in Frontiers of Marine Science as:

Mihaila, A. A., C. R. K. Glasson, R. J. Lawton R. Huerlimann, and M. Magnusson. 2024. Metabolomic and transcriptomic changes during tetrasporogenesis induction of the red seaweed *Asparagopsis armata*.

5.1. Abstract

The red seaweed *Asparagopsis armata*, known for its ability to reduce methane emissions from enteric fermentation when incorporated as a ruminant feed additive, is a key target for aquaculture development. However, despite advancements in this field, there remains a critical gap in understanding the internal mechanisms governing reproduction in *A. armata*, as well as seaweeds in general. In this study, we examined metabolomic and transcriptomic changes throughout the induction of tetrasporogenesis in *A. armata*, utilising both targeted and untargeted approaches. Key findings included the accumulation of several metabolites, notably the eicosanoid precursor arachidonic acid, and high upregulation of genes associated with polyamine metabolism, particularly the candidate ornithine decarboxylase (ODC) gene previously linked to seaweed reproduction, during the lead up to tetrasporogenesis. Pathways related to environmental signalling, carbon metabolism, and steroid hormone production also showed significant enrichment

throughout the induction of tetrasporogenesis, although a significant portion of the genes involved in these pathways have unknown function. These findings collectively offer a detailed overview of the processes underlying tetrasporogenesis in *A. armata*, facilitating further targeted investigations into the internal regulation of seaweed reproductive biology.

5.2. Introduction

Red seaweeds have complex triphasic reproductive cycles that are controlled by a combination of environmental and endogenous (molecular and biochemical) factors (Lüning and Dieck 1989, de Bettignies et al. 2018). Extensive research has investigated the environmental triggers for reproduction, with temperature, light intensity, or their combination often implicated in inducing reproductive transitions in red seaweeds (Lüning 1981, Guiry 1984, Liu et al. 2017, de Bettignies et al. 2018). In contrast, the molecular and biochemical mechanisms underlying life cycle control remain largely unexplored for most seaweeds, resulting in limited understanding of these internal processes (García-Jiménez and Robaina 2015, Liu et al. 2017). In terrestrial plants, research elucidating the internal regulators of reproduction has aided in understanding species level responses to climate-change induced stressors and enabling crop breeders to manipulate targeted reproductive traits for improved crop production (Davies 2004, Dwivedi et al. 2008, Iqbal et al. 2017, Yang et al. 2021). A deeper understanding of the endogenous controls of life cycle transitions in seaweeds, including the associated biochemical pathways and important genes, may deliver similar benefits for overcoming reproduction-associated barriers in aquaculture and managing the effects of climate change on these ecologically and commercially important organisms.

The integration of metabolomic analysis with transcriptomic and/or proteomic data is a powerful tool for deciphering the genes and intricate metabolic pathways regulating primary metabolic processes, including reproduction (Gupta et al. 2014, Tanna and Mishra 2018). For instance, a comparative transcriptomic investigation of wild non-reproductive and wild reproductive tetrasporophytes of the red seaweed *Asparagopsis taxiformis* identified 44 putative reproduction-associated genes, encoding proteins with enzymatic, structural, and transport functions (Patwary 2023). Moreover, transcriptomic analyses of the red seaweed *Grateloupia imbricata* during cystocarp development identified the upregulation of the ornithine decarboxylase (ODC) gene, which is involved in polyamine biosynthesis (Garcia-Jimenez et al. 2017). Several genes associated with the metabolism of jasmonate and ethylene were also identified during cystocarp development (Garcia-Jimenez et al. 2018). Omics investigations have highlighted the significance of plant growth regulators (PGRs) in seaweed reproduction (Stirk and Van Staden 2014, Garcia-Jimenez and Robaina 2017, Uji and Mizuta 2022). Notably, several PGRs, such as 1-aminocyclopropane-1-carboxylic acid (ACC) (Uji et al. 2020), ethylene (García-Jiménez and Robaina 2012) and methyl jasmonate (MeJa) (Pilar et al. 2016), have been linked to reproduction in red seaweeds. In certain cases, the exogenous application of PGRs significantly improved reproductive output and/or reduced maturation periods of reproductive structures (Stirk and Van Staden 2014, Pilar et al. 2016, Liu et al. 2017, Uji et al. 2020). However, there is limited understanding regarding the role of PGRs in controlling reproduction in seaweeds, and the physiological processes relating these PGRs to reproduction remain elusive (Stirk and Van Staden 2014, García-Jiménez and Robaina 2015, Liu et al. 2017). Advancing our understanding of this is likely to have benefits for aquaculture, given the noted improvements in reproductive processes.

The red seaweeds *Asparagopsis taxiformis* and *A. armata* (order Bonnemaisoniales) have gained scientific and commercial interest due to their capacity to effectively mitigate enteric methane emissions from ruminant livestock when included at low levels in their feed (Kinley et al. 2020, Roque et al. 2021, Ridoutt et al. 2022). Consequently, these species have emerged as targets for aquaculture (Duarte et al. 2017, Hunter 2022, Zanolla et al. 2022). Commercial seaweed aquaculture requires a high degree of control over both the environmental conditions and endogenous factors regulating reproductive transitions (García-Jiménez and Robaina 2015, Charrier et al. 2017). Previous studies have documented the induction of tetrasporogenesis in *A. armata* under an 8 h Light:16 h Dark (L:D) photoperiod (Oza 1977, Lüning and Dieck 1989, Guiry and Dawes 1992, Mihaila et al. 2023a). Recent work also showed that the transition to tetrasporogenesis can be vastly improved by exposure to 18 °C for 14 days, 15 µmol photons m^{-2} s^{-1}, and 3.5 mg nitrogen (N) L^{-1} and 0.3 mg phosphorus (P) L^{-1} (F/8) (Chapter 3/Mihaila et al. (2023a)). However, unlike these environmental factors used for optimal reproductive output, the biochemical and molecular factors underpinning reproductive processes in *A. armata* have not yet been examined.

The ability to effectively induce tetrasporogenesis in cultured *A. armata* provides an excellent opportunity to analyse the biochemical and molecular mechanisms involved in the onset of tetrasporogenesis and improve our understanding of this fundamental process. Therefore, in the present study, we examined metabolomic and transcriptomic dynamics in *A. armata* at different time points during tetrasporogenesis following induction under the aforementioned conditions. We combined targeted and untargeted metabolomic profiling with differential gene expression analysis to identify changes in PGR production, related

metabolites, and gene expression. These findings represent a first exploration into the biochemical pathways and genes involved in tetrasporogenesis of *A. armata*.

5.3. Materials and methods

5.3.1. Seaweed collection and cultivation

Tetrasporophyte cultures of *A. armata* were established from wild collected cystocarpic individuals and have been maintained at the University of Waikato Coastal Marine Field Station, New Zealand, since September 2022. Sample transport and preparation, including carpospore release and upscaling were carried out as described previously (Chapter 3/Mihaila et al. (2023a)). Tetrasporophytes were maintained in autoclaved filtered seawater (AFSW) with gentle aeration under the following conditions: temperature, 18 °C; irradiance, ~15 µmol photons m^{-2} s^{-1}; photoperiod, 12 h D:12 h D (L:D); and nutrients, 3.5 mg N L^{-1} and 0.3 mg P L^{-1} (F/8) (Varicon Aqua, Cell-Hi F2P). The medium was changed weekly.

5.3.2. Experimental setup and sample collection

Ten individual tetrasporophytes were transferred from the tetrasporophyte stock cultures into separate 50 mL conical centrifuge tubes containing 25 mL of AFSW. To obtain a homogenous mass of filaments, samples were fragmented for 30 sec at 10,000 rpm using a laboratory homogeniser equipped with a 10 x 115 mm generator probe with a sawtooth tip (Omni GLH 850). This approach has previously been shown to enhance the rate of tetrasporogenesis (de Nys et al. 2023). The resulting samples (approximately 0.5 mm length

fragments, 200 mg fresh weight (FW) per replicate) were then transferred into individual 2 L plastic cylinder containers containing 1.8 L of AFSW with nutrients added at F/8. Samples were placed in environmental control cabinets (Panasonic, MLR-352) set at 18 °C and 15 µmol photons m^{-2} s^{-1} with a photoperiod of 12 h L:12 h D, replicating the original maintenance conditions. All samples were subject to a seven-day acclimation period under maintenance conditions to facilitate recovery from the stress induced by the fragmentation process. This allowed filaments to return to a stable physiological state before starting the experiment. After seven days, the biomass from each container was strained through a cell strainer (100 µm, Fisherbrand™), secured into a 50 mL conical centrifuge tube, and centrifuged for 2 min at 685 *g* to remove excess water. Individual subsamples for Gas Chromatography Mass Spectrometry (GC-MS) (50 mg) and RNA-sequencing (RNA-seq) (50 mg) analyses were then collected from each replicate, denoted as 'day 0' samples (*n* = 10). Additionally, extra subsamples for each analysis were collected directly from the stock cultures (i.e., non-fragmented), denoted as 'baseline samples' (*n* = 5). Each container was then restocked with 150 mg (FW) of the spun biomass and filled with 1.8 L of fresh nutrient enriched (F/8) AFSW. Samples were then placed under experimental conditions as described below.

The experimental design comprised of two treatments: control (*n* = 5) and induction (*n* = 5), as per Chapter 3/Mihaila et al. (2023a). Control treatments were maintained under original maintenance conditions, while induction treatments were transferred to a separate environmental control cabinet set at 18 °C and 15 µmol photons m^{-2} s^{-1} with a photoperiod of 8 h L:16 h D to induce tetrasporogenesis (Chapter 3/Mihaila et al. (2023a)). Tetrasporogenesis initiates after 14 days of exposure to inducing conditions, followed by a subsequent increase in the frequency of tetraspore production and release continuing until

day 29 (Chapter 3/Mihaila et al. (2023a)). Therefore, both control and induction cultures were maintained under their respective conditions for a period of 21 days. This duration allowed for the analysis of changes in metabolite levels and gene expression leading up to and during tetrasporogenesis. Every seven days, nutrient medium in each container was replaced by centrifuging replicates through a strainer as described above, and subsamples for GC-MS and RNA-seq analysis were collected (prior to restocking into new nutrient medium). A total of five timepoints were sampled: baseline, day 0, day 7, day 14, and day 21. GC-MS samples were analysed immediately after collection, while RNA-seq samples were snap-frozen in liquid nitrogen and stored at -80 °C until analysis. Regular checks were conducted on subsamples from each culture (approximately 50 filaments per replicate) using a stereomicroscope (Olympus SZX2-ILLTQ) to confirm the presence/absence of tetrasporangia in each treatment.

5.3.3. Metabolite extraction and identification

The extraction and derivatisation of metabolites for untargeted metabolic profiling by GC-MS was conducted as per Rawlinson et al. (2015) with some modification. Samples for each timepoint (50 mg FW per replicate) were suspended in 200 µL of sodium hydroxide solution (1% w/v) and 147 µL of HPLC grade methanol in 2 mL screwcap microcentrifuge tubes (Heathrow Scientific, HS10060). Two zirconia/silica beads (2.3 mm, Dnature, 11079125z) were added to each suspension before homogenisation using a Precellys Evolution Tissue Homogeniser (10,000 rpm, 3 x 20 sec with 1 min intervals), followed by immediate transfer to 4 °C where samples were left to extract overnight (20 h). The next day, samples were vortexed for 15 sec and centrifuged for 30 sec at 16,000 *g.* The supernatant was then carefully transferred by pipette into a fresh 1.5 mL Eppendorf tube,

followed by derivatisation using methyl chloroformate (MCF) (Rawlinson et al. 2015). Deuterated cinnamic acid (20 µL of 20 µg mL^{-1} in methanol) was used as an internal standard. The derivatised products were then extracted into chloroform and transferred to GC-MS vials for analysis. For the targeted analysis of PGRs (abscisic acid (ABA), azelaic acid (AZ), 3-indole acetic acid (IAA), jasmonic acid (JA), and salicylic acid (SA)) or PGR precursors/related metabolites (1-aminocyclopropane-1-carboxylic acid (ACC), benzoic acid (BA), linolenic acid, and linoleic acid), stock standard solutions (2 µg mL^{-1}) of each chemical were prepared and subsequently derivatised as per Rawlinson et al. (2015). The derivatised samples were analysed on a Nexis GC-2030 - Shimadzu gas chromatograph coupled with a single quadrupole mass spectrometer (GCMS-QP2020 NX) using an SH-I-5Sil MS column (30m x 0.25mm x 0.25µm) and a Topaz Splitless Single Taper Liner (3.5mm x 5.0 mm x 95 mm) (Shimadzu, REST-23336). The ion source used electron ionisation, and the MS was run in scan mode and selected ion monitoring (SIM) mode to identify the analytes. Helium was used as the carrier at a flow rate of 0.96 mL min^{-1}. The flow control mode was set to linear velocity, and the pressure was set to 9.0 psi. The injection volume was set to 2 µL in splitless injection mode and the injection port temperature was set to 250 °C. The oven temperature for the method was set at 80 °C, held for 1 min, and ramped up to 320 °C at a rate of 10 °C min^{-1}, and held for 2 min. Compounds were identified based on the National Institute of Standards and Technology (NIST) and MassBank website (http://www.massbank.jp/) according to mass/charge value (*m/z*) and relative abundance, with an 85% Similarity Index threshold.

5.3.4. Targeted metabolomic analysis

Significant differences in the production of identified target PGRs and related metabolites were assessed using MetaboAnalyst software (ver. 3.0) (http://metaboanalyst.ca/). Data were normalised to the internal standard (cinnamic acid), "none" was selected for data transformation, and "pareto scaling" was selected for data scaling. To examine differences at specific timepoints representing: 1) the effect of fragmentation, 2) pre-tetrasporogenesis, 3) the onset of tetrasporogenesis, and 4) active tetrasporogenesis, *t* tests were conducted for the following pairwise contrasts: 1) baseline vs. day 0, 2) day 7 control vs. day 7 induction, 3) day 14 control vs. day 14 induction, 4) day 21 control vs. day 21 induction. Significant differences in metabolite production were determined using a false discovery rate (FDR) adjusted *P*-value threshold of ≤0.05.

5.3.5. Untargeted metabolomic analysis

For untargeted metabolic profiling analysis, GC-MS raw data files were exported as mzXML files and processed using XCMS software (ver. 3.7.1) with optimised parameters: peak picking method = matchedFilter, peak width = 1–10 sec, ppm = 500, mzdiff = 0.01, prefilter = 0, retention time correction method = "none", and matching peaks across samples (bw = 3, mzwid = 1, minfrac = 0.1). A compound matrix containing peak intensity, *m/z* value, and retention time was extracted for statistical analysis in MetaboAnalyst software (ver. 3.0) (http://metaboanalyst.ca/). Data were normalised to the internal standard, "none" was selected for data transformation, and "pareto scaling" was selected for data scaling. To detect changes in metabolite production, *t* tests were conducted for the contrasts at each timepoint as described above (Section 5.3.4). Significant differences were

determined using an FDR adjusted *P*-value threshold of ≤0.05. Principal component analysis (PCA), partial least squares discriminant analysis (PLS-DA), and heatmap analysis were all performed with default parameters.

5.3.6. RNA extraction and sequencing

Total RNA was extracted from each algal sample using an RNeasy Plant Mini Kit (Qiagen, Germany) with an additional DNase I (Thermo Fisher Scientific) treatment to remove residual genomic DNA, both following the manufacturer's instructions. RNA quantity and purity were assessed using a DS-11 Series spectrophotometer (Denovix) before shipping to Novogene (Singapore) on dry ice, where RNA concentration and integrity was verified using an Agilent 2100 Bioanalyzer. Whole mRNA-seq (paired-end 150 bp) was performed using the Next-Generation Illumina NovaSeq 6000 platform using an HiSeq sequencer according to the standardised Illumina pipeline by Novogene. A summary of total reads per sample is presented in Table S1 (Appendix 7). Raw sequence data was deposited into the Sequence Read Archive (SRA) database (NCBI BioProject ID 1098997, accession number PRJNA109899).

5.3.7. Transcriptome de novo assembly and functional annotation

Raw read data quality control, transcriptome reconstruction, and gene functional annotation were conducted by Novogene (Singapore). Raw reads in FASTQ format underwent processing using custom scripts developed in-house. This process involved trimming reads containing adapters and removing poly-N sequences and low-quality reads from the raw data. Only clean, high-quality data were retained for downstream analysis. *De*

novo assembly of a reference transcriptome was performed using Trinity ver. 2.6.6 (Grabherr et al. 2011), followed by hierarchical clustering with Corset ver. 1.09 to remove redundancy (Davidson and Oshlack 2014). Clean RNA-seq reads were then mapped to the reference Corset-filtered transcriptome assembly using RSEM ver. 1.2.28 (Li and Dewey 2011), and gene expression levels were quantified as fragments per kilobase of exon per million fragments mapped (FPKM) (Trapnell et al. 2010). The average mapping rate was 87% ± 3 (mean ± stdev) (Appendix 7). For gene functional annotation, seven databases were queried using the following software: NCBI blast for the NT database (Altschul et al. 1997), Diamond for NR, SwissProt, and KOG databases (Buchfink et al. 2015), HMMER package hmmscan for PFAM, Blast2GO and a Novogene script for Gene Ontology (GO) annotations (Götz et al. 2008), and KAAS (https://www.kegg.jp/kegg/ko.html) for Kyoto Encyclopedia of Genes and Genomes (KEGG) annotations (Moriya et al. 2007). Among the 245,537 unigenes identified, 157,880 unigenes (63.4%) were successfully annotated in at least one database.

5.3.8. Differential gene expression analysis

The DESeq2 R-package (ver. 3.4.2) was used to identify differentially expressed genes (DEGs) using normalised raw count data processed through the inbuilt normalisation method in DESeq2. Pairwise contrasts were conducted at each timepoint (n = 5 for baseline, day 7, day 14, and day 21 samples, and n = 10 for day 0 samples), as described in the metabolomic analysis (Section 5.3.4), to determine differential expression. Genes with significant upregulation or downregulation were determined using an FDR adjusted P-value threshold of ≤0.05 and minimum Log2 Fold Change of ≥1.

5.3.9. Functional enrichment analysis

For the untargeted metabolomic data, pathway impact analysis was carried out for the metabolites detected in each contrast according to the pathway analysis module of MetaboAnalyst 3.0 (Xia et al. 2015), selecting the *Arabidopsis* metabolic pathway database as the reference and relative-betweenness centrality as the pathway analysis algorithm. Significantly affected pathways were identified using an adjusted *P*-value threshold of ≤0.05 and minimum impact value ≥0.1 (Xia et al. 2015).

For the transcriptomic data, both GO term and KEGG pathway enrichment analyses were performed for the DEGs identified in each contrast using the clusterProfiler R-package ver. 4.10.0 (Wu et al. 2021). Significantly enriched GO terms and KEGG pathways were defined as those with adjusted *P*-values ≤0.05. We prioritised GO terms annotated to the category 'Biological Process' and focused on enriched GO terms and KEGG pathways associated with metabolism. This approach enabled us to target specific biological processes and metabolic pathways most relevant to the induction of tetrasporogenesis. Additionally, we explored genes and pathways associated with the synthesis of PGRs and environmental information processing, considering the significance of these factors in seaweed reproduction (Stirk and Van Staden 2014, García-Jiménez and Robaina 2015, Zhang et al. 2021, Uji and Mizuta 2022).

5.4. Results and discussion

5.4.1. Post-fragmentation recovery and induction of tetrasporogenesis

Following fragmentation, the pigmentation of the filaments noticeably declined across all treatments. This is a consistent outcome resulting from the mechanical stress

induced by the fragmentation process. During the seven-day acclimation period that followed, the pigmentation notably improved across all samples. Despite initial signs of stress, including partial bleaching observed in some filaments of day 0 samples, the pigmentation of the filaments was completely restored by day 7, indicating a successful recovery from the mechanical stress. After 14 days, tetrasporogenesis was induced in all induction treatments, and by day 21, the biomass across all induction treatments had prolific tetraspore output.

5.4.2. Targeted metabolomic analysis

Out of the nine targeted metabolites analysed in *A. armata*, only four were detected with the method employed: benzoic acid, azelaic acid, linoleic acid, and proline (Figure 5.1). Induction samples had elevated levels of benzoic acid on day 7 and azelaic acid on day 14 compared to control samples; however, these increases did not reach statistical significance (P >0.05). Further investigations into other PGRs and related metabolites are necessary to better understand their role in seaweed reproduction (García-Jiménez and Robaina 2015, Uji and Mizuta 2022). Potential candidates for such investigation are discussed in Section 5.4.5, where we examine the expression of genes associated with PGRs outside those specifically targeted in this study.

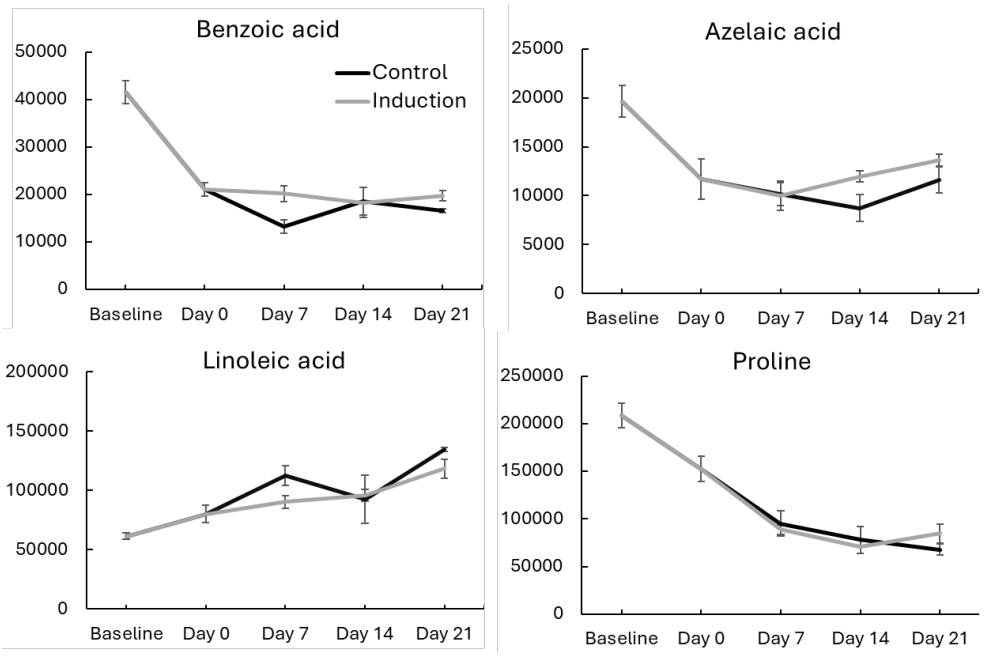

Figure 5.1 Peak areas (± SE) of targeted metabolites detected in *A. armata* across different sampling timepoints baseline and day 0 samples, as well as control samples on days 7, 14, and 21.

5.4.3. Untargeted metabolomic analysis

The metabolic profiles of control samples varied notably on day 7, and also on days 14 and 21, which could reflect minor differences in the rates of processes associated with growth or recovery. Despite this variability, control samples showed significant overlap across timepoints (Figure 5.2). In contrast, induction samples at each timepoint were more tightly clustered and showed increased separation across timepoints, though with some overlap (Figure 5.2). The most notable disparity in metabolic profiles between control and induction samples occurred on day 14. A total of 155 peaks were detected across samples from day 7 through to day 21. Of these, 42 metabolites were identified, including amino acids, fatty acids, carboxylic acids, and other compounds (Appendix 7).

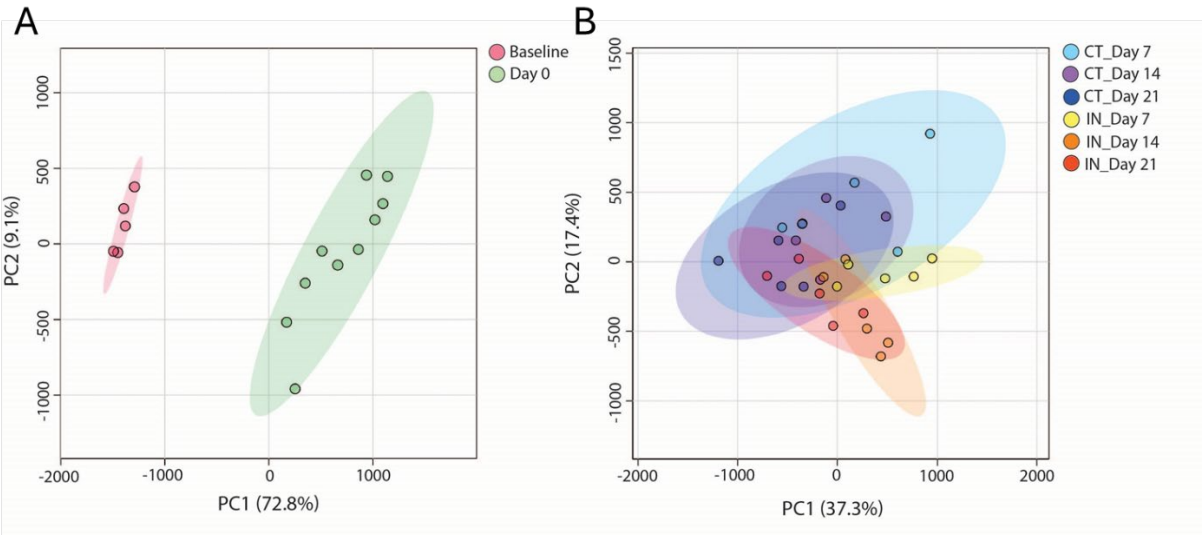

Figure 5.2 PCA plots showing the metabolic profiles of *A. armata* during tetrasporogenesis, comparing (A) baseline and day 0 samples, and (B) control (CT) and induction (IN) samples on days 7, 14, and 21. In (A), red and green circles represent baseline (*n* = 5) and day 0 samples (*n* = 10), respectively. In (B), light blue, purple, and dark blue circles represent control samples on days 7, 14, and 21 (*n* = 5), while the yellow, orange, and red circles represent induction samples on days 7, 14, and 21 (*n* = 5), respectively.

Among the identified metabolites, 14 were significantly different between control and induction samples at one or more of the three timepoints related to tetrasporogenesis (Appendix 7). These metabolites are visually represented in the heat map (Figure 5.3). Several metabolites, including arachidonic acid, which was most accumulated (2.6-fold change (FC)), followed by 2-bromofumaric acid (2.1-FC), tricarballylic acid (1.5-FC), and two unidentified metabolites (1.5 and 2.4-FC) were significantly accumulated in day 7 induction samples (Figure 5.3). Arachidonic acid, a long-chain polyunsaturated fatty acid, is an important component of cellular membrane phospholipids (Guschina and Harwood 2009). Conversely, tricarballylic acid, a dicarboxylic acid, is known to inhibit aconitase, a key enzyme in the citrate cycle (TCA cycle) affecting energy metabolism and various biosynthetic pathways (Villafranca 1974, Forsberg and Russell 1986). Although none of these metabolites have been explicitly studied in the context of seaweed metabolism, insights from higher

plants and microalgae suggest that arachidonic acid is involved in environmental stress response (Savchenko et al. 2010). For instance, in the green microalga *Lobosphaera incisa*, nitrogen starvation and increases in light intensity induce strong accumulation of arachidonic acid (Khozin-Goldberg et al. 2002, Kokabi et al. 2019). Elevated levels of arachidonic acid in response to the reduction in photoperiod applied to induction samples may have contributed to triggering tetrasporogenesis, yet the relationship between such metabolic alterations and seaweed reproduction remains ambiguous. In animals, arachidonic acid serves as a precursor for the synthesis of eicosanoids – essential bioregulators of many cellular processes (Gerwick et al. 1990, Mišurcová et al. 2011). While it has been speculated that eicosanoids can play a role in coordinating reproductive events in red seaweeds (Gerwick et al. 1990), this hypothesis remains untested.

Homophenylalanine was the most accumulated metabolite identified in day 14 induction samples (2.3-FC), followed by valeric acid (1.6-FC) (Figure 5.3). Notably, valeric acid was the sole fatty acid with significant accumulation across all timepoints. Knowledge regarding the functions of homophenylalanine and valeric acid in seaweed metabolism is sparse (Koketsu et al. 2013). Nonetheless, their accumulation at this specific timepoint indicates a possible role in initiating reproduction. Cholesteryl nonanoate was the sole metabolite significantly accumulated in day 21 samples, marking the later stages of tetrasporogenesis (Appendix 7). This result suggests that the majority of metabolic alterations associated with tetrasporogenesis occur during the earlier stages of this process. The remaining metabolites accumulated in day 7 and day 14 induction samples were primarily amino acids, including sarcosine, phenylalanine, and notably aspartate, which was accumulated at both timepoints. However, increases in all amino acids were relatively modest (1.3 to 1.4-FC) (Figure 5.3). Amino acids play pivotal roles in a multitude of

physiological processes in seaweeds, including reproduction (Wu 2010, Harnedy and FitzGerald 2011). Yet, without a more comprehensive list of metabolites facilitating detailed functional pathway analysis, it remains challenging to speculate on the specific roles of these amino acids in our study. A more sensitive metabolomic analysis, ideally utilising LC-MS-MS for its enhanced capability in untargeted metabolomic profiling, is therefore recommended to gain deeper insights into the metabolomic changes during tetrasporogenesis. Nevertheless, this study serves as a foundational exploration into this area for *A. armata*.

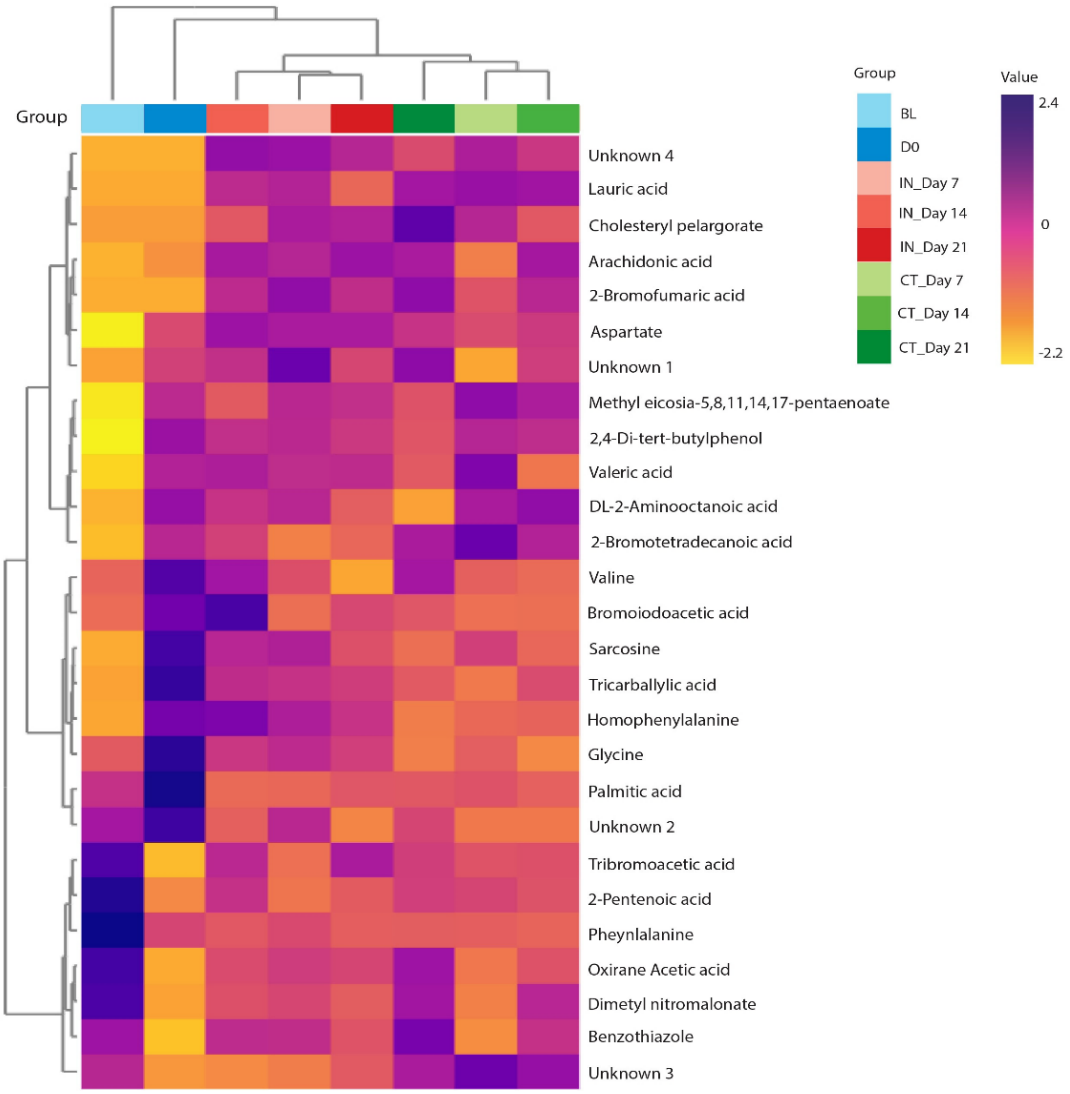

Figure 5.3 Heatmap with hierarchical clustering of the significantly different ($P \leq 0.05$) metabolites identified in *A. armata* between baseline (BL) and day 0 (D0) samples and between control (CT) and induction (IN) samples on days 7, 14, and 21 (group averages). Colours from yellow to deep purple indicate the relative abundances of metabolites from low to high according to the scale bar.

5.4.4. Differential gene expression analysis

Gene expression profiles for control and induction samples on day 7 and day 21 showed low variability, whereas those on day 14 showed high variability (Appendix 8). The high variability in gene expression profiles, especially in induction samples, could be attributed to the dynamic nature of tetrasporogenesis, as precise quantities of reproductive

structures per individual were not measured. Varied numbers of upregulated and downregulated DEGs were observed for the contrasts at each timepoint (Figure 5.4, see Appendix 9 for gene expression and annotation details), reflecting different phases of tetrasporogenesis. The contrast between control and induction samples identified 12,400 DEGs on day 7 (pre-tetrasporogenesis) and 5,557 DEGs on day 14 (the onset of tetrasporogenesis) (Figure 5.4). The majority of DEGs at these timepoints were upregulated (Figure 5.4). Overall, these DEG figures were higher compared to those found in the closely related species *A. taxiformis* between wild reproductive and non-reproductive tetrasporophytes (Patwary 2023) and between mature female and immature gametophyte tips (Patwary et al. 2023). This difference likely stems from our focused experimental design aimed at investigating tetrasporogenesis and our use of a *de novo* transcriptome assembly approach, contrasting with the availability of an assembled reference genome for *A. taxiformis* (Zhao et al. 2022). In our study, the lowest number of DEGs (3,730) was detected on day 21 (active tetrasporogenesis), with similar numbers of upregulated and downregulated genes (Figure 5.4). This result supports the finding of fewer metabolic alterations at this timepoint compared to preceding timepoints (Section 5.4.3), further reinforcing that the majority of biochemical changes linked to tetrasporogenesis occur during its earlier stages.

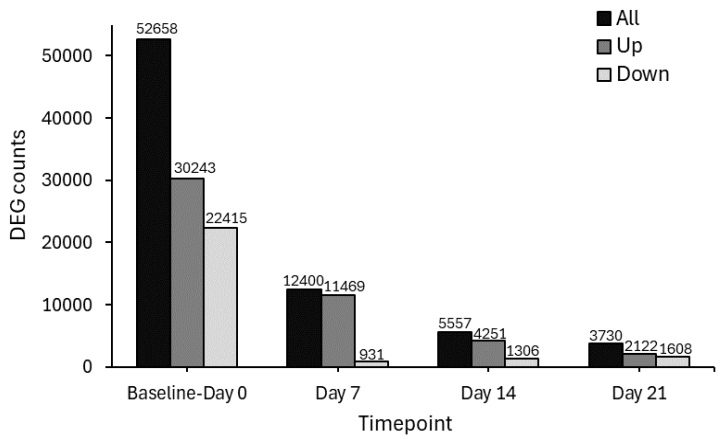

Figure 5.4 Differentially expressed genes (DEGs) (*P* ≤0.05 and Log2 Fold Change ≥1) between baseline and day 0 samples and between control and induction samples on days 7, 14, and 21. Refer to Appendix 9 for gene expression and annotation details.

5.4.5. Functional enrichment analysis

Functional enrichment analysis of both metabolomic and transcriptomic data provides valuable insights into the key biological pathways involved during tetrasporogenesis in *A. armata*. When examining differences in metabolite production and gene expression across the different phases of tetrasporogenesis, day 7 emerged as the most significant timepoint, followed by day 14. Therefore, we primarily focused our investigation into functional enrichment on day 7, while also considering results from day 14.

Metabolomic analysis of induction samples on day 7 and 14 showed impacts on pathways primarily related to amino acid metabolism (Figure 5.5). However, the analysis yielded only a low number of metabolites matched (≤3) to each pathway, highlighting the constraints of GC-MS in capturing the full spectrum of metabolites present in our samples. In contrast, the transcriptomes of induction samples across day 7 and day 14 were enriched in numerous GO terms and KEGG pathways with a significant number of genes matched to each pathway (refer to Appendix 10 for full lists of enriched GO terms, KEGG pathways and associated genes). While integrating metabolomic and transcriptomic data would provide a

deeper understanding of the biochemical mechanisms underpinning reproduction, insufficient metabolomic data prevented such integration here. Therefore, further investigation proceeded solely based on transcriptomic data.

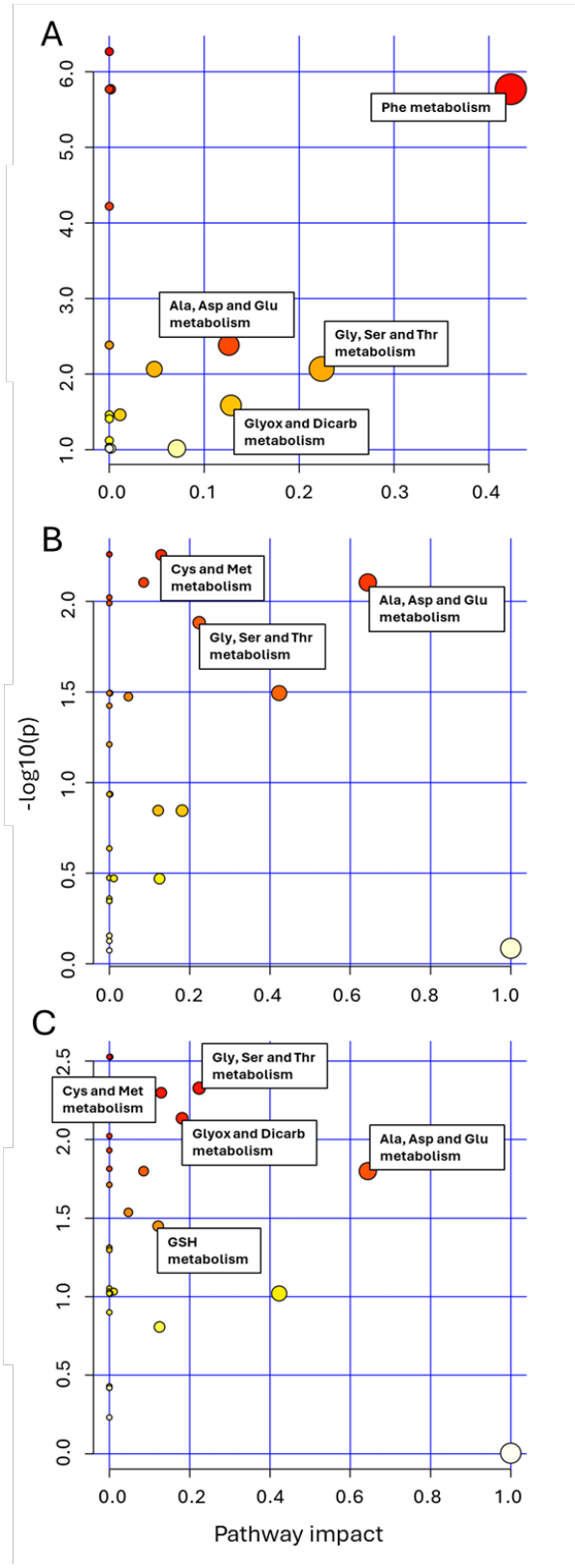

Figure 5.5 Metabolomic pathway analysis showing impacted pathways between (A) baseline and day 0 and between control and induction samples on (B) day 7 and (C) day 14. Darker circle colours indicate more significant changes of metabolites in the corresponding pathway, whereas the size of the circle represents the pathway impact score. Significantly impacted pathways ($P \leq 0.05$ and pathway impact ≥0.1) are annotated. Analysis for day 21 are not shown as no pathways were significantly impacted at this timepoint.

Top GO terms enriched for induction samples on day 7 included cellular response to oxidative stress, proteolysis involved in protein catabolic processes, carbohydrate transport, and glycerolipid biosynthetic process (Figure 5.6). Additionally, the primary KEGG pathways enriched on day 7 were associated with energy production, the metabolism of carbohydrates, amino acids, cofactors, glutathione, terpenoids, inositol phosphates (IPs), glycerophospholipids (GPLs), and the phosphatidylinositol (PI) signalling system (Figure 5.7), highlighting the dynamic metabolic activity during this timepoint. The complex PI signalling system is highly responsive to environmental cues and plays a critical role in activating signalling pathways involved in regulating reproductive processes in higher plants (Yang 1996). Notably, IPs – important lipid signalling molecules derived from PIs (Williams et al. 2015) – have been associated with the activation of plant hormone receptors in higher plants (Smart and Fleming 1993, Tan and Zheng 2009, Tsui and York 2010, Gillaspy 2011). The observed enrichment of the PI signalling system pathway at this timepoint suggests its potential activation in response to the reduction in photoperiod, the sole environmental change between control and induction samples and known inducer of tetrasporogenesis (Chapter 3/Mihaila et al. (2023a)). Such light signals are typically perceived and transduced through membrane associated photoreceptors, such as cryptochromes (CRYs) and phototropins (PHOTs) (Gyula et al. 2003). In this study, genes encoding these photoreceptors were highly upregulated in day 7 induction samples (ranging from 3.5 to 4.6-Log2 Fold Change (LFC)) (Appendix 11), underscoring their active response to changes in light conditions and possible role in initiating cellular responses associated with tetrasporogenesis.

The significance of the PI signalling system pathway is further highlighted by its enrichment during reproductive processes in other seaweeds, such as the maturation of

conchosporangia in the red alga *Pyropia haitanensis* (Lin et al. 2021) and initial stages of gametogenesis in *Saccharina japonica* (Liang et al. 2023). In *P. haitanensis*, several hub genes encoding diacylglycerol kinase (DGK), which are involved in synthesising phosphatidic acid – a key component of lipid metabolism – were upregulated during conchosporangia maturation (Lin et al. 2021). However, these genes showed no significant changes in expression levels in day 7 samples in our study. Instead, genes encoding phosphatidylinositol phospholipase C (PI-PLC) and phosphatidylinositol 4-phosphate 5-kinase (PIP5K) were markedly upregulated (3.7 and 3.4-LFC, respectively) in our day 7 induction samples as part of the PI signalling system and IP metabolism pathways (Appendix 11). PLCs are important lipid-modifying enzymes linked to reproductive development in rice (Singh et al. 2013), while PIP5K is a key enzyme producing the signalling lipid phosphatidylinositol 4,5-bisphosphate (PIP2) and plays a role in pollen development in *Arabidopsis thaliana* (Kato et al. 2024). We suggest that PLCs also play a role in seaweed reproduction, although the specific function of these enzymes in seaweeds remains to be elucidated.

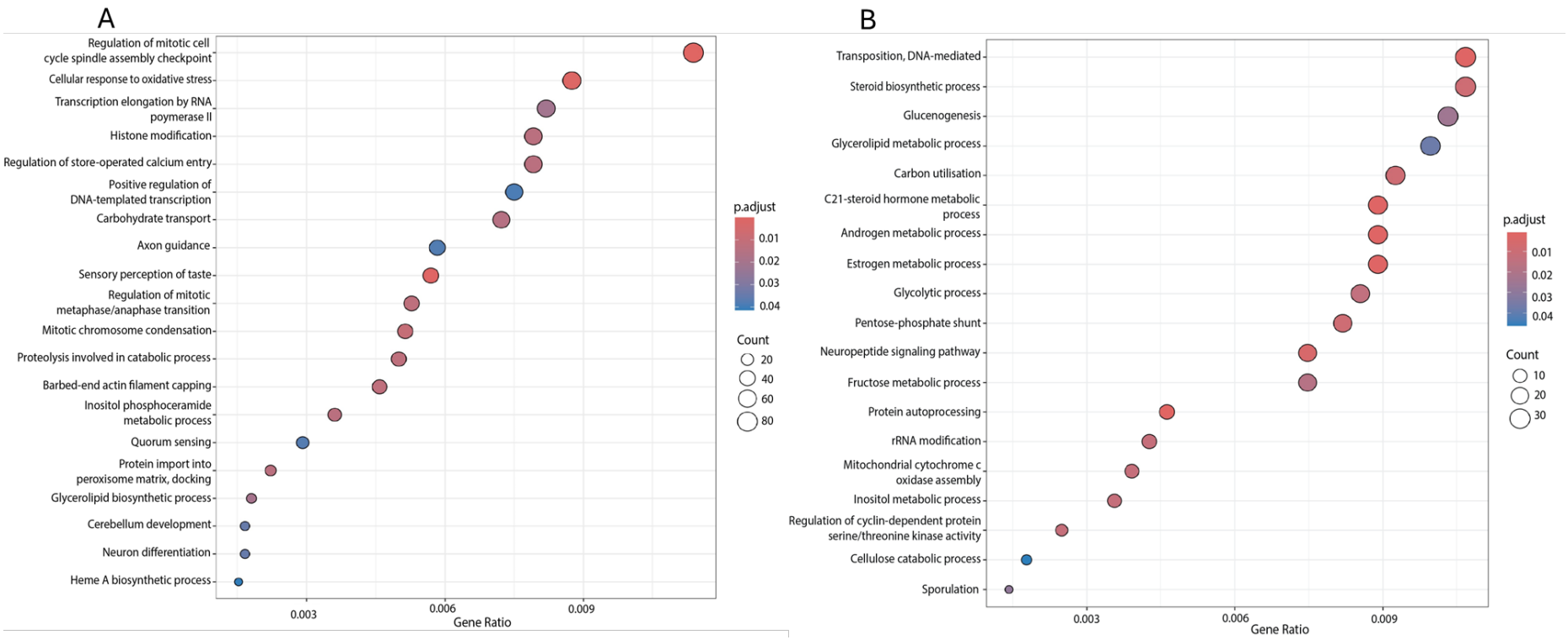

Figure 5.6 Top 20 Enriched Gene Ontology (GO) terms associated with differentially expressed genes (DEGs) identified between control and induction samples on (A) day 7 and (B) day 14, within the category 'Biological Process'. Red circle colours indicate more significant enrichment ($P \leq 0.05$). The size of the circle represents the number of genes associated with each term. If less than 20 terms were enriched, all are displayed. Refer to Appendix 10 for full lists of enriched GO terms for all contrasts.

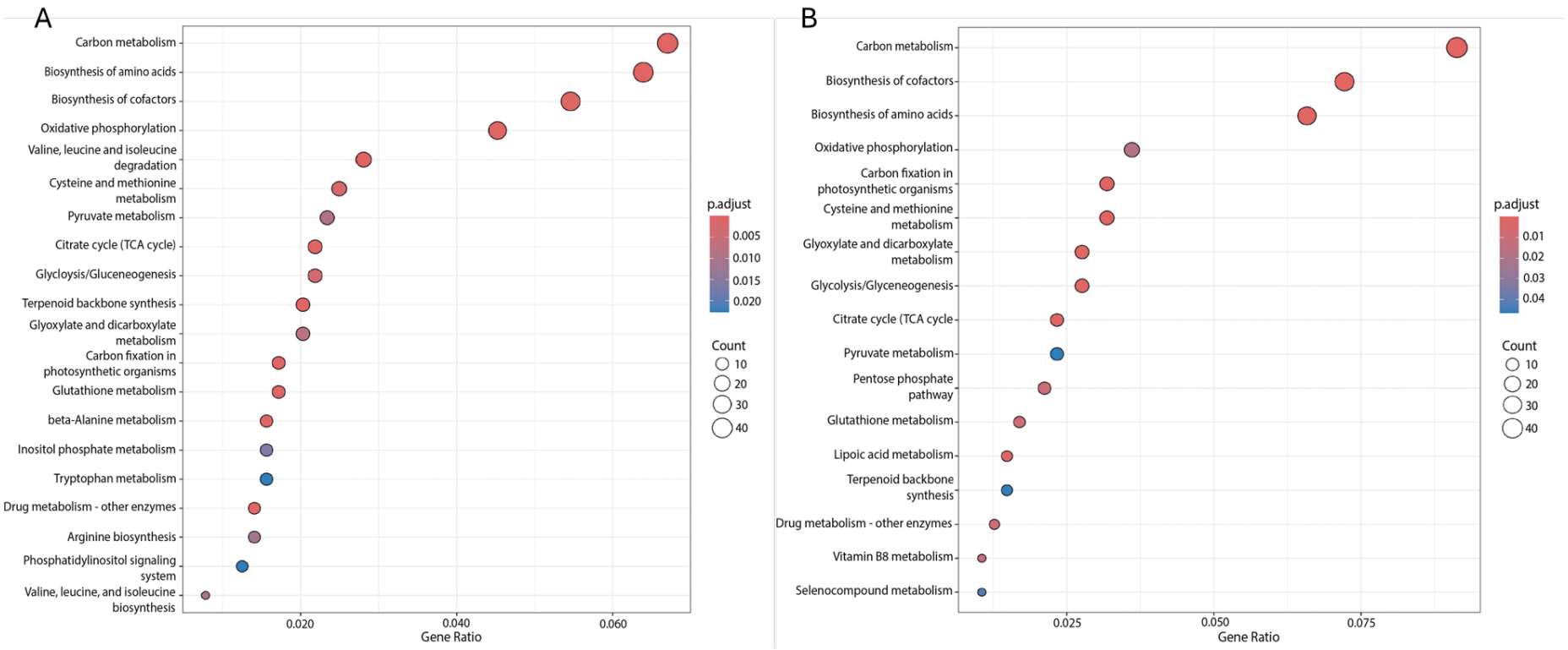

Figure 5.7 Top 20 Enriched Kyoto Encyclopedia of Genes and Genomes (KEGG) pathways associated with differentially expressed genes (DEGs) identified between control and induction samples on (A) day 7 and (B) day 14. Red circle colours indicate more significant enrichment ($P \leq 0.05$). The size of the circle represents the number of genes associated with each pathway. If less than 20 pathways were enriched, all are displayed. Refer to Appendix 10 for full lists of enriched KEGG pathways for all contrasts.

Recent research highlights the involvement of plant growth hormones, including polyamines (spermine, spermidine, and putrescine), jasmonates, and ethylene, in controlling the transition from vegetative to reproductive stages in red seaweeds (Guzmán-Urióstegui et al. 2002, Sacramento et al. 2007, García-Jiménez and Robaina 2015, Uji and Mizuta 2022). Polyamines are synthesised through the reproduction-candidate gene ornithine decarboxylase (ODC) (García-Jiménez et al. 2009, Pilar and Rafael 2019), which produces the polyamine precursor, putrescine, from the non-proteinogenic amino acid L-ornithine (Sacramento et al. 2004, Garcia-Jimenez et al. 2018). Notably, increased expression of the candidate gene ODC is an established indicator of cystocarp maturation and sporulation in *G. imbricata* (García-Jiménez et al. 2009, Montero-Fernández et al. 2016, Garcia-Jimenez et al. 2017). In day 7 induction samples, we detected high upregulation of the ODC gene (5.3-LFC), as well as several genes involved in polyamine biosynthesis, such as S-adenosyl methionine synthase (SAMS) (4.3-LFC) and spermidine/spermine synthase (Spd/Spm synthase) (3.7-LFC) (Garcia-Jimenez et al. 2018) (Appendix 11). The gene encoding for ornithine aminotransferase (OAT), a key enzyme involved in L-ornithine metabolism (Anwar et al. 2018), was also significantly upregulated in day 7 induction samples (4.4-LFC), implying its active role during this phase. Conversely, in day 14 induction samples, coinciding with the onset of tetrasporogenesis, expression levels of polyamine-related genes reverted to baseline or lower levels, while amine oxidase expression increased (3.8-LFC) (Appendix 11). As reproductive processes are initiated, polyamines undergo degradation by amine oxidases, leading to a stark decline in ODC expression, almost reaching undetectable levels (Sacramento et al. 2007, García-Jiménez et al. 2009). Although the precise involvement of polyamines and the ODC gene in tetrasporogenesis requires targeted investigation, these

collective observations strongly suggest their participation in regulating this reproductive process in *A. armata*.

Enrichment analysis showed an increase in the number of terms and pathways related to energy production and carbohydrate metabolism in day 14 induction samples compared to day 7 (Figures 5.6 and 5.7). Significant enrichment in carbon metabolism was also identified during tetraspore formation in *G. lemaneiformis* (Sun et al. 2023). These results align with the heightened energy demand for tetrasporogenesis (De Wreede and Klinger 1988, Guillemin et al. 2014). Supporting this notion, genes associated with carbon metabolism were significantly downregulated in cultured non-reproductive tetrasporophytes of *A. taxiformis* compared to wild reproductive tetrasporophytes, highlighting the importance of carbon metabolism during reproduction in *Asparagopsis* (Patwary 2023). Furthermore, additional terms and pathways enriched in day 14 induction samples were associated with biosynthesis of amino acids and steroids, as well as the metabolism of cofactors and vitamins, such as lipoic acid and vitamin B6, C21-steroid hormones, and glutathione (Figures 5.6 and 5.7). Genes associated with steroid/steroid hormone pathways were predominantly classified as hypothetical or unnamed/uncharacterised, with functional annotations tied to “androgen and estrogen metabolic processes” (Appendix 11). Primarily recognised for their involvement in animal reproduction, their presence in this context underscores the limited availability of molecular information regarding seaweed reproduction. Nonetheless, these annotations could indicate potential similarities to enzymes involved in the plant equivalents of these hormones. For instance, certain hypothetical proteins identified in *A. armata* show similarities to enzymes such as beta-hydroxysteroid-dehydrogenases or decarboxylases

(Appendix 11) that have been associated with the production of brassinosteroids (Zhang et al. 2017, Pan et al. 2023). Brassinosteroids are vital steroid hormones regulating various reproductive processes in higher plants (Fujioka and Yokota 2003, Asami et al. 2005, Li et al. 2010), and have been detected in microalgae and kelps (Stirk et al. 2013, Stirk et al. 2014). More targeted research is needed to define the roles of these genes in seaweeds, which may provide useful insights into the fundamental biochemical mechanisms governing seaweed reproduction. This is especially pertinent considering the prospective link between these genes and reproductive hormones across different organisms.

5.4.6. Response to fragmentation

Our analysis comparing baseline (pre-fragmentation) and day 0 (seven days post-fragmentation) samples aimed to broadly describe the metabolic and transcriptomic responses to fragmentation. Since all samples underwent the same fragmentation treatment prior to experimental conditions, any observed changes after the seven-day post-fragmentation recovery period should be attributed to the specific treatments applied. The PCAs conducted on metabolic (Figure 5.1) and transcriptomic data (Appendix 8) (separate analyses) both showed clear separation between baseline and day 0 samples. This highlights distinct alterations in both metabolite production and gene expression in response to fragmentation.

Nineteen metabolites exhibited significant differences in day 0 samples compared to baseline, with 13 showing accumulation, including tricarballylic acid, aspartate, homophenylalanine, sarcosine, and arachidonic acid (Figure 5.3 and Appendix 7). Some of these metabolites, such as aspartate, known for its role in plant stress response (Han et al.

2021) and potential involvement in reproductive processes (Wang et al. 2018), were also accumulated in induction samples, underscoring their diverse functions. Post-fragmentation uniquely accumulated metabolites such as valine, glycine, valeric acid, 2,4-Di-tert-butylphenol, 2-bromotetradecanoic acid, and methyl eicosia-5,8,11,14,17-pentaenoate, indicating their likely role in stress response and/or recovery and growth. Notably, the production of phenylalanine significantly decreased in day 0 samples (Figures 5.3 and 5.5), contrasting with its elevated levels in day 7 induction samples, suggesting shifts in amino acid synthesis leading up to tetrasporogenesis induction (Sun et al. 2023). Furthermore, metabolic pathway analysis revealed significant enrichment of pathways associated with alanine/aspartate/glutamine and glycine/serine/threonine metabolism in day 0 samples, as well as in day 7 and 14 induction samples (Figure 5.5), emphasising the diverse metabolic functions performed by these amino acids.

Alongside metabolomic findings, a total of 52,658 DEGs were identified between baseline and day 0 samples (Figure 5.4, Appendix 9), indicating marked changes in gene expression induced by fragmentation. This process induces significant physical disruption and stress, necessitating the activation of various physiological mechanisms in response (Vega-Muñoz et al. 2020). Enriched GO terms and KEGG pathways in day 0 samples were primarily linked to cellular signalling, antioxidant defence, energy production, and growth (Appendix 10). Additionally, numerous pathways related to amino acid production, including lysine, tryptophan, tyrosine, phenylalanine, alanine, aspartate, and glutamate metabolic pathways, were enriched in day 0 samples (Appendix 10), aligning with findings from metabolomic analysis. Before fragmentation, tetrasporophyte cultures were maintained under conditions conducive to minimal growth. However, following stress recovery post-fragmentation, a pronounced growth response is initiated. Thus, it was expected that

fragmentation would result in upregulation of metabolic pathways linked to recovery and growth, aligning with observations.

5.5. Conclusion

This study provides insights into the metabolomic and transcriptomic dynamics underlying the induction of tetrasporogenesis in *A. armata*, highlighting key metabolites, pathways, and genes for more targeted investigation. Our findings indicate a potential role of the phosphatidylinositol signalling system, along with possible involvement of phospholipase C enzymes, in responding to the reduced photoperiod triggering tetrasporogenesis. While significant differences in targeted plant growth regulators/related metabolites were not detected, gene expression analysis strongly implicates polyamines as worthy of further investigation for their involvement in tetrasporogenesis in *A. armata*. Amino acid and carbohydrate metabolism were identified as crucial not only for inducing tetrasporogenesis but also in responding to fragmentation. The variability in gene expression and metabolite production leading up to and during the initiation of tetrasporogenesis underscores the dynamic nature of this process. These findings lay the groundwork for future research endeavours aimed at disentangling the complexities of this fundamental biological processes.

Chapter 6

General Discussion

6.1. Main research findings and implications

The aim of this thesis was to provide a foundation for developing closed-life cycle aquaculture of the anti-methanogenic red seaweed *Asparagopsis armata*. This involved monthly field sampling and quantification of reproductive phenology on the North Island of New Zealand, hatchery- and nursery-based cultivation experiments, targeted and untargeted metabolomic profiling, and transcriptomic analysis.

Understanding the reproductive phenology of *A. armata* and its response to rising sea temperatures is crucial for sustainable aquaculture (Charrier et al. 2017, de Bettignies et al. 2018, Kim et al. 2019). Comparing reproductive phenology to a 1978–1981 assessment, when temperatures were 1–2 °C cooler, showed no apparent shift in the timing of tetrasporogenesis (Chapter 2/Mihaila et al. (2023b)). However, tetraspore release was inconsistent in natural populations, rendering them unreliable for research or aquaculture purposes. The delayed and shortened duration of cystocarp production, along with limited viable carpospore released compared to 1978–1981, presents significant challenges for achieving scalability and consistency in aquaculture operations reliant on carpospore release cultures. Therefore, developing methods for inducing viable cystocarp production and subsequent carpospore release is recommended to ensure sustainable and dependable aquaculture practises of *A. armata*. The timing of spermatangia and cystocarp production reported in this study will aid in guiding such research efforts. The heatwave recorded in 2022 likely contributed to poor pigmentation, low reproductive output, and high mortality

of both tetrasporophytes and gametophytes in natural populations (Bartsch et al. 2013, Endo et al. 2017, Kreusch et al. 2019, Kumar et al. 2020). Therefore, decreasing dependence on natural reproductive process for aquaculture production will become increasingly important considering the increases in frequency, duration, and intensity of marine heatwaves predicted in future climate change scenarios (Oliver et al. 2018). Overall, these findings establish a quantitative baseline for tracking how climate-induced rises in sea temperature impact reproductive patterns in *A. armata*, potentially serving as a marker for understanding the broader effects of climate change on seaweed reproduction (Mihaila et al. 2023b). Moreover, these results demonstrate that closed life cycle production of tetraspores is essential for both research and farming purposes due to seasonal and variable availability.

Previous research has suggested that a decrease in photoperiod can trigger the onset of tetrasporogenesis (Oza 1977, Lüning and Dieck 1989, Guiry and Dawes 1992). However, despite this knowledge, effectively replicating this life cycle transition for hatchery production has proven challenging due to limited information on timing and practical implementation (Zhu et al. 2021, Zanolla et al. 2022). To address this gap, hatchery protocols were developed to induce, improve, and regulate tetrasporogenesis through experiments manipulating various environmental factors (Chapter 3/Mihaila et al. (2023a)). It was found that reducing the light period by 4 h to an 8 h L:16 h D photoperiod was crucial for inducing tetrasporogenesis, and that this process can be optimised by exposing cultures to 18 °C, 15 µmol photons m^{-2} s^{-1}, and F/8 (3.5 mg N L^{-1} and 0.3 mg P L^{-1}) for 14 days. These experiments not only establish a detailed method for inducing tetrasporogenesis in a significantly shorter timeframe than previous studies (Oza 1977, Lüning and Dieck 1989, Guiry and Dawes 1992), thereby improving hatchery efficiency, but also provide a basis for

adjusting these methods to suit specific temperature and light conditions across different strains. Moreover, the established hatchery protocols enable on-demand mass production and release of tetraspores, facilitating timed seeding with optimal ocean outplanting conditions, which is likely to improve post-outplanting gametophyte survival and growth. Based on the optimised protocol, seeding can be conducted over a 15-day period from the onset of tetrasporogenesis, yielding an estimated >10 million tetraspores per g FW of tetrasporophyte biomass. Alternatively, concentrating seeding efforts during the primary peak in tetraspore production (from day 27 to day 29) results in an estimated 7–8 million tetraspores. These first estimates of spore production for *A. armata* will help to determine seeding densities and forecast harvest yields. Overall, the induction of tetrasporogenesis through methods scalable for commercial aquaculture (de Nys et al. 2023, Mihaila et al. 2023a) overcomes a significant bottleneck to progressing closed life cycle cultivation. This advancement now allows for the development and refinement of optimal conditions for nursery production, as well as protocols for line seeding and processes for automation.

Developing and maximising nursery production is critical for implementing closed-life cycle cultivation of *A. armata*, yet no studies have successfully determined the culture requirements of juvenile gametophytes. Thus, drawing on protocols obtained in Chapter 3 (Mihaila et al. 2023a), key parameters for enhancing early-stage development and growth of juvenile gametophytes were identified using laboratory-induced tetraspores (Chapter 4/Mihaila et al. (2024)). Moderate temperature and water flow were identified as critical drivers of juvenile gametophyte growth and are highly recommended for maximising nursery cultivation of *A. armata*. Moreover, water flow, when combined with the optimal environmental conditions, substantially increased biomass productivity, resulting in well-branched gametophytes with a combined total branch length of 6.2 mm and a height of

3.5–4 mm after three weeks. This nursery period is significantly shorter than the timeframes typically needed for kelps and nori (Sahoo and Yarish 2005, Redmond et al. 2014, Forbord et al. 2020), with potential for further reduction, given that *A. armata* gametophytes reached assumed outplanting size (1–2 mm height) after 2 weeks (Redmond et al. 2014, Forbord et al. 2020). These results mark the first successful demonstration of laboratory-induced tetraspores leading to well-branched juvenile gametophytes, supporting the feasibility and effectiveness of closed life cycle cultivation of *A. armata*. Furthermore, this study showcases successful cultivation of gametophytes in indoor cultures, a notable progression given previous inconclusive results and high mortality rates in laboratory experiments with mature gametophytes (Chualáin et al. 2004, Mickelson 2013, Batista 2020, Zanolla et al. 2022). Cultivation under a 12 h L: 12 h D photoperiod and 15 µmol photons m^{-2} s^{-1} improved development and growth, while maintaining a nutrient concentration of F/8 minimised fouling without impeding growth. These insights are crucial for cost and contamination control in commercial settings. Together with outcomes from chapter three, these findings lay the foundation for designing streamlined *A. armata* hatcheries and nurseries for both research and commercial production (Mihaila et al. 2024).

Deciphering the internal mechanisms governing seaweed reproduction, particularly in red seaweeds with their complex life cycles, presents a significant challenge (García-Jiménez and Robaina 2015, Sun et al. 2023). However, such knowledge is imperative for ensuring the effectiveness and sustainability of seaweed farming practises (Loureiro et al. 2015, Liu et al. 2017, Hwang et al. 2019). Thus, the final part of this thesis sought to investigate biochemical and molecular dynamics underlying tetrasporogenesis induction. Although variations in the production of targeted phytohormones lacked significance, there was a notable accumulation of various metabolites, including the eicosanoid precursor

arachidonic acid, alongside specific amino acids, leading up to and during the onset of tetrasporogenesis. Furthermore, genes associated with phospholipase C (PLC) enzymes and polyamine production also showed high upregulation pre-tetrasporogenesis, suggesting their involvement in coordinating tetrasporogenesis in *A. armata*. These data provide a foundational information base by offering new biochemical and molecular insights on *A. armata*, essential for understanding the internal mechanisms of reproduction. Such knowledge is invaluable for selective breeding programs to advance seaweed aquaculture production (Hwang et al. 2019). Analysis of thousands of differentially expressed genes throughout the phases of tetrasporogenesis revealed numerous enriched pathways. Among these, pathways related to the phosphatidylinositol (PI) signalling system (Lin et al. 2021, Liang et al. 2023), carbon metabolism (Patwary 2023, Sun et al. 2023), and steroid hormone production (Pan et al. 2023), show promise for key participation in seaweed reproduction based on previous research. Overall, these results offer new perspectives on possible key regulators of tetrasporogenesis, an area of research that has been explored by only a few previous studies (García-Jiménez and Robaina 2012, Sun et al. 2023). Moreover, they underscore the complexity of the endogenous mechanisms controlling seaweed reproduction and offer a comprehensive range of genes and pathways to facilitate more targeted molecular and biochemical investigations.

6.2. Future research directions

This research has significant implications for *A. armata* aquaculture and directions for future research.

Chapter 2 identified potential climate driven shifts in the reproductive phenology of *A. armata* in New Zealand since 1978–1981. Yet, to confirm the drivers of these shifts and

inform aquaculture development, it is essential to gain a more comprehensive understanding of the environmental factors affecting reproductive processes in *A. armata* gametophytes (de Bettignies et al. 2018). Previous laboratory culture studies with gametophytes have shown low survival rates (Chualáin et al. 2004, Mickelson 2013, Batista 2020, Hunter 2022), indicating the need for careful consideration of experimental methods. Moreover, heat stress was identified as a probable factor explaining low reproductive success and high mortality rates in the field in 2022, emphasising the need for temperature tolerance experiments. Data from this study, together with findings from Chapter 4 (Mihaila et al. 2024), strongly indicate that gametophytes have limited tolerance to continuous exposure to temperatures of 21 °C. Understanding the effect of heat stress on gametophyte reproduction and survival will be critical for determining the timing of outplanting and harvesting, particularly in light of projected increases in the frequency and intensity of marine heatwaves (Allen 2018). Exceedance of thermal tolerance could also bring about shifts in population dynamics, with reduced reproductive success and survival rates potentially leading to population declines and decreased availability. Limited carpospore release could also reduce genetic diversity within populations, as there may be fewer opportunities for genetic recombination. This would result in populations becoming less adaptable to changing environmental conditions. It is worth noting that our study was conducted at a single site over a two-year period, with intermittent gaps due to COVID-19 restrictions and poor weather conditions. Therefore, repeated sampling and longer-term quantitative monitoring at the same site and additional sites would allow further accounting for short-term variation and comparison across temporal and spatial scales.

Chapter 3 presents a method for inducing tetrasporogenesis and the release and germination of tetraspores in domesticated *A. armata* tetrasporophytes acclimated at 18 °C,

~15 µmol photons m^{-2} s^{-1}, and 12 h L:12 h D for 18 months, likely belonging to the L1B lineage. Assessing this method on tetrasporophytes with varied environmental histories and across different strains would be beneficial to determine its applicability for general aquaculture of *A. armata*. A reduced photoperiod (8 h L:16 h D–10 h L:14 h D) appears to be a universal requirement for inducing tetrasporogenesis in *A. armata*, as indicated by previous controlled laboratory studies (Oza 1977, Lüning and Dieck 1989, Guiry and Dawes 1992). Nevertheless, the experimental design employed here provides a practical template for fast forwarding strain specific adjustments that may be required for other environmental parameters. Despite the emerging benefits of plant growth regulators (PGRs) for enhancing seaweed reproduction (Nimura and Mizuta 2002, García-Jiménez and Robaina 2012, Uji et al. 2020), the exogenous application of select PGRs did not positively affect tetrasporogenesis in *A. armata*. Subsequent targeted metabolomic analysis conducted in Chapter 5 was unable to detect the production of PGRs selected in this study. Thus, additional PGRs should be further explored to identify those involved in regulating tetrasporogenesis in *A. armata* and ascertain their potential application during the hatchery phase to enhance efficiency. Specific parameters identified for ceasing and re-inducing tetrasporogenesis in the same biomass should also be evaluated for commercial feasibility. Notably, the development of tetraspores develop on newly grown tissue (Guiry and Dawes 1992) and rapid growth of filaments under the established protocols suggest that repeated induction is unlikely to have negative effects on reproductive output or viability. Therefore, it is likely that re-inducing tetrasporogenesis in the same biomass and maintaining that biomass at scale is feasible for preserving valuable selected cultivars/strains.

Chapter 4 elucidates the essential drivers for successful nursery production of *A. armata*. With these critical parameters identified, processes and systems can confidently be

developed for implementation in large-scale nursery settings. Furthermore, while temperature conditions are expected to remain consistent across nursery systems, optimal water flow, light exposure, and nutrient concentrations may fluctuate depending on the scale and configuration of the cultivation setup (Hurd 2000, Caines et al. 2014, Redmond et al. 2014). Therefore, it is recommended that these parameters are further fine-tuned according to individual system requirements. Theoretically, juvenile gametophytes could be outplanted after two weeks of exposure to nursery conditions, based on the recommended outplanting size for kelps and nori (Sahoo and Yarish 2005, Redmond et al. 2014, Forbord et al. 2020). However, marine farm experiments assessing varying nursery phase duration will be important to confirm the optimal nursery period and maximise outplanting success. The optimal temperature (18 °C) and photoperiod (12 h L:12 h D) for juvenile gametophyte growth coincided with the long-term maintenance conditions of parental tetrasporophyte stock cultures. This alignment implies the possibility of predetermining optimal growth conditions by manipulating the environmental conditions of the parental tetrasporophyte conditions. Such thermal priming techniques offer potential for enhancing the temperature tolerance of gametophytes (Wang et al. 2017, Jueterbock et al. 2021), a critical factor given the challenges posed by climate change, such as heatwaves, which are likely to diminish outplanting success (Nepper-Davidsen et al. 2023). Additionally, an important progression after establishing conditions for hatchery and nursery production is the refinement of methods for tetraspore seeding. This will involve determining suitable seeding techniques, densities, and rope selection.

Chapter 5 provides a first exploration into the biochemical and molecular dynamics underlying the induction of tetrasporogenesis in *A. armata*. Substantial transcriptomic changes were detected throughout all phases of tetrasporogenesis, while metabolic

changes were less conspicuous, likely attributed to methodological sensitivity constraints. Therefore, future investigations employing LC-MS-MS and/or alternative techniques (Kumar et al. 2016, Tanna and Mishra 2018) are recommended to gain deeper insights into the biochemical changes during tetrasporogenesis. Expression patterns of polyamine-related genes during pre-tetrasporogenesis imply their involvement in controlling tetrasporogenesis in *A. armata*, consistent with prior research demonstrating the role of polyamines in regulating various reproductive processes in seaweeds (Sacramento et al. 2004, Sacramento et al. 2007, Kumar et al. 2015). Further targeted exploration of polyamine-related genes, potentially in conjunction with exposing cultures to polyamines during induction (similar to the approach taken with methyl jasmonate in *Grateloupia* spp. (Pilar et al. 2016, Garcia-Jimenez et al. 2017)), is warranted to elucidate their contribution to tetrasporogenesis in *A. armata*. Certain metabolites, enzymes, and genes were pinpointed as potentially involved in regulating tetrasporogenesis in *A. armata*. Nevertheless, many identified genes, similar to reproductive sex-biased genes identified in *A. taxiformis* (Patwary et al. 2023), remain classified as hypothetical or unnamed. The ambiguity of these classifications could be attributed to the unique roles of genes involved the reproduction of red seaweeds, influenced by the rapid evolutionary rates of reproduction-associated genes (Liu et al. 2017, Hatchett et al. 2023). The scarcity of molecular data relating to seaweed reproduction also presents further challenges for classification (García-Jiménez and Robaina 2015, Kumar et al. 2015). This emphasises the need for further molecular research aimed at the structural and functional characterisation of genes involved in biochemical pathways with prospective links to seaweed reproduction. For instance, focusing on genes linked to steroid hormone pathways, primarily annotated to animal sex hormone production in this study, could provide valuable insights into seaweed metabolites with modulating roles in reproduction.

Nonetheless, the absence of an assembled reference genome for *A. armata* remains a significant bottleneck, hindering efforts to conduct high-quality comparative transcriptomic and proteomic analyses aimed at identifying candidate tetrasporogenesis-associated genes. To address this limitation, the next logical step should be to prioritise the assembly of a reference genome for *A. armata*.

6.3. Conclusion

This thesis addresses key knowledge gaps for understanding the biology and developing closed-life cycle cultivation of *A. armata* within four research areas that have not previously been addressed.

1) The assessment of reproductive phenology demonstrated changes in the timing and extent of reproductive processes and provides a detailed measurable baseline to detect future phenological shifts.
2) The hatchery cultivation experiments delivered comprehensive methods for mass induction and release of tetraspores and attaining a high degree of control over tetrasporogenesis to enable commercial hatchery production.
3) The nursery cultivation experiments identified temperature and water flow as pivotal drivers of juvenile gametophyte growth and development and defined the necessary cultivation conditions for facilitating the establishment of commercial nurseries.
4) The metabolomic and transcriptomic analyses demonstrated that multiple mechanisms are involved in regulating tetrasporogenesis in *Asparagopsis* and

identified key directions for future research in this emerging field within phycology.

Collectively, these findings substantially drive our progress towards achieving closed-life cycle aquaculture of *A. armata*, providing a framework upon which to implement commercial production. Moreover, they improve our understanding of seaweed reproduction from both exogenous and endogenous perspectives. The latter will be particularly crucial as *Asparagopsis* aquaculture evolves, leading to genetic optimisation and further strain selection.

In summary, this thesis advances understanding of diverse aspects of *Asparagopsis* biology and aquaculture, spanning knowledge of reproductive phenology, the innovation of hatchery and nursery protocols, and the elucidation of biochemical and molecular mechanisms governing reproduction. To deepen understanding of *A. armata* biology and further progress closed life cycle aquaculture development, future research should focus on:

1) Understanding the environmental factors affecting *A. armata* gametophyte reproduction to verify climate-driven shifts in reproductive phenology and guide aquaculture practises; and implementing repeated sampling across multiple sites to enhance our comprehension of *A. armata* reproductive phenology and provide insights for broader aquaculture applications.
2) Refining line seeding techniques and automating processes, streamlining the design of hatcheries and nurseries, assessing strategies to enhance gametophyte temperature tolerance for resilient aquaculture in the face of climate change, and determining optimal nursery duration through outplanting trials.
3) Further exploring the role of PGRs on tetrasporogenesis, particularly focusing on polyamines, and continuing to decipher the intricate mechanisms underlying

seaweed reproduction to address existing knowledge gaps and support the development of selective breeding programs.

References

Abad, M., L. Bedoya, and P. Bermejo. 2011. Marine compounds and their antimicrobial activities. In: Science against microbial pathogens: communicating current research and technological advances, Formatex, Badajoz, Spain, pp 1293-1306.

Abbott, D. W., I. M. Aasen, K. A. Beauchemin, F. Grondahl, R. Gruninger, M. Hayes, S. Huws, D. A. Kenny, S. J. Krizsan, and S. F. Kirwan. 2020. Seaweed and seaweed bioactives for mitigation of enteric methane: challenges and opportunities. Animals **10**:2432.

Allen, M. R., O.P. Dube, W. Solecki, F. Aragón-Durand, W. Cramer, S. Humphreys, M. Kainuma, J. Kala, N. Mahowald, Y. Mulugetta, R. Perez, M. Wairiu, and K. Zickfeld. 2018. Framing and context. In: Global warming of 1.5°C. An IPCC special report on the impacts of global warming of 1.5°C above pre-industrial levels and related global greenhouse gas emission pathways, in the context of strengthening the global response to the threat of climate change, sustainable development, and efforts to eradicate poverty. Cambridge University Press, Cambridge, UK and New York, USA, pp 49-92.

Altschul, S. F., T. L. Madden, A. A. Schäffer, J. Zhang, Z. Zhang, W. Miller, and D. J. Lipman. 1997. Gapped BLAST and PSI-BLAST: a new generation of protein database search programs. Nucleic Acids Research **25**:3389-3402.

Amsler, C. D. 2008. Algal chemical ecology. Springer-Verlag, Berlin, Germany.

Amsler, C. D., and M. Neushul. 1989. Chemotactic effects of nutrients on spores of the kelps *Macrocytis pyrifera* and *Pterygophora california*. Marine Biology **102**:557-564.

Anderson, M., R. Gorley, K. Clarke, M. Anderson, R. Gorley, K. Clarke, M. Anderson, R. Gorley, and M. Andersom. 2008. PERMANOVA+ for PRIMER. Guide to software and statistical methods. PRIMER-E, Plymouth, UK.

Anis, M., S. Ahmed, and M. Hasan. 2017. Algae as nutrition, medicine and cosmetic: the forgotten history, present status and future trends. World Journal of Pharmacy and Pharmaceutical Sciences **6**:1934-1959.

Anwar, A., M. She, K. Wang, B. Riaz, and X. Ye. 2018. Biological roles of ornithine aminotransferase (OAT) in plant stress tolerance: Present progress and future perspectives. International Journal of Molecular Sciences **19**:3681.

Aono, Y., and K. Kazui. 2008. Phenological data series of cherry tree flowering in Kyoto, Japan, and its application to reconstruction of springtime temperatures since the 9th century. International Journal of Climatology **28**:905-914.

Arndt, C., A. N. Hristov, W. J. Price, S. C. McClelland, A. M. Pelaez, S. F. Cueva, J. Oh, J. Dijkstra, A. Bannink, A. R. Bayat, L. A. Crompton, M. A. Eugène, D. Enahoro, E. Kebreab, M. Kreuzer, M. McGee, C. Martin, C. J. Newbold, C. K. Reynolds, A. Schwarm, K. J. Shingfield, J. B. Veneman, D. R. Yáñez-Ruiz, and Z. Yu. 2022. Full adoption of the most effective strategies to mitigate methane emissions by ruminants can help meet the 1.5 °C target by 2030 but not 2050. Proceedings of the National Academy of Sciences **119**:e2111294119.

Asami, T., T. Nakano, and S. Fujioka. 2005. Plant brassinosteroid hormones. Vitamins and Hormones **72**:479-504.

Asch, R. G. 2015. Climate change and decadal shifts in the phenology of larval fishes in the California Current ecosystem. Proceedings of the National Academy of Sciences **112**:e4065-e4074.

Auckland Council. 2023. Environmental data portal. Available at: http://environmentauckland.org.nz.

Azanza, R. V., and T. T. Aliaza. 1999. In vitro carpospore release and germination in *Kappaphycus alvarezii* (Doty) Doty from Tawi-Tawi, Philippines. Botanica Marina **42**:281-284.

Bansemir, A., M. Blume, S. Schröder, and U. Lindequist. 2006. Screening of cultivated seaweeds for antibacterial activity against fish pathogenic bacteria. Aquaculture **252**:79-84.

Bartsch, I., J. Vogt, C. Pehlke, and D. Hanelt. 2013. Prevailing sea surface temperatures inhibit summer reproduction of the kelp *Laminaria digitata* at Helgoland (North Sea). Journal of Phycology **49**:1061-1073.

Basarab, J. A., K. A. Beauchemin, V. S. Baron, K. H. Ominski, L. L. Guan, S. P. Miller, and J. J. Crowley. 2013. Reducing GHG emissions through genetic improvement for feed efficiency: effects on economically important traits and enteric methane production. Animal **7**:303-315.

Batista, M. 2020. Reproduction and cultivation of *Asparagopsis taxiformis* (Delile) Trevisan. Master's Dissertation, Universidade do Algarve, Portugal.

Bayat, A. R., I. Tapio, J. Vilkki, K. J. Shingfield, and H. Leskinen. 2018. Plant oil supplements reduce methane emissions and improve milk fatty acid composition in dairy cows fed grass silage-based diets without affecting milk yield. Journal of Dairy Science **101**:1136-1151.

Beauchemin, K. A., M. Kreuzer, F. O'Mara, and T. A. McAllister. 2008. Nutritional management for enteric methane abatement: A review. Australian Journal of Experimental Agriculture **48**:21-27.

Beauchemin, K. A., E. M. Ungerfeld, A. L. Abdalla, C. Alvarez, C. Arndt, P. Becquet, C. Benchaar, A. Berndt, R. M. Mauricio, T. A. McAllister, W. Oyhantçabal, S. A. Salami, L. Shalloo, Y. Sun, J. Tricarico, A. Uwizeye, C. De Camillis, M. Bernoux, T. Robinson, and E. Kebreab. 2022. Invited review: Current enteric methane mitigation options. Journal of Dairy Science **105**:9297-9326.

Beaugrand, G. 2009. Decadal changes in climate and ecosystems in the North Atlantic Ocean. Deep Sea Research Part II: Topical Studies in Oceanography **56**:656-673.

Beef+LambNZ. 2017. Guide to New Zealand cattle farming. Beef+Lamb New Zealand, Wellington, New Zealand.

Behera, D. P., K. N. Ingle, D. E. Mathew, A. Dhimmar, H. Sahastrabudhe, S. K. Sahu, M. G. Krishnan, P. B. Shinde, M. Ganesan, and V. A. Mantri. 2022. Epiphytism, diseases and grazing in seaweed aquaculture: A comprehensive review. Reviews in Aquaculture **14**:1345-1370.

Blunt, J. W., B. R. Copp, W.-P. Hu, M. H. Munro, P. T. Northcote, and M. R. Prinsep. 2007. Marine natural products. Natural product reports **24**:31-86.

Blunt, J. W., B. R. Copp, W.-P. Hu, M. H. Munro, P. T. Northcote, and M. R. Prinsep. 2009. Marine natural products. Natural product reports **26**:170-244.

Boderskov, T., M. M. Nielsen, M. B. Rasmussen, T. J. S. Balsby, A. Macleod, S. L. Holdt, J. J. Sloth, and A. Bruhn. 2021a. Effects of seeding method, timing and site selection on the production and quality of sugar kelp, *Saccharina latissima*: A Danish case study. Algal Research **53**:102160.

Boderskov, T., M. B. Rasmussen, and A. Bruhn. 2021b. Obtaining spores for the production of *Saccharina latissima*: seasonal limitations in nature, and induction of sporogenesis in darkness. Journal of Applied Phycology **33**:1035-1046.

Bolton, J. 2020. The problem of naming commercial seaweeds. Journal of Applied Phycology **32**:1-8.

Bonin, D. R., and M. W. Hawkes. 1987. Systematics and life histories of New Zealand Bonnemaisoniaceae (Bonnemaisoniales, Rhodophyta): I. The genus *Asparagopsis*. New Zealand Journal of Botany **25**:577-590.

Boucher, O., P. Friedlingstein, B. Collins, and K. P. Shine. 2009. The indirect global warming potential and global temperature change potential due to methane oxidation. Environmental Research Letters **4**:044007.

Brawley, S. H., and L. E. Johnson. 1992. Gametogenesis, gametes and zygotes: An ecological perspective on sexual reproduction in the algae. British Phycological Journal **27**:233-252.

Brooke, C. G., B. M. Roque, C. Shaw, N. Najafi, M. Gonzalez, A. Pfefferlen, V. DeAnda, D. W. Ginsburg, M. C. Harden, S. V. Nuzhdin, J. K. Salwen, E. Kebreab, and M. Hess. 2020. Methane reduction potential of two pacific coast macroalgae during in vitro ruminant fermentation. Frontiers in Marine Science **7**:561.

Buchfink, B., C. Xie, and D. H. Huson. 2015. Fast and sensitive protein alignment using DIAMOND. Nature Methods **12**:59-60.

Burrows, M. T., D. S. Schoeman, L. B. Buckley, P. Moore, E. S. Poloczanska, K. M. Brander, C. Brown, J. F. Bruno, C. M. Duarte, B. S. Halpern, J. Holding, C. V. Kappel, W. Kiessling, M. I. O'Connor, J. M. Pandolfi, C. Parmesan, F. B. Schwing, W. J. Sydeman, and A. J. Richardson. 2011. The pace of shifting climate in marine and terrestrial ecosystems. Science **334**:652.

Burtin, P. 2003. Nutritional value of seaweeds. Electronic journal of Environmental, Agricultural and Food chemistry **2**:498-503.

Buschmann, A. H., and C. Camus. 2019. An introduction to farming and biomass utilisation of marine macroalgae. Phycologia **58**:443-445.

Buschmann, A. H., C. Camus, J. Infante, A. Neori, Á. Israel, M. C. Hernández-González, S. V. Pereda, J. L. Gomez-Pinchetti, A. Golberg, N. Tadmor-Shalev, and A. T. Critchley. 2017. Seaweed production: overview of the global state of exploitation, farming and emerging research activity. European Journal of Phycology **52**:391-406.

Butler, A., and J. N. Carter-Franklin. 2004. The role of vanadium bromoperoxidase in the biosynthesis of halogenated marine natural products. Natural product reports **21**:180-188.

Butler, A., and M. Sandy. 2009. Mechanistic considerations of halogenating enzymes. Nature **460**:848-854.

Cabrita, M. T., C. Vale, and A. P. Rauter. 2010. Halogenated compounds from marine algae. Marine drugs **8**:2301-2317.

Caines, S., J. A. Manríquez-Hernández, J. Duston, P. Corey, and D. J. Garbary. 2014. Intermittent aeration affects the bioremediation potential of two red algae cultured in finfish effluent. Journal of Applied Phycology **26**:2173-2181.

Camus, C., and A. H. Buschmann. 2017. *Macrocystis pyrifera* aquafarming: Production optimization of rope-seeded juvenile sporophytes. Aquaculture **468**:107-114.

Caro, D., E. Kebreab, and F. Mitloehner. 2016. Mitigation of enteric methane emissions from global livestock systems through nutrition strategies. Climatic Change **137**:467-480.

Chagas, J. C., M. Ramin, and S. J. Krizsan. 2019. In vitro evaluation of different dietary methane mitigation strategies. Animals **9**:1120.

Charrier, B., M. H. Abreu, R. Araujo, A. Bruhn, J. C. Coates, O. De Clerck, C. Katsaros, R. R. Robaina, and T. Wichard. 2017. Furthering knowledge of seaweed growth and development to facilitate sustainable aquaculture. New Phytologist **216**:967-975.

Chijioke, A. O., and E. S. Rudinow. 2018. Meta-analysis of methane mitigation strategies: Improved predictions of mitigation potentials and production implications. Iranian Journal of Applied Animal Science **8**:567-573.

Choi, H. G., Y. S. Kim, J. H. Kim, S. J. Lee, E. J. Park, J. Ryu, and K. W. Nam. 2006. Effects of temperature and salinity on the growth of *Gracilaria verrucosa* and *G. chorda*, with the potential for mariculture in Korea. Journal of Applied Phycology **18**:269-277.

Chopin, T., and A. G. J. Tacon. 2021. Importance of seaweeds and extractive species in global aquaculture production. Reviews in Fisheries Science & Aquaculture **29**:139-148.

Chualáin, F. N., C. A. Maggs, G. W. Saunders, and M. D. Guiry. 2004. The invasive genus *Asparagopsis* (Bonnemaisoniaceae, Rhodophyta): Molecular systematics, morpholoy, and ecophysiology of *Falkenbergia* isolates. Journal of Phycology **40**:1112-1126.

Clark, H., F. Kelliher, and C. Pinares-Patino. 2011. Reducing CH4 emissions from grazing ruminants in New Zealand: challenges and opportunities. Asian-Australasian Journal of Animal Sciences **24**:295-302.

Cleland, E. E., I. Chuine, A. Menzel, H. A. Mooney, and M. D. Schwartz. 2007. Shifting plant phenology in response to global change. Trends in Ecology & Evolution **22**:357-365.

Climate Action Tracker. 2023. Available at: http://www.climateactiontracker.org/countries/new-zealand/. Accessed 9 Oct. 2023.

Climate Change Comission. 2023. Full report: 2023 Draft advice to inform the strategic direction of the Government's second emissions reduction plan (April 2023).

ClimateWatch. 2022. Available at: https://www.climatewatchdata.org/sectors/agriculture?contextBy=indicator#drivers-of-emissions. Wasington, DC, World Resources Institute.

Collins, W. J., C. P. Webber, P. M. Cox, C. Huntingford, J. Lowe, S. Sitch, S. E. Chadburn, E. Comyn-Platt, A. B. Harper, and G. Hayman. 2018. Increased importance of methane reduction for a 1.5 degree target. Environmental Research Letters **13**:054003.

Cook, F., R. O. Smith, M. Roughan, N. J. Cullen, N. Shears, and M. Bowen. 2022. Marine heatwaves in shallow coastal ecosystems are coupled with the atmosphere: Insights from half a century of daily in situ temperature records. Frontiers in Climate **4**.

Davidson, N. M., and A. Oshlack. 2014. Corset: enabling differential gene expression analysis for *de novo*assembled transcriptomes. Genome Biology **15**:410.

Davies, P. J. 2004. Plant hormones: biosynthesis, signal transduction, action! Springer-Dordrecht, Berlin, Germany.

de Bettignies, T., T. Wernberg, and C. F. D. Gurgel. 2018. Exploring the influence of temperature on aspects of the reproductive phenology of temperate seaweeds. Frontiers in Marine Science **5**:1-8.

de Haas, Y., J. J. Windig, M. P. L. Calus, J. Dijkstra, M. de Haan, A. Bannink, and R. F. Veerkamp. 2011. Genetic parameters for predicted methane production and potential for reducing enteric emissions through genomic selection. Journal of Dairy Science **94**:6122-6134.

de Nys, R., M. Tatsumi, M. Magnusson, A. Mihaila, C. Glasson, and R. Lawton. 2023. *Asparagopsis* life cycle improvements, AU Patent No. PCT/AU2023/050396.

De Wreede, R., and T. Klinger. 1988. Reproductive strategies in algae. Plant reproductive ecology: patterns and strategies, Oxford University Press, USA, pp 267-284.

DeBusk, T. A., and J. H. Ryther. 1984. Effects of seawater exchange, pH and carbon supply on the growth of *Gracilaria tikvahiae* (Rhodophyceae) in large-scale cultures. Botanica Marina **27**:357-362.

Denman, S. E., N. W. Tomkins, and C. S. McSweeney. 2007. Quantitation and diversity analysis of ruminal methanogenic populations in response to the antimethanogenic compound bromochloromethane. FEMS Microbiology Ecology **62**:313-322.

Dijoux, L., F. Viard, and C. Payri. 2014. The more we search, the more we find: Discovery of the new lineage and a new species complex in the genus *Asparagopsis*. PLOS ONE **9**:e103826.

Dillehay, T., C. Ramírez, M. Pino, M. Collins, J. Rossen, and J. Pino-Navarro. 2008. Monte Verde: Seaweed, food, medicine, and the peopling of South America. Science **320**:784-786.

DSM. 2019. Summary of scientific research how 3-NOP effectively reduces enteric methane emissions from cows. Version 1. 7th Greenhouse Gas and Animal Agriculture Conference, Brazil.

Duarte, C. M., J. Wu, X. Xiao, A. Bruhn, and D. Krause-Jensen. 2017. Can seaweed farming play a role in climate change mitigation and adaptation? Frontiers in Marine Science **4**:100.

Durmic, Z., P. J. Moate, R. Eckard, D. K. Revell, R. Williams, and P. E. Vercoe. 2014. In vitro screening of selected feed additives, plant essential oils and plant extracts for rumen methane mitigation. Journal of the Science of Food and Agriculture **94**:1191-1196.

Dwivedi, S., E. Perotti, and R. Ortiz. 2008. Towards molecular breeding of reproductive traits in cereal crops. Plant Biotechnology Journal **6**:529-559.

Eggert, A. 2012. Seaweed responses to temperature. Seaweed biology: Novel insights into ecophysiology, ecology and utilization. Springer-Verlag, Berlin, Germany, pp 47-66.

Endo, H., Y. Okumura, Y. Sato, and Y. Agatsuma. 2017. Interactive effects of nutrient availability, temperature, and irradiance on photosynthetic pigments and color of the brown alga *Undaria pinnatifida*. Journal of Applied Phycology **29**:1683-1693.

FAO. 2018a. The global status of seaweed production, trade, and utilization. Globefish Research Programme Volume 124. Food and agriculture organization of the United States, Rome, Italy.

FAO. 2018b. The State of World Fisheries and Aquaculture 2018 - Meeting the sustainable development goals. Food and agriculture organization of the United States, Rome, Italy.

FAO. 2020. The State of World Fisheries and Aquaculture 2020. Sustainability in action. Food and agriculture organization of the United States, Rome, Italy.

FAO. 2022. The State of World Fisheries and Aquaculture 2022. Towards blue transformation. Food and agriculture organization of the United Nations, Rome, Italy.

FAO, and WHO. 2022. Report of the expert meeting on food safety for seaweed - Current status and future perspectives. Rome, 28 -29 October 2021. Food safety and quality series No. 13. Food and agriculture organization of the United Nations, Rome, Italy.

Fernand, F., A. Israel, J. Skjermo, T. Wichard, K. R. Timmermans, and A. Golberg. 2017. Offshore macroalgae biomass for bioenergy production: Environmental aspects, technological achievements and challenges. Renewable and Sustainable Energy Reviews **75**:35-45.

Fitter, A. H., R. S. R. Fitter, I. T. B. Harris, and M. H. Williamson. 1995. Relationships between first flowering date and temperature in the flora of a locality in central England. Functional Ecology **9**:55-60.

Forbord, S., K. B. Steinhovden, T. Solvang, A. Handå, and J. Skjermo. 2020. Effect of seeding methods and hatchery periods on sea cultivation of *Saccharina latissima* (Phaeophyceae): a Norwegian case study. Journal of Applied Phycology **32**:2201-2212.

Forsberg, N., and J. B. Russell. 1986. Production of tricarballylic acid by rumen microorganisms and its potential toxicity in ruminant tissue metabolism. British Journal of Nutrition **56**:153-162.

Fujioka, S., and T. Yokota. 2003. Biosynthesis and metabolism of brassinosteroids. Annual Review of Plant Biology **54**:137-164.

García-Jiménez, P., F. García-Maroto, J. A. Garrido-Cárdenas, C. Ferrandiz, and R. R. Robaina. 2009. Differential expression of the ornithine decarboxylase gene during carposporogenesis in the thallus of the red seaweed *Grateloupia imbricata* (Halymeniaceae). Journal of Plant Physiology **166**:1745-1754.

Garcia-Jimenez, P., C. Llorens, F. J. Roig, and R. R. Robaina. 2018. Analysis of the transcriptome of the red seaweed *Grateloupia imbricata* with emphasis on reproductive potential. Marine drugs **16**:490.

Garcia-Jimenez, P., M. Montero-Fernández, and R. R. Robaina. 2017. Molecular mechanisms underlying *Grateloupia imbricata* (Rhodophyta) carposporogenesis induced by methyl jasmonate. Journal of Phycology **53**:1340-1344.

Garcia-Jimenez, P., and R. Robaina. 2017. Volatiles in the aquatic marine ecosystem: Ethylene and related plant hormones and sporulation in red seaweeds. Systems Biology of Marine Ecosystems. Springer, Cham, Switzerland, pp 99-116.

García-Jiménez, P., and R. R. Robaina. 2012. Effects of ethylene on tetrasporogenesis in *Pterocladiella capillaceae* (Rhodophyta). Journal of Phycology **48**:710-715.

García-Jiménez, P., and R. R. Robaina. 2015. On reproduction in red algae: further research needed at the molecular level. Frontiers in Plant Science **6**:93.

Ge, Q., H. Wang, T. Rutishauser, and J. Dai. 2015. Phenological response to climate change in China: a meta-analysis. Global Change Biology **21**:265-274.

Gerard, V. A. 1982. In situ water motion and nutrient uptake by the giant kelp *Macrocystis pyrifera*. Marine Biology **69**:51-54.

Gerard, V. A., and K. H. Mann. 1979. Growth and production of *Laminaria longicruris* (Phaeophyta) populations exposed to different intensities of water movement. Journal of Phycology **15**:33-41.

Gerber, P. J., B. Henderson, H. Makkar, A. Hristov, J. Oh, C.-C. Lee, R. Meinen, F. Montes, T. Ott, J. Firkins, C. A. Rotz, C. Dell, A. Adesogan, W. Yang, J. Tricarico, E. Kebreab, G. Waghorn, J. Dijkstra, and S. Oosting. 2013. Mitigation of greenhouse gas emissions in livestock production-a review of technical options for non-CO2 emissions. No.177. Food and agriculture organization of the United Nations, Rome, Italy.

Gerwick, W., M. Bernart, M. Moghaddam, Z. Jiang, M. Solem, and D. Nagle. 1990. Eicosanoids from the Rhodophyta: New metabolism in the algae. Hydrobiologia **204-205**:621-628.

Gibbs, J. P., and A. R. Breisch. 2001. Climate warming and calling phenology of frogs near Ithaca, New York, 1900–1999. Conservation Biology **15**:1175-1178.

Gillaspy, G. E. 2011. The cellular language of myo-inositol signaling. New Phytologist **192**:823-839.

Glasson, C. R. K., R. D. Kinley, R. de Nys, N. King, S. L. Adams, M. A. Packer, J. Svenson, C. T. Eason, and M. Magnusson. 2022. Benefits and risks of including the bromoform containing seaweed *Asparagopsis* in feed for the reduction of methane production from ruminants. Algal Research **64**:e102673.

Glenn, E. P., and M. S. Doty. 1992. Water motion affects the growth rates of *Kappaphycus alvarezii* and related red seaweeds. Aquaculture **108**:233-246.

Gonen, Y., E. Kimmel, and M. Friedlander. 1993. Effect of relative water motion on photosynthetic rate of red alga *Gracilaria conferta*. Hydrobiologia **260/261**:493-498.

Gordo, O., L. Brotons, X. Ferrer, and P. Comas. 2005. Do changes in climate patterns in wintering areas affect the timing of the spring arrival of trans-Saharan migrant birds? Global Change Biology **11**:12-21.

Gordo, O., and J. J. Sanz. 2005. Phenology and climate change: a long-term study in a Mediterranean locality. Oecologia **146**:484-495.

Götz, S., J. M. García-Gómez, J. Terol, T. D. Williams, S. H. Nagaraj, M. J. Nueda, M. Robles, M. Talón, J. Dopazo, and A. Conesa. 2008. High-throughput functional annotation and data mining with the Blast2GO suite. Nucleic Acids Research **36**:3420-3435.

Grabherr, M. G., B. J. Haas, M. Yassour, J. Z. Levin, D. A. Thompson, I. Amit, X. Adiconis, L. Fan, R. Raychowdhury, Q. Zeng, Z. Chen, E. Mauceli, N. Hacohen, A. Gnirke, N. Rhind, F. di Palma, B. W. Birren, C. Nusbaum, K. Lindblad-Toh, N. Friedman, and A. Regev. 2011. Full-length transcriptome assembly from RNA-Seq data without a reference genome. Nature Biotechnology **29**:644-652.

Graiff, A., D. Liesner, U. Karsten, and I. Bartsch. 2015. Temperature tolerance of western Baltic Sea *Fucus vesiculosus* – growth, photosynthesis and survival. Journal of Experimental Marine Biology and Ecology **471**:8-16.

Grainger, C., M. J. Auldist, T. Clarke, K. A. Beauchemin, S. M. McGinn, M. C. Hannah, R. J. Eckard, and L. B. Lowe. 2008. Use of monensin controlled-release capsules to reduce methane emissions and improve milk production of dairy cows offered pasture supplemented with grain. Journal of Dairy Science **91**:1159-1165.

Guillemin, M. L., P. Valenzuela, J. D. Gaitán-Espitia, and C. Destombe. 2014. Evidence of reproductive cost in the triphasic life history of the red alga *Gracilaria chilensis* (Gracilariales, Rhodophyta). Journal of Applied Phycology **26**:569-575.

Guinguina, A., M. Hayes, F. Gröndahl, and S. Krizsan. 2023. *Bonnemaisonia hamifera*, a temperate macroalga to reduce methane emissions from ruminants. Animals **13**:2925.

Guiry, M. D. 1984. Photoperiodic and temperature responses in the growth and tetrasporogenesis of *Gigartina acicularis* (Rhodophyta) from Ireland. Helgoländer Meeresuntersuchungen **38**:335.

Guiry, M. D., and C. J. Dawes. 1992. Daylength, temperature and nutrient control of tetrasporogenesis in *Asparagopsis armata* (Rhodophyta). Journal of Experimental Marine Biology and Ecology **158**:197-217.

Gupta, V., R. Thakur, R. Baghel, C. R. K. Reddy, and B. Jha. 2014. Seaweed metabolomics: A new facet of functional genomics. Advances in Botanical Research, Academic Press, Elsevier Limited, pp 31-52.

Guschina, I. A., and J. L. Harwood. 2009. Algal lipids and effect of the environment on their biochemistry. Lipids in Aquatic Ecosystems. Springer, New York, pp 1-24.

Guzmán-Urióstegui, A., P. García-Jiménez, F. Marián, D. Robledo, and R. Robaina. 2002. Polyamines influence maturation in reproductive structures of *Gracilaria cornea* (Gracilariales, Rhodophyta). Journal of Phycology **38**:1169-1175.

Hammond, K. J., J. L. Burke, J. P. Koolaard, S. Muetzel, C. S. Pinares-Patiño, and G. C. Waghorn. 2013. Effects of feed intake on enteric methane emissions from sheep fed fresh white clover (*Trifolium repens*) and perennial ryegrass (*Lolium perenne*) forages. Animal Feed Science and Technology **179**:121-132.

Han, M., C. Zhang, P. Suglo, S. Sun, M. Wang, and T. Su. 2021. l-Aspartate: An essential metabolite for plant growth and stress acclimation. Molecules **26**:1877.

Harnedy, P. A., and R. J. FitzGerald. 2011. Bioactive proteins, peptides, and amino acids from macroalgae. Journal of Phycology **47**:218-232.

Harrison, P., and C. Hurd. 2001. Nutrient physiology of seaweeds: Application of concepts to aquaculture. Cahiers De Biologie Marine **42**:71-82.

Hart, K. J., J. A. Huntington, R. G. Wilkinson, C. G. Bartram, and L. A. Sinclair. 2015. The influence of grass silage-to-maize silage ratio and concentrate composition on methane emissions, performance and milk composition of dairy cows. Animal **9**:983-991.

Hatchett, W. J., A. O. Jueterbock, M. Kopp, J. A. Coyer, S. M. Coelho, G. Hoarau, and A. P. Lipinska. 2023. Evolutionary dynamics of sex-biased gene expression in a young XY system: insights from the brown alga genus Fucus. New Phytologist **238**:422-437.

Hoffmann, A. J. 1987. The arrival of seaweed propagules at the shore: A review. Botanica Marina **30**:151-166.

Holdt, S. L., and S. Kraan. 2011. Bioactive compounds in seaweed: functional food applications and legislation. Journal of Applied Phycology **23**:543-597.

Howells, R. J., S. J. Burthe, J. A. Green, M. P. Harris, M. A. Newell, A. Butler, D. G. Johns, E. J. Carnell, S. Wanless, and F. Daunt. 2017. From days to decades: short- and long-term variation in environmental conditions affect offspring diet composition of a marine top predator. Marine Ecology Progress Series **583**:227-242.

Hristov, A. N., J. Oh, J. L. Firkins, J. Dijkstra, E. Kebreab, G. Waghorn, H. P. S. Makkar, A. T. Adesogan, W. Yang, C. Lee, P. J. Gerber, B. Henderson, and J. M. Tricarico. 2013. Special topics — Mitigation of methane and nitrous oxide emissions from animal operations: I. A review of enteric methane mitigation options. Journal of Animal Science **91**:5045-5069.

Hunter, S. 2022. Asexual cultivation techniques of the red macroalgae *Asparagopsis taxiformis* for commercial application. Master's Dissertation, Murdoch University, Western Australia.

Hurd, C. L. 2000. Water motion, marine macroalgal physiology, and production. Journal of Phycology **36**:453-472.

Hurd, C. L. 2017. Shaken and stirred: the fundamental role of water motion in resource acquisition and seaweed productivity. Perspectives in Phycology **4**:73-81.

Hurd, C. L., P. J. Harrison, K. Bischof, and C. S. Lobban. 2014. Seaweed ecology and physiology. 2nd edition. Cambridge University Press, Cambridge, UK.

Hutjens, M. F. 1991. Feed additives. Veterinary Clinics of North America: Food Animal Practice **7**:525-540.

Hutson, K. S., L. Mata, N. A. Paul, and R. de Nys. 2012. Seaweed extracts as a natural control against the monogenean ectoparasite, *Neobenedenia* sp., infecting farmed barramundi (*Lates calcarifer*). **42**:1135-1141.

Hwang, E. K., N. Yotsukura, S. J. Pang, L. Su, and T. F. Shan. 2019. Seaweed breeding programs and progress in eastern Asian countries. Phycologia **58**:484-495.

Ims, R. A. 1990. The ecology and evolution of reproductive synchrony. Trends in Ecology & Evolution **5**:135-140.

IPCC. 2007. Climate change 2007: Synthesis report. Contribution of working groups I, II and III to the fourth assessment report of the Intergovernmental Panel on Climate Change [Core writing team, Pachauri, R.K and Reisinger, A. (eds.)]. IPCC, Geneva, Switzerland.

IPCC. 2014. Climate change 2014: Synthesis report. Contribution of working groups I, II and III to the fifth assessment report of the Intergovernmental Panel on Climate Change [Core writing team, R.K. Pachauri and L.A. Meyer (eds.)]. IPCC, Geneva, Switzerland.

IPCC. 2018. Global warming of 1.5°C. An IPCC special report on the impacts of global warming of 1.5°C above pre-industrial levels and related global greenhouse gas emission pathways, in the context of strengthening the global response to the threat of climate change, sustainable development, and efforts to eradicate poverty [Masson-Delmotte, V., P. Zhai, H.-O. Pörtner, D. Roberts, J. Skea, P.R. Shukla, A. Pirani, W. Moufouma-Okia, C. Péan, R. Pidcock, S. Connors, J.B.R. Matthews, Y. Chen, X. Zhou, M.I. Gomis, E. Lonnoy, T. Maycock, M. Tignor, and T. Waterfield (eds.)]. World Meteorological Organization, Geneva, Swizterland.

Iqbal, N., N. A. Khan, A. Ferrante, A. Trivellini, A. Francini, and M. I. R. Khan. 2017. Ethylene role in plant growth, development and senescence: Interaction with other phytohormones. Frontiers in Plant Science **8**:475.

Ito, K., and K. Hori. 1989. Seaweed: Chemical composition and potential food uses. Food Reviews International **5**:101-144.

Jansen, H. M., M. S. Bernard, M. A. J. Nederlof, I. M. van der Meer, and A. van der Werf. 2022. Seasonal variation in productivity, chemical composition and nutrient uptake of *Ulva* spp. (Chlorophyta) strains. Journal of Applied Phycology **34**:1649-1660.

Jayanegara, A., K. A. Sarwono, M. Kondo, H. Matsui, M. Ridla, E. B. Laconi, and Nahrowi. 2018. Use of 3-nitrooxypropanol as feed additive for mitigating enteric methane emissions from ruminants: a meta-analysis. Italian Journal of Animal Science **17**:650-656.

Jeliani, Z. Z., M. Yousefzadi, J. S. Pour, and H. Toiserkani. 2018. Growth, phytochemicals, and optimal timing of planting *Gracilariopsis persica*: an economic red seaweed. Journal of Applied Phycology **30**:525-533.

Johnson, J. R., G. E. Carstens, W. K. Krueger, P. A. Lancaster, E. G. Brown, L. O. Tedeschi, R. C. Anderson, K. A. Johnson, and A. Brosh. 2019. Associations between residual feed intake and apparent nutrient digestibility, in vitro methane-producing activity, and volatile fatty acid concentrations in growing beef cattle. Journal of Animal Science **97**:3550-3561.

Jueterbock, A., A. J. P. Minne, J. M. Cock, M. A. Coleman, T. Wernberg, L. Scheschonk, R. Rautenberger, J. Zhang, and Z.-M. Hu. 2021. Priming of marine macrophytes for

enhanced restoration success and food security in future oceans. Frontiers in Marine Science **8**:658485.
Jun Pang, S., and K. Lüning. 2004. Breaking seasonal limitation: year-round sporogenesis in the brown alga *Laminaria saccharina* by blocking the transport of putative sporulation inhibitors. Aquaculture **240**:531-541.
Kai, T., K. Nimura, H. Yasui, and H. Mizuta. 2006. Regulation of sorus formation by auxin in Laminariales sporophyte. Journal of Applied Phycology **18**:95.
Kakinuma, M., I. Kaneko, D. A. Coury, T. Suzuki, and H. Amano. 2006. Isolation and identification of gametogenesis-related genes in *Porphyra yezoensis* (Rhodophyta) using subtracted cDNA libraries. Journal of Applied Phycology **18**:489-496.
Kato, M., M. Watari, T. Tsuge, S. Zhong, H. Gu, L.-J. Qu, T. Fujiwara, and T. Aoyama. 2024. Redundant function of the *Arabidopsis* phosphatidylinositol 4-phosphate 5-kinase genes PIP5K4–6 is essential for pollen germination. The Plant Journal **117**:212-225.
Kelly, J. 2020. Australian seaweed industry blueprint – a blueprint for growth. Agrifutures Australia, Wagga Wagga, Australia.
Kerrison, P. D., M. S. Stanley, M. Kelly, A. MacLeod, K. D. Black, and A. D. Hughes. 2016. Optimising the settlement and hatchery culture of *Saccharina latissima* (Phaeophyta) by manipulation of growth medium and substrate surface condition. Journal of Applied Phycology **28**:1181-1191.
Key, N., and G. Tallard. 2012. Mitigating methane emissions from livestock: A global analysis of sectoral policies. Climatic Change **112**:387-414.
Khan, W., U. Menon, S. Subramanian, M. Jithesh, P. Rayorath, D. Hodges, A. Critchley, J. Craigie, J. Norrie, and B. Prithiviraj. 2009. Seaweed extracts as biostimulants of plant growth and development. Journal of Plant Growth Regulation **28**:386-399.
Khozin-Goldberg, I., C. Bigogno, P. Shrestha, and Z. Cohen. 2002. Nitrogen starvation induces the accumulation of arachidonic acid in the freshwater green alga *Parietochloris incisa* (Trebuxiophyceae). Journal of Phycology **38**:991-994.
Kim, J., M. Stekoll, and C. Yarish. 2019. Opportunities, challenges and future directions of open-water seaweed aquaculture in the United States. Phycologia **58**:446-461.
Kim, J. K., C. Yarish, E. K. Hwang, M. Park, and Y. Kim. 2017. Seaweed aquaculture: cultivation technologies, challenges and its ecosystem services. Algae **32**:1-13.
Kinley, R., G. Martinez-Fernandez, M. Matthews, R. de Nys, M. Magnusson, and N. Tomkins. 2020. Mitigating the carbon footprint and improving productivity of ruminant livestock agriculture using a red seaweed. Journal of Cleaner Production **259**:e120836.
Kinley, R., S. Tan, J. Turnbull, S. Askew, and B. Roque. 2021. Changing the proportions of grass and grain in feed substrate impacts the efficacy of *Asparagopsis taxiformis* to inhibit methane production *in vitro*. American Journal of Plant Sciences **12**:1835-1858.
Kinley, R. D., R. de Nys, M. J. Vucko, L. Machado, and N. W. Tomkins. 2016. The red macroalgae *Asparagopsis taxiformis* is a potent natural antimethanogenic that reduces methane production during *in vitro* fermentation with rumen fluid. Animal Production Science **56**:282-289.
Kinley, R. D., and A. H. Fredeen. 2015. In vitro evaluation of feeding North Atlantic stormtoss seaweeds on ruminal digestion. Journal of Applied Phycology **27**:2387-2393.

Knapp, J. R., G. L. Laur, P. A. Vadas, W. P. Weiss, and J. M. Tricarico. 2014. Invited review: Enteric methane in dairy cattle production: Quantifying the opportunities and impact of reducing emissions. Journal of Dairy Science **97**:3231-3261.

Kokabi, K., O. Gorelova, T. Ismagulova, M. Itkin, S. Malitsky, S. Boussiba, A. Solovchenko, and I. Khozin-Goldberg. 2019. Metabolomic foundation for differential responses of lipid metabolism to nitrogen and phosphorus deprivation in an arachidonic acid-producing green microalga. Plant Science **283**:95-115.

Koketsu, K., S. Mitsuhashi, and K. Tabata. 2013. Identification of homophenylalanine biosynthetic genes from cyanobacterium *Nostoc punctiforme* PCC73102 and application to its microbial production by *Escherichia coli*. Applied and Environmental Microbiology **79**:2201–2208.

Kraan, S., and K. A. Barrington. 2005. Commercial farming of *Asparagopsis armata* (Bonnemaisoniceae, Rhodophyta) in Ireland, maintenance of an introduced species? Journal of Applied Phycology **17**:103-110.

Kregting, L., A. J. Blight, B. Elsäßer, and G. Savidge. 2016. The influence of water motion on the growth rate of the kelp *Laminaria digitata*. Journal of Experimental Marine Biology and Ecology **478**:86-95.

Kreusch, M., E. Poltronieri, F. Bouvie, D. T. Pereira, D. Batista, F. Ramlov, M. Maraschin, Z. L. Bouzon, and C. Simioni. 2019. Cellular responses of *Gelidium floridanum* (Gelidiales, Rhodophyta) tetraspores under heat wave and copper pollution. Journal of Phycology **55**:1394-1400.

Krizsan, S. J., M. Ramin, J. C. C. Chagas, A. Halmemies-Beauchet-Filleau, A. Singh, A. Schnürer, and R. Danielsson. 2023. Effects on rumen microbiome and milk quality of dairy cows fed a grass silage-based diet supplemented with the macroalga *Asparagopsis taxiformis*. Frontiers in Animal Science **4**:1112969.

Krone, U. E., K. Laufer, R. K. Thauer, and H. P. Hogenkamp. 1989. Coenzyme F430 as a possible catalyst for the reductive dehalogenation of chlorinated C1 hydrocarbons in methanogenic bacteria. Biochemistry **28**:10061-10065.

Kumar, M., U. Kuzhiumparambil, M. Pernice, Z. Jiang, and P. J. Ralph. 2016. Metabolomics: an emerging frontier of systems biology in marine macrophytes. Algal Research **16**:76-92.

Kumar, M., C. R. Reddy, and P. J. Ralph. 2015. Polyamines in morphogenesis and development: a promising research area in seaweeds. Frontiers in Plant Science **6**:27.

Kumar, Y. N., S. W. Poong, C. Gachon, J. Brodie, A. Sade, and P. E. Lim. 2020. Impact of elevated temperature on the physiological and biochemical responses of *Kappaphycus alvarezii* (Rhodophyta). PLOS ONE **15**:e0239097.

Leahy, S. C., L. Kearney, A. Reisinger, and H. Clark. 2019. Mitigating greenhouse gas emissions from New Zealand pasture-based livestock farm systems. Journal of New Zealand Grasslands **81**:101-110.

Leal, P. P., M. Y. Roleda, P. A. Fernández, U. Nitschke, and C. L. Hurd. 2021. Reproductive phenology and morphology of *Macrocystis pyrifera* (Laminariales, Ochrophyta) from southern New Zealand in relation to wave exposure. Journal of Phycology **57**:1619-1635.

Lee, J.-A., and B. H. Brinkhuis. 1986. Reproductive phenology of *Laminaria saccharina* (L.) Lamour. (Phaeophyta) at the southern limit of its distribution in the northwestern Atlantic ocean. Journal of Phycology **22**:276-285.

Levy, I., S. Beer, and M. Friedlander. 1990. Strain selection in *Gracilaria* spp. 2. Selection for high and low temperature resistance in *G. verrucosa* sporelings. Journal of Applied Phycology **2**:163-171.

Li, B., and C. N. Dewey. 2011. RSEM: accurate transcript quantification from RNA-Seq data with or without a reference genome. BMC Bioinformatics **12**:323.

Li, J., Y. Li, S. Chen, and L. An. 2010. Involvement of brassinosteroid signals in the floral-induction network of *Arabidopsis*. Journal of Experimental Botany **61**:4221-4230.

Li, X., H. C. Norman, R. D. Kinley, M. Laurence, M. Wilmot, H. Bender, R. de Nys, and N. Tomkins. 2016. *Asparagopsis taxiformis* decreases enteric methane production from sheep. Animal Production Science **58**:681-688.

Liang, Z., X. Wang, P. Zhang, W. Liu, W. Wang, and F. Liu. 2023. Chronological development of the morphological, physiological, biochemical, and transcriptomic changes provides insights into the mechanisms of gametogenesis in *Saccharina japonica*. Journal of Applied Phycology **35**:785-802.

Lima, F. P., P. A. Ribeiro, N. Queiroz, S. J. Hawkins, and A. M. Santos. 2007. Do distributional shifts of northern and southern species of algae match the warming pattern? Global Change Biology **13**:2592-2604.

Lin, Y., K. Xu, Y. Xu, D. Ji, C. Chen, W. Wang, and C. Xie. 2021. Transcriptome co-expression network analysis identifies key genes regulating conchosporangia maturation of *Pyropia haitanensis*. Frontiers in Genetics **12**:680120.

Liu, N., X. Fu, D. Duan, J. Xu, X. Gao, and L. Zhao. 2018. Evaluation of bioactivity of phenolic compounds from the brown seaweed of *Sargassum fusiforme* and development of their stable emulsion. Journal of Applied Phycology **30**:1955-1970.

Liu, X., K. Bogaert, A. H. Engelen, F. Leliaert, M. Y. Roleda, and O. D. Clerck. 2017. Seaweed reproductive biology: environmental and genetic controls. Botanica Marina **60**:89-108.

Liu, Z., T. Zhou, and D. Gao. 2022. Genetic and epigenetic regulation of growth, reproduction, disease resistance and stress responses in aquaculture. Frontiers in Genetics **13**:994471.

Lobban, C. S., and P. J. Harrison. 1994. Morphology, life histories, and morphogenesis. In: Seaweed ecology and physiology. Cambridge University Press, Cambridge, UK, pp 1-68.

Loureiro, R., C. M. M. Gachon, and C. Rebours. 2015. Seaweed cultivation: potential and challenges of crop domestication at an unprecedented pace. New Phytologist **206**:489-492.

Lubchenco, J., and S. D. Gaines. 1981. A unified approach to marine plant-herbivore interactions. I. Populations and communities. Annual Review of Ecology and Systematics **12**:405-437.

Lüning, K. 1980. Critical levels of light and temperature regulating the gametogenesis of three Laminaria species (Phaeophyceae). Journal of Phycology **16**:1-15.

Lüning, K. 1981. Photomorphogenesis of reproduction in marine macroalgae. Plant Biology **94**:401-417.

Lüning, K., and I. t. Dieck. 1989. Environmental triggers in algal seasonality. Botanica Marina **32**:389-398.

Lüning, K., P. Kadel, and S. Pang. 2008. Control of reproductive rhythmicity by environmental and endogenous signals in *Ulva pseudocurvata* (Chlorophyta). Journal of Phycology **44**:866-873.

Lüning, K., and M. Neushul. 1978. Light and temperature demands for growth and reproduction of laminarian gametophytes in southern and central California. Marine Biology **45**:297-309.

Lüning, K., and S. Pang. 2003. Mass cultivation of seaweeds: current aspects and approaches. Journal of Applied Phycology **15**:115-119.

Lüning, K., and C. Yarish. 1990. Seaweeds: their environment, biogeography, and ecophysiology. John Wiley & Sons, New York, USA.

Machado, L., M. Magnusson, N. Paul, R. Kinley, R. Nys, and N. Tomkins. 2016a. Identification of bioactives from the red seaweed *Asparagopsis taxiformis* that promote antimethanogenic activity in vitro. Journal of Applied Phycology **28**:3117-3126.

Machado, L., M. Magnusson, N. A. Paul, R. de Nys, and N. Tomkins. 2014. Effects of marine and freshwater macroalgae on in vitro total gas and methane production. PLOS ONE **9**:e85289.

Machado, L., M. Magnusson, N. A. Paul, R. Kinley, R. de Nys, and N. Tomkins. 2016b. Dose-response effects of *Asparagopsis taxiformis* and *Oedogonium* sp. on in vitro fermentation and methane production. Journal of Applied Phycology **28**:1443-1452.

Machado, L., N. Tomkins, M. Magnusson, D. J. Midgley, R. de Nys, and C. P. Rosewarne. 2018. In vitro response of rumen microbiota to the antimethanogenic red macroalga *Asparagopsis taxiformis*. Microbial Ecology **75**:811-818.

Magnusson, M., M. J. Vucko, T. L. Neoh, and R. de Nys. 2020. Using oil immersion to deliver a naturally-derived, stable bromoform product from the red seaweed *Asparagopsis taxiformis*. Algal Research **51**:102065.

Maia, M. R. G., A. J. M. Fonseca, H. M. Oliveira, C. Mendonça, and A. R. J. Cabrita. 2016. The potential role of seaweeds in the natural manipulation of rumen fermentation and methane production. Scientific Reports **6**:32321.

Martin, C., D. P. Morgavi, and M. Doreau. 2010. Methane mitigation in ruminants: from microbe to the farm scale. Animal **4**:351-365.

Martins, G. M., C. D. Harley, J. Faria, M. Vale, S. J. Hawkins, A. I. Neto, and F. Arenas. 2019. Direct and indirect effects of climate change squeeze the local distribution of a habitat-forming seaweed. Marine Ecology Progress Series **626**:43-52.

Masson-Delmotte, V. 2018. Global warming of 1.5°C: An IPCC special report on impacts of global warming of 1.5°C above pre-industrial levels and related global greenhouse gas emission pathways, in the contex of strengthening the global response to the thereat of blimate change, sustainable development, and efforts to eradicate poverty. [Masson-Delmotte, V., P. Zhai, H.-O. Pörtner, D. Roberts, J. Skea, P.R. Shukla, A. Pirani, W. Moufouma-Okia, C. Péan, R. Pidcock, S. Connors, J.B.R. Matthews, Y. Chen, X. Zhou, M.I. Gomis, E. Lonnoy, T. Maycock, M. Tignor, and T. Waterfield (eds.)]. In Press.

Mata, L., H. Gaspar, and R. Santos. 2012. Carbon/nutrient balance in relation to biomass production and halogenated compound content in the red alga *Asparagopsis taxiformis* (Bonnemaisoniaceae). Journal of Phycology **48**:248-253.

Mata, L., R. J. Lawton, M. Magnusson, N. Andreakis, R. de Nys, and N. A. Paul. 2017. Within-species and temperature-related variation in the growth and natural products of the red alga *Asparagopsis taxiformis*. Journal of Applied Phycology **29**:1437-1447.

Mata, L., A. Schuenhoff, and R. Santos. 2010. A direct comparison of the performance of the seaweed biofilters, *Asparagopsis armata* and *Ulva rigida*. Journal of Applied Phycology **22**:639-644.

Mata, L., J. Silva, A. Schuenhoff, and R. Santos. 2006. The effects of light and temperature on the photosynthesis of the *Asparagopsis armata* tetrasporophyte (*Falkenbergia rufolanosa*), cultivated in tanks. Aquaculture **252**:12-19.

Matinfar, M., F. Rafiee, P. Nejatkhah Manavi, I. Joon Lee, and Y.-K. Hong. 2013. Optimal conditions for tissue growth and branch induction of *Gracilariopsis persica*. Iranian Journal of Fisheries Sciences **12**:24-33.

Mayberry, D., H. Bartlett, J. Moss, T. Davison, and M. Herrero. 2019. Pathways to carbon-neutrality for the Australian red meat sector. Agricultural Systems **175**:13-21.

McConnell, O., and W. Fenical. 1977. Halogen chemistry of the red alga *Asparagopsis*. Phytochemistry **16**:367-374.

McGrath, J., S. M. Duval, L. F. M. Tamassia, M. Kindermann, R. T. Stemmler, V. N. de Gouvea, T. S. Acedo, I. Immig, S. N. Williams, and P. Celi. 2018. Nutritional strategies in ruminants: A lifetime approach. Research in Veterinary Science **116**:28-39.

Melgar, A., M. Harper, J. Oh, F. Giallongo, M. Young, T. Ott, S. Duval, and A. Hristov. 2020. Effects of 3-nitrooxypropanol on rumen fermentation, lactational performance, and resumption of ovarian cyclicity in dairy cows. Journal of Dairy Science **103**:410-432.

Menzel, A., and V. Dose. 2005. Analysis of long-term time series of the beginning of flowering by Bayesian function estimation. Meteorologische Zeitschrift **14**:429-434.

Menzel, A., and P. Fabian. 1999. Growing season extended in Europe. Nature **397**:659-659.

Menzel, A., T. H. Sparks, N. Estrella, E. Koch, A. Aasa, R. Ahas, K. Alm-Kübler, P. Bissolli, O. g. Braslavská, A. Briede, F. M. Chmielewski, Z. Crepinsek, Y. Curnel, Å. Dahl, C. Defila, A. Donnelly, Y. Filella, K. Jatczak, F. Mäge, A. Mestre, Ø. Nordli, J. Peñuelas, P. Pirinen, V. Remišová, H. Scheifinger, M. Striz, A. Susnik, A. J. H. Van Vliet, F.-E. Wielgolaski, S. Zach, and A. Zust. 2006. European phenological response to climate change matches the warming pattern. Global Change Biology **12**:1969-1976.

MfE. 2020. New Zealand's greenhouse gas inventory 1990-2018. Ministry for the Environment, Wellington, New Zealand.

Mickelson, A. 2013. Defining culture requirements for reproduction and growth of *Asparagopsis taxiformis*, a Hawaiian native red alga. Master's Dissertation, University of Hawai'i, US.

Mihaila, A. A. 2020. Investigating the anti-methanogenic properties of select species of seaweed in New Zealand. Master's Dissertation, The University of Waikato, New Zealand.

Mihaila, A. A., R. J. Lawton, C. R. K. Glasson, and M. Magnusson. 2023a. Early hatchery protocols for tetrasporogenesis of the antimethanogenic seaweed *Asparagopsis armata*. Journal of Applied Phycology **35**:2323-2335.

Mihaila, A. A., R. J. Lawton, C. R. K. Glasson, and M. Magnusson. 2024. Moderate temperature and water flow increase growth during the nursery phase of *Asparagopsis armata*. Algal Research **78**:103380.

Mihaila, A. A., M. Magnusson, C. R. K. Glasson, and R. J. Lawton. 2023b. The reproductive phenology of *Asparagopsis armata* in New Zealand - potential shifts 35 years later. Algal Research **76**:103318.

Min, B. R., D. Parker, D. Brauer, H. Waldrip, C. Lockard, K. Hales, A. Akbay, and S. Augyte. 2021. The role of seaweed as a potential dietary supplementation for enteric methane mitigation in ruminants: Challenges and opportunities. Animal Nutrition **7**:1371-1387.

Mišurcová, L., J. Ambrožová, and D. Samek. 2011. Seaweed lipids as nutraceuticals. Advances in Food and Nutrition Research **64**:339-355.
Mohring, M. B., T. Wernberg, G. A. Kendrick, and M. J. Rule. 2013. Reproductive synchrony in a habitat-forming kelp and its relationship with environmental conditions. Marine Biology **160**:119-126.
Moigne, J. 1998. Use of algae extracts as antibacterial and/or antifungal agent and composition containing same, PCT Patent WO1998010656:A1.
Molenaar, F. J., A. M. Breeman, and L. A. H. Venekamp. 1996. Ecotypic variation in *Cystoclonium purpureum* (Rhodophyta) synchronizes life history events in different regions. Journal of Phycology **32**:516-525.
Molina-Alcaide, E., M. D. Carro, M. Y. Roleda, M. R. Weisbjerg, V. Lind, and M. Novoa-Garrido. 2017. In vitro ruminal fermentation and methane production of different seaweed species. Animal Feed Science and Technology **228**:1-12.
Montero-Fernández, M., R. R. Robaina, and P. Garcia-Jimenez. 2016. In silico characterization of DNA motifs associated with the differential expression of the ornithine decarboxylase gene during in vitro cystocarp development in the red seaweed *Grateloupia imbricata*. Journal of Plant Physiology **195**:31-38.
Mooney-McAuley, K., M. Edwards, J. Champenois, and E. Gorman. 2016. Best practice guidelines for seaweed cultivation and analysis: Public output report [WP1A5.01] of the EnAlgae project. WP1A5.01, EnAlgae, Swansea, UK.
Moore, P. J., R. C. Thompson, and S. J. Hawkins. 2011. Phenological changes in intertidal con-specific gastropods in response to climate warming. Global Change Biology **17**:709-719.
Morais, T., A. Inácio, T. Coutinho, M. Ministro, J. Cotas, L. Pereira, and K. Bahcevandziev. 2020. Seaweed potential in the animal feed: A review. Journal of Marine Science and Engineering **8**:559.
Morelissen, B., B. D. Dudley, S. W. Geange, and N. E. Phillips. 2013. Gametophyte reproduction and development of *Undaria pinnatifida* under varied nutrient and irradiance conditions. Journal of Experimental Marine Biology and Ecology **448**:197-206.
Moriya, Y., M. Itoh, S. Okuda, A. C. Yoshizawa, and M. Kanehisa. 2007. KAAS: an automatic genome annotation and pathway reconstruction server. Nucleic Acids Research **35**:W182-185.
Narassimhan, E., K. S. Gallagher, S. Koester, and J. R. Alejo. 2018. Carbon pricing in practice: a review of existing emissions trading systems. Climate Policy **18**:967-991.
National Institute of of Water and Atmospheric Research [NIWA]. 2022a. The national climate database. Available at: http://cliflo.niwa.co.nz.
National Institute of of Water and Atmospheric Research [NIWA]. 2022b. Monthly climate summaries from December 2001 to the present. Available at: http://niwa.co.nz/climate/monthly.
Nepper-Davidsen, J., M. Magnusson, C. R. K. Glasson, and R. J. Lawton. 2023. Line configuration and farming depth markedly affect survival and growth in the kelp *Ecklonia radiata*. New Zealand Journal of Marine and Freshwater Research **1**:1-17.
Neto, A. 2001. Macroalgal species diversity and biomass of subtidal communities of São Miguel (Azores). Helgoland Marine Research **55**:101-111.
Neto, A. I. 2000. Observations on the biology and ecology of selected macroalgae from the littoral of São Miguel (Azores). Botanica Marina **43**:483-498.

Nimura, K., and H. Mizuta. 2002. Inducible effects of abscisic acid on sporophyte discs from *Laminaria japonica* Areschoug (Laminariales, Phaeophyceae). Journal of Applied Phycology **14**:159-163.

Niwa, K., and K. Harada. 2013. Physiological responses to nitrogen deficiency and resupply in different blade portions of *Pyropia yezoensis* f. *narawaensis* (Bangiales, Rhodophyta). Journal of Experimental Marine Biology and Ecology **439**:113-118.

O'Mara, F. P. 2011. The significance of livestock as a contributor to global greenhouse gas emissions today and in the near future. Animal Feed Science and Technology **166-167**:7-15.

Odongo, N. E., R. Bagg, G. Vessie, P. Dick, M. M. Or-Rashid, S. E. Hook, J. T. Gray, E. Kebreab, J. France, and B. W. McBride. 2007. Long-term effects of feeding monensin on methane production in lactating dairy cows. Journal of Dairy Science **90**:1781-1788.

Oh, K.-B., J. H. Lee, S.-C. Chung, J. Shin, H. J. Shin, H.-K. Kim, and H.-S. Lee. 2008. Antimicrobial activities of the bromophenols from the red alga *Odonthalia corymbifera* and some synthetic derivatives. Bioorganic & Medicinal Chemistry Letters **18**:104-108.

Oliveira, E. C., K. Alveal, and R. J. Anderson. 2000. Mariculture of the agar-producing gracilarioid red algae. Reviews in Fisheries Science **8**:345-377.

Oliver, E. C. J., M. G. Donat, M. T. Burrows, P. J. Moore, D. A. Smale, L. V. Alexander, J. A. Benthuysen, M. Feng, A. Sen Gupta, A. J. Hobday, N. J. Holbrook, S. E. Perkins-Kirkpatrick, H. A. Scannell, S. C. Straub, and T. Wernberg. 2018. Longer and more frequent marine heatwaves over the past century. Nature Communications **9**:1324.

Oza, R. M. 1977. Culture studies on induction of tetraspores and their subsequent development in the red alga *Falkenbergia rufolanosa* (Harvey) Schmitz. Botanica Marina **20**:29-32.

Pan, J., W. Li, B. Chen, L. Liu, J. Zhang, and J. Li. 2023. *Arabidopsis* 3β-hydroxysteroid dehydrogenases/C4-decarboxylases are essential for the pollen and embryonic development. International Journal of Molecular Sciences **24**:15565.

Pandey, D., M. Mansouryar, M. Novoa-Garrido, G. Næss, V. Kiron, H. H. Hansen, M. O. Nielsen, and P. Khanal. 2021. Nutritional and anti-methanogenic potentials of macroalgae for ruminants. In: Seaweed and microalgae as alternative sources of protein. Burleigh Dodds Science Publishing Limited, Cambridge, UK, pp 344-379.

Pang, S. J., and K. Lüning. 2006. Tank cultivation of the red alga *Palmaria palmata*: year-round induction of tetrasporangia, tetraspore release in darkness and mass cultivation of vegetative thalli. Aquaculture **252**:20-30.

Parmesan, C. 2006. Ecological and evolutionary responses to recent climate change. Annual Review of Ecology, Evolution, and Systematics **37**:637-669.

Parmesan, C. 2007. Influences of species, latitudes and methodologies on estimates of phenological response to global warming. Global Change Biology **13**:1860-1872.

Patwary, Z. P. 2023. Multi-omics investigation across the life-history stages of the red seaweed, *Asaparagopsis taxiformis.* PhD Dissertation, University of the Sunshine Coast, Queensland, Australia.

Patwary, Z. P., M. Zhao, N. A. Paul, and S. F. Cummins. 2023. Identification of reproductive sex-biased gene expression in *Asparagopsis taxiformis* (lineage 6) gametophytes. Journal of Phycology **00**:1-16.

Paul, N. A., R. d. Nys, and P. D. Steinberg. 2006. Chemical defence against bacteria in the red alga *Asparagopsis armata*: linking structure with function. Marine Ecology Progress Series **306**:87-101.

Pérez, M. J., E. Falqué, and H. Domínguez. 2016. Antimicrobial action of compounds from marine seaweed. Marine drugs **14**:52.

Peteiro, C., G. Bidegain, and N. Sánchez. 2019. Experimental evaluation of the effect of water velocity on the development of string-attached kelp seedlings (Laminariales) with implications for hatchery and nursery production. Algal Research **44**:101678.

Peteiro, C., and Ó. Freire. 2011. Effect of water motion on the cultivation of the commercial seaweed *Undaria pinnatifida* in a coastal bay of Galicia, Northwest Spain. Aquaculture **314**:269-276.

Philippart, C. J. M., H. M. van Aken, J. J. Beukema, O. G. Bos, G. C. Cadée, and R. Dekker. 2003. Climate-related changes in recruitment of the bivalve *Macoma balthica*. Limnology and Oceanography **48**:2171-2185.

Philippart, C. J. M., J. D. L. van Bleijswijk, J. C. Kromkamp, A. F. Zuur, and P. M. J. Herman. 2014. Reproductive phenology of coastal marine bivalves in a seasonal environment. Journal of Plankton Research **36**:1512-1527.

Pickering, N. K., V. H. Oddy, J. Basarab, K. Cammack, B. Hayes, R. S. Hegarty, J. Lassen, J. C. McEwan, S. Miller, C. S. Pinares-Patiño, and Y. de Haas. 2015. Animal board invited review: genetic possibilities to reduce enteric methane emissions from ruminants. Animal **9**:1431-1440.

Pilar, G.-J., B.-R. Olegario, and R. R. Rafael. 2016. Occurrence of jasmonates during cystocarp development in the red alga *Grateloupia imbricata*. Journal of Phycology **52**:1085-1093.

Pilar, G.-J., and R. R. Rafael. 2019. Insight into the mechanism of red elga reproduction. What else is beyond cystocarps development? In: Systems biology. IntechOpen, Rijeka, Croatia, pp 94-106.

Poloczanska, E. S., C. J. Brown, W. J. Sydeman, W. Kiessling, D. S. Schoeman, P. J. Moore, K. Brander, J. F. Bruno, L. B. Buckley, M. T. Burrows, C. M. Duarte, B. S. Halpern, J. Holding, C. V. Kappel, M. I. O'Connor, J. M. Pandolfi, C. Parmesan, F. Schwing, S. A. Thompson, and A. J. Richardson. 2013. Global imprint of climate change on marine life. Nature Climate Change **3**:919-925.

Prayitno, C. H., F. K. Utami, A. Nugroho, and T. Widyastuti. 2019. The effect of seaweed (Gracilaria sp.) supplementation in sheep feed on methanogenesis inhibition in vitro. IOP Conference Series: Earth and Environmental Science **247**:012069.

Preuss, M., W. A. Nelson, and R. D'Archino. 2022. Cryptic diversity and phylogeographic patterns in the *Asparagopsis armata* species complex (Bonnemaisoniales, Rhodophyta) from New Zealand. Phycologia **61**:89-96.

Quigley, C. T. C. 2018. Thermal and microbial effects on brown macroalgae: Heat acclimation and the biodiversity of the microbiome. PhD Dissertation, The University of Maine, US.

Rawlinson, C., L. G. Kamphuis, J. P. A. Gummer, K. B. Singh, and R. D. Trengove. 2015. A rapid method for profiling of volatile and semi-volatile phytohormones using methyl chloroformate derivatisation and GC–MS. Metabolomics **11**:1922-1933.

Redmond, S., L. Green-Gavrielidis, C. Yarish, J. Kim, and C. Neefus. 2014. New England seaweed culture handbook: Nursery systems. Connecticut Sea Grant, Connecticut, USA.

Reisinger, A., S. F. Ledgard, and S. J. Falconer. 2017. Sensitivity of the carbon footprint of New Zealand milk to greenhouse gas metrics. Ecological Indicators **81**:74-82.
Reusch, T. B. H. 2014. Climate change in the oceans: evolutionary versus phenotypically plastic responses of marine animals and plants. Evolutionary Applications **7**:104-122.
Richards, A. 2012. Phenological shifts in hatch timing of northern shrimp *Pandalus borealis*. Marine Ecology Progress Series **456**:149-158.
Richardson, A. J., and E. S. Poloczanska. 2008. Under-resourced, under threat. Science **320**:1294.
Richardson, J. T. E. 2011. Eta squared and partial eta squared as measures of effect size in educational research. Educational Research Review **6**:135-147.
Ridoutt, B., S. A. Lehnert, S. Denman, E. Charmley, R. Kinley, and S. Dominik. 2022. Potential GHG emission benefits of *Asparagopsis taxiformis* feed supplement in Australian beef cattle feedlots. Journal of Cleaner Production **337**:130499.
Robinson, N., P. Winberg, and L. Kirkendale. 2013. Genetic improvement of macroalgae: status to date and needs for the future. Journal of Applied Phycology **25**:703-716.
Rogers, L. A., and A. B. Dougherty. 2019. Effects of climate and demography on reproductive phenology of a harvested marine fish population. Global Change Biology **25**:708-720.
Roleda, M. Y., and C. L. Hurd. 2019. Seaweed nutrient physiology: application of concepts to aquaculture and bioremediation. Phycologia **58**:552-562.
Roque, B. M., C. G. Brooke, J. Ladau, T. Polley, L. J. Marsh, N. Najafi, P. Pandey, L. Singh, R. Kinley, J. K. Salwen, E. Eloe-Fadrosh, E. Kebreab, and M. Hess. 2019a. Effect of the macroalgae *Asparagopsis taxiformis* on methane production and rumen microbiome assemblage. Animal Microbiome **1**:3.
Roque, B. M., J. K. Salwen, R. Kinley, and E. Kebreab. 2019b. Inclusion of *Asparagopsis armata* in lactating dairy cows' diet reduces enteric methane emission by over 50 percent. Journal of Cleaner Production **234**:132-138.
Roque, B. M., M. Venegas, R. D. Kinley, R. de Nys, T. L. Duarte, X. Yang, and E. Kebreab. 2021. Red seaweed (*Asparagopsis taxiformis*) supplementation reduces enteric methane by over 80 percent in beef steers. PLOS ONE **16**:e0247820.
Rule, M., T. Wernberg, G. Kendrick, and M. Rule. 2013. Reproductive synchrony in a habitat-forming kelp and its relationship with environmental conditions. Marine Biology **160**:119-126.
Sacramento, A. T., P. García-Jiménez, R. Alcázar, A. F. Tiburcio, and R. R. Robaina. 2004. Influence of polyamines on the sporulation of *Grateloupia* (Halymeniaceae, Rhodophyta). Journal of Phycology **40**:887-894.
Sacramento, A. T., P. García-Jiménez, and R. R. Robaina. 2007. The polyamine spermine induces cystocarp development in the seaweed *Grateloupia* (Rhodophyta). Plant Growth Regulation **53**:147-154.
Sahoo, D., and C. Yarish. 2005. Mariculture of seaweeds. Phycological Methods: Algal Culturing Techniques. Academic Press, New York, US, pp 219-237.
Santelices, B. 1989. Algas marinas de Chile: distribución, ecología, utilización, diversidad. Ediciones Universidad Católica de Chile, Santiago, Chile.
Savchenko, T., J. W. Walley, E. W. Chehab, Y. Xiao, R. Kaspi, M. F. Pye, M. E. Mohamed, C. M. Lazarus, R. M. Bostock, and K. Dehesh. 2010. Arachidonic acid: an evolutionarily conserved signaling molecule modulates plant stress signaling networks. The Plant Cell **22**:3193-3205.

Schuenhoff, A., L. Mata, and R. Santos. 2006. The tetrasporophyte of *Asparagopsis armata* as a novel seaweed biofilter. Aquaculture **252**:3-11.
Sea Temperature Info. 2022. Water temperature in Goat Island. Available at: https://seatemperature.info/new-zealand/goat-island-water-temperature.html.
Searles, R. B. 1980. The strategy of the red algal life history. The American Naturalist **115**:113-120.
Shears, N. T., and R. C. Babcock. 2007. Quantitative description of mainland New Zealand's shallow subtidal reef communities. Science & Technical Publishing, Department of Conservation, Wellington, New Zealand.
Shears, N. T., and M. M. Bowen. 2017. Half a century of coastal temperature records reveal complex warming trends in western boundary currents. Scientific Reports **7**:14527.
Singh, A., P. Kanwar, A. Pandey, A. K. Tyagi, S. K. Sopory, S. Kapoor, and G. K. Pandey. 2013. Comprehensive genomic analysis and expression profiling of phospholipase C gene family during abiotic stresses and development in rice. PLOS ONE **8**:e62494.
Singh, S. P., and P. Singh. 2015. Effect of temperature and light on the growth of algae species: A review. Renewable and Sustainable Energy Reviews **50**:431-444.
Sirirustananun, N., J.-C. Chen, Y.-C. Lin, S.-T. Yeh, C.-H. Liou, L.-L. Chen, S. S. Sim, and S. L. Chiew. 2011. Dietary administration of a *Gracilaria tenuistipitata* extract enhances the immune response and resistance against *Vibrio alginolyticus* and white spot syndrome virus in the white shrimp *Litopenaeus vannamei*. Fish & Shellfish Immunology **31**:848-855.
Slesinger, E., O. P. Jensen, and G. Saba. 2021. Spawning phenology of a rapidly shifting marine fish species throughout its range. ICES Journal of Marine Science **78**:1010-1022.
Smart, C. C., and A. J. Fleming. 1993. A plant gene with homology to d-myo-inositol-3-phosphate synthase is rapidly and spatially up-regulated during an abscisic-acid-induced morphogenic response in *Spirodela polyrrhiza*. The Plant Journal **4**:279-293.
Stewart, H. L., and R. C. Carpenter. 2003. The effects of morphology and water flow on photosynthesis of marine macroalgae. Ecology **84**:2999-3012.
Stirk, W. A., P. Bálint, D. Tarkowská, O. Novák, M. Strnad, V. Ördög, and J. van Staden. 2013. Hormone profiles in microalgae: Gibberellins and brassinosteroids. Plant Physiology and Biochemistry **70**:348-353.
Stirk, W. A., D. Tarkowská, V. Turečová, M. Strnad, and J. van Staden. 2014. Abscisic acid, gibberellins and brassinosteroids in Kelpak®, a commercial seaweed extract made from *Ecklonia maxima*. Journal of Applied Phycology **26**:561-567.
Stirk, W. A., and J. Van Staden. 2014. Plant growth regulators in seaweeds: occurrence, regulation and functions. Advances in botanical research. Elsevier Limited, London, UK, pp 125-159.
Su, L., S. J. Pang, T. F. Shan, and X. Li. 2017. Large-scale hatchery of the kelp *Saccharina japonica*: a case study experience at Lvshun in northern China. Journal of Applied Phycology **29**:3003-3013.
Sudatti, D. B., M. T. Fujii, S. V. Rodrigues, A. Turra, and R. C. Pereira. 2018. Prompt induction of chemical defenses in the red seaweed *Laurencia dendroidea*: The role of herbivory and epibiosis. Journal of Sea Research **138**:48-55.
Sun, D., X. Zhou, X. Sun, and N. Xu. 2023. Transcriptomic analysis reveals the regulatory mechanism of tetraspore formation in *Gracilariopsis lemaneiformis*. Frontiers in Marine Science **9**:1080474.

Sunrise and sunset. 2020. Sunrise and sunset Auckland, New Zealand. Available at: https://www.sunrise-and-sunset.com/en/sun/new-zealand/auckland.
Taelman, S. E., J. Champenois, M. D. Edwards, S. De Meester, and J. Dewulf. 2015. Comparative environmental life cycle assessment of two seaweed cultivation systems in North West Europe with a focus on quantifying sea surface occupation. Algal Research **11**:173-183.
Tan, X., and N. Zheng. 2009. Hormone signaling through protein destruction: a lesson from plants. American Journal of Physiology-Endocrinology and Metabolism **296**:e223-e227.
Tanna, B., and A. Mishra. 2018. Chapter 2 - metabolomics of seaweeds: Tools and techniques. In: Plant metabolites and regulation under environmental stress. Academic Press, Elsevier Limited, pp 37-52.
Thépot, V., A. H. Campbell, N. A. Paul, and M. A. Rimmer. 2021. Seaweed dietary supplements enhance the innate immune response of the mottled rabbitfish, *Siganus fuscescens*. Fish and Shellfish Immunology **113**:176-184.
Tomkins, N., S. Colegate, and R. Hunter. 2009. A bromochloromethane formulation reduces enteric methanogenesis in cattle fed grain-based diets. Animal Production Science **49**:1053-1058.
Torres, R., L. Mata, R. Santos, and A. Alexandre. 2021. Nitrogen uptake kinetics of an enteric methane inhibitor, the red seaweed *Asparagopsis armata*. Journal of Applied Phycology **33**:4001-4009.
Trapnell, C., B. A. Williams, G. Pertea, A. Mortazavi, G. Kwan, M. J. van Baren, S. L. Salzberg, B. J. Wold, and L. Pachter. 2010. Transcript assembly and quantification by RNA-Seq reveals unannotated transcripts and isoform switching during cell differentiation. Nature Biotechnology **28**:511-515.
Tsui, M. M., and J. D. York. 2010. Roles of inositol phosphates and inositol pyrophosphates in development, cell signaling and nuclear processes. Advances in Enzyme Regulation **50**:324-337.
Tubiello, F. N., M. Salvatore, S. Rossi, A. Ferrara, N. Fitton, and P. Smith. 2013. The FAOSTAT database of greenhouse gas emissions from agriculture. Environmental Research Letters **8**:015009.
Uji, T., H. Endo, and H. Mizuta. 2020. Sexual reproduction via a 1-aminocyclopropane-1-carboxylic acid-dependent pathway through redox modulation in the marine red alga *Pyropia yezoensis* (Rhodophyta). Frontiers in Plant Science **11**:60.
Uji, T., and H. Mizuta. 2022. The role of plant hormones on the reproductive success of red and brown algae. Frontiers in Plant Science **13**:1019334.
Ungerfeld, E., K. Beauchemin, and C. Muñoz. 2022. Current perspectives on achieving pronounced enteric methane mitigation from ruminant production. Frontiers in Animal Science **2**:795200.
Vadas, R. L., S. Johnson, and T. A. Norton. 1992. Recruitment and mortality of early post-settlement stages of benthic algae. British Phycological Journal **27**:331-351.
Vairappan, C. S., M. Suzuki, T. Ishii, T. Okino, T. Abe, and M. Masuda. 2008. Antibacterial activity of halogenated sesquiterpenes from Malaysian *Laurencia* spp. Phytochemistry **69**:2490-2494.
Vatsos, I. N., and C. Rebours. 2015. Seaweed extracts as antimicrobial agents in aquaculture. Journal of Applied Phycology **27**:2017-2035.

Vega-Muñoz, I., D. Duran-Flores, Á. D. Fernández-Fernández, J. Heyman, A. Ritter, and S. Stael. 2020. Breaking bad news: Dynamic molecular mechanisms of wound response in plants. Frontiers in Plant Science **11**:610445.

Vergés, A., C. Doropoulos, H. A. Malcolm, M. Skye, M. Garcia-Pizá, E. M. Marzinelli, A. H. Campbell, E. Ballesteros, A. S. Hoey, A. Vila-Concejo, Y.-M. Bozec, and P. D. Steinberg. 2016. Long-term empirical evidence of ocean warming leading to tropicalization of fish communities, increased herbivory, and loss of kelp. Proceedings of the National Academy of Sciences **113**:13791.

Vergés, A., E. McCosker, M. Mayer-Pinto, M. A. Coleman, T. Wernberg, T. Ainsworth, and P. D. Steinberg. 2019. Tropicalisation of temperate reefs: Implications for ecosystem functions and management actions. Functional Ecology **33**:1000-1013.

Vergés, A., P. D. Steinberg, M. E. Hay, A. G. B. Poore, A. H. Campbell, E. Ballesteros, K. L. Heck, D. J. Booth, M. A. Coleman, D. A. Feary, W. Figueira, T. Langlois, E. M. Marzinelli, T. Mizerek, P. J. Mumby, Y. Nakamura, M. Roughan, E. van Sebille, A. S. Gupta, D. A. Smale, F. Tomas, T. Wernberg, and S. K. Wilson. 2014. The tropicalization of temperate marine ecosystems: climate-mediated changes in herbivory and community phase shifts. Proceedings of the Royal Society B **281**:20140846.

Vesty, E. F., R. W. Kessler, T. Wichard, and J. C. Coates. 2015. Regulation of gametogenesis and zoosporogenesis in *Ulva linza* (Chlorophyta): comparison with *Ulva mutabilis* and potential for laboratory culture. Frontiers in Plant Science **6**:15.

Viejo, R. M., B. Martínez, J. Arrontes, C. Astudillo, and L. Hernández. 2011. Reproductive patterns in central and marginal populations of a large brown seaweed: drastic changes at the southern range limit. Ecography **34**:75-84.

Vijn, S., D. P. Compart, N. Dutta, A. Foukis, M. Hess, A. N. Hristov, K. F. Kalscheur, E. Kebreab, S. V. Nuzhdin, N. N. Price, Y. Sun, J. M. Tricarico, A. Turzillo, M. R. Weisbjerg, C. Yarish, and T. D. Kurt. 2020. Key considerations for the use of seaweed to reduce enteric methane emissions from cattle. Frontiers in Veterinary Science **7**:e597430.

Villafranca, J. J. 1974. The mechanism of aconitase action: Evidence for an enzyme isomerization by studies of inhibition by tricarboxylic acids. Journal of Biological Chemistry **249**:6149-6155.

Visch, W., H. Lush, J. Schwoerbel, and C. L. Hurd. 2023. Nursery optimization for kelp aquaculture in the Southern Hemisphere: the interactive effects of temperature and light on growth and contaminants. Applied Phycology **4**:44-53.

Vitasse, Y., F. Baumgarten, C. M. Zohner, T. Rutishauser, B. Pietragalla, R. Gehrig, J. Dai, H. Wang, Y. Aono, and T. H. Sparks. 2022. The great acceleration of plant phenological shifts. Nature Climate Change **12**:300-302.

Vucko, M. J., M. Magnusson, R. D. Kinley, C. Villart, and R. de Nys. 2017. The effects of processing on the in vitro antimethanogenic capacity and concentration of secondary metabolites of *Asparagopsis taxiformis*. Journal of Applied Phycology **29**:1577-1586.

Wang, W., M. Xu, G. Wang, and G. Galili. 2018. New insights into the metabolism of aspartate-family amino acids in plant seeds. Plant Reproduction **31**:203-211.

Wang, X., L. He, Y. Ma, L. Huan, Y. Wang, B. Xia, and G. Wang. 2020. Economically important red algae resources along the Chinese coast: History, status, and prospects for their utilization. Algal Research **46**:101817.

Wang, X., F.-l. Liu, and D. Jiang. 2017. Priming: A promising strategy for crop production in response to future climate. Journal of Integrative Agriculture **16**:2709-2716.
Wang, Y., Z. Xu, S. Bach, and T. McAllister. 2008. Effects of phlorotannins from *Ascophyllum nodosum* (brown seaweed) on in vitro ruminal digestion of mixed forage or barley grain. Animal Feed Science and Technology **145**:375-395.
Watson, L., and M. Dring. 2011. Business plan for the establishment of a seaweed hatchery and grow-out farm (part 2). PBA/SW/07/001 (01), Irish Sea Fisheries Board, Dublin, Ireland.
Wedlock, D. N., G. Pedersen, M. Denis, D. Dey, P. H. Janssen, and B. M. Buddle. 2010. Development of a vaccine to mitigate greenhouse gas emissions in agriculture: vaccination of sheep with methanogen fractions induces antibodies that block methane production in vitro. New Zealand Veterinary Journal **58**:29-36.
Wernberg, T., D. A. Smale, and M. S. Thomsen. 2012. A decade of climate change experiments on marine organisms: procedures, patterns and problems. Global Change Biology **18**:1491-1498.
Werner, A., D. Clarke, and S. Kraan. 2004. Strategic review and the feasibility of seaweed aquaculture in Ireland. Marine Institute, Ireland.
Werner, A., and M. Dring. 2011. Aquaculture explained no. 27-cultivating *Palmaria palmata*. PBA/SW/07/001 (27), Irish Sea Fisheries Board, Dublin, Ireland.
West, J. A., and D. L. McBride. 1999. Long-term and diurnal carpospore discharge patterns in the Ceramiaceae, Rhodomelaceae and Delesseriaceae (Rhodophyta). Hydrobiologia **398/399**:101-114.
Wiencke, C., and M. Clayton. 1990. Sexual reproduction, life history, and early development in culture of the Antarctic brown alga *Himantothallus grandifolius* (Desmarestiales, Phaeophyceae). Phycologia **29**:9-18.
Wiencke, C., M. Clayton, and C. Langreder. 1996. Life history and seasonal morphogenesis of the endemic Antarctic brown alga *Desmarestia anceps* Montagne. Botanica Marina **39**:435-444.
Wiencke, C., U. Stolpe, and H. Lehmann. 1991. Morphogenesis of the brown alga *Desmarestia antarctica* cultivated under seasonally fluctuating Antarctic daylegths. Serie Scientifica INACH **41**:65-78.
Wijesekara, I., N. Y. Yoon, and S. K. Kim. 2010. Phlorotannins from *Ecklonia cava* (Phaeophyceae): Biological activities and potential health benefits. Biofactors **36**:408-414.
Williams, S. P., G. E. Gillaspy, and I. Y. Perera. 2015. Biosynthesis and possible functions of inositol pyrophosphates in plants. Frontiers in Plant Science **6**:67.
Williams, Y. J., S. Popovski, S. M. Rea, L. C. Skillman, A. F. Toovey, K. S. Northwood, and A.-D. G. Wright. 2009. A vaccine against rumen methanogens can alter the composition of archaeal populations. Applied and Environmental Microbiology **75**:1860-1866.
Wood, J. M., F. S. Kennedy, and R. S. Wolfe. 1968. Reaction of multihalogenated hydrocarbons with free and bound reduced vitamin B12. Biochemistry **7**:1707-1713.
World Data Info. 2022. Sunrise and sunset data. Available at: https://www.worlddata.info/.
Wright, A. D. G., P. Kennedy, C. J. O'Neill, A. F. Toovey, S. Popovski, S. M. Rea, C. L. Pimm, and L. Klein. 2004. Reducing methane emissions in sheep by immunization against rumen methanogens. Vaccine **22**:3976-3985.

Wright, J. T., E. J. Kennedy, R. de Nys, and M. Tatsumi. 2022. Asexual propagation of *Asparagopsis armata* gametophytes: fragmentation, regrowth and attachment mechanisms for sea-based cultivation. Journal of Applied Phycology **1**:1-10.

Wu, G. 2010. Amino acids: Biochemistry and nutrition. 1st edition. CRC Press, Boca Raton, Florida, US.

Wu, T., E. Hu, S. Xu, M. Chen, P. Guo, Z. Dai, T. Feng, L. Zhou, W. Tang, L. Zhan, X. Fu, S. Liu, X. Bo, and G. Yu. 2021. clusterProfiler 4.0: A universal enrichment tool for interpreting omics data. Innovation (Camb) **2**:100141.

Xia, J., I. V. Sinelnikov, B. Han, and D. S. Wishart. 2015. MetaboAnalyst 3.0—making metabolomics more meaningful. Nucleic Acids Research **43**:W251-W257.

Yan, X.-H., F. Lv, C.-J. Liu, and Y.-F. Zheng. 2010. Selection and characterization of a high-temperature tolerant strain of *Porphyra haitanensis* Chang et Zheng (Bangiales, Rhodophyta). Journal of Applied Phycology **22**:511-516.

Yang, Y., M. A. Saand, L. Huang, W. B. Abdelaal, J. Zhang, Y. Wu, J. Li, M. H. Sirohi, and F. Wang. 2021. Applications of multi-omics technologies for crop improvement. Frontiers in Plant Science **12**:563953.

Yang, Z. 1996. Signal transducing proteins in plants: an overview. In: Signal transduction in plant growth and development. Springer, Vienna, Austria, pp 1-37.

Yu, K.-X., I. Jantan, R. Ahmad, and C.-L. Wong. 2014. The major bioactive components of seaweeds and their mosquitocidal potential. Parasitology Research **113**:3121-3141.

Zanolla, M., R. Carmona, and M. Altamirano. 2017. Reproductive ecology of an invasive lineage 2 population of *Asparagopsis taxiformis* (Bonnemaisoniales, Rhodophyta) in the Alboran Sea (western Mediterranean Sea). Botanica Marina **60**:627-638.

Zanolla, M., R. Carmona, L. Mata, J. De la Rosa, A. Sherwood, C. N. Barranco, A. R. Muñoz, and M. Altamirano. 2022. Concise review of the genus *Asparagopsis* Montagne, 1840. Journal of Applied Phycology **34**:1-17.

Zerrifi, S. E. A., F. El Khalloufi, B. Oudra, and V. Vasconcelos. 2018. Seaweed bioactive compounds against pathogens and microalgae: Potential uses on pharmacology and harmful algae bloom control. Marine drugs **16**:55.

Zhang, J., X. Li, F. Lu, S. Wang, Y. An, X. Su, X. Li, L. Ma, and G. Han. 2017. De novo sequencing and transcriptome analysis reveal key genes regulating steroid metabolism in leaves, roots, adventitious roots and calli of *Periploca sepium* Bunge. Frontiers in Plant Science **8**:594.

Zhang, Q., S. Song, D. Gao, H. Ding, and X. Yan. 2021. Time-series transcriptomic analysis reveals potential genes and pathways involved in the process of monospore formation in *Phycocalida chauhanii*. Journal of Applied Phycology **33**:1925-1937.

Zhao, M., A. Campbell, Z. Patwary, T. Wang, T. Lang, J. Webb, G. Zuccarello, A. Wegner, D. Heyne, L. McKinnie, C. Pascelli, N. Satoh, E. Shoguchi, N. Paul, and S. Cummins. 2022. The red seaweed *Asparagopsis taxiformis* genome and integrative -omics analysis. Preprint (Version 1). Research Square, 09 November 2022.

Zhou, W., Z. Sui, J. Wang, and L. Chang. 2013. An orthogonal design for optimization of growth conditions for all life history stages of *Gracilariopsis lemaneiformis* (Rhodophyta). Aquaculture **392**:98-105.

Zhu, P., D. Li, Q. Yang, P. Su, H. Wang, K. Heimann, and W. Zhang. 2021. Commercial cultivation, industrial application, and potential halocarbon biosynthesis pathway of *Asparagopsis* sp. Algal Research **56**:102319.

Zubia, M., Y. Freile-Pelegrín, and D. Robledo. 2014. Photosynthesis, pigment composition and antioxidant defences in the red alga *Gracilariopsis tenuifrons* (Gracilariales, Rhodophyta) under environmental stress. Journal of Applied Phycology **26**:2001-2010.

Appendices

Appendix 1 Immature tetrasporangia (arrowhead) in poorly pigmented tetrasporophytes of *A. armata* collected during March and April in 2021 and 2022. Scale bar = 50 µm.

Appendix 2 Colour image of thallus, cystocarps, and carpospores (arrowhead) in poorly pigmented gametophytes of *A. armata* collected during October in 2022 that became discoloured within 24 h of exposure to controlled conditions (18 °C, 20 – 25 µmol photos m^{-2} s^{-1}, 12 h L:12 h D). Scale bar = 1 mm.

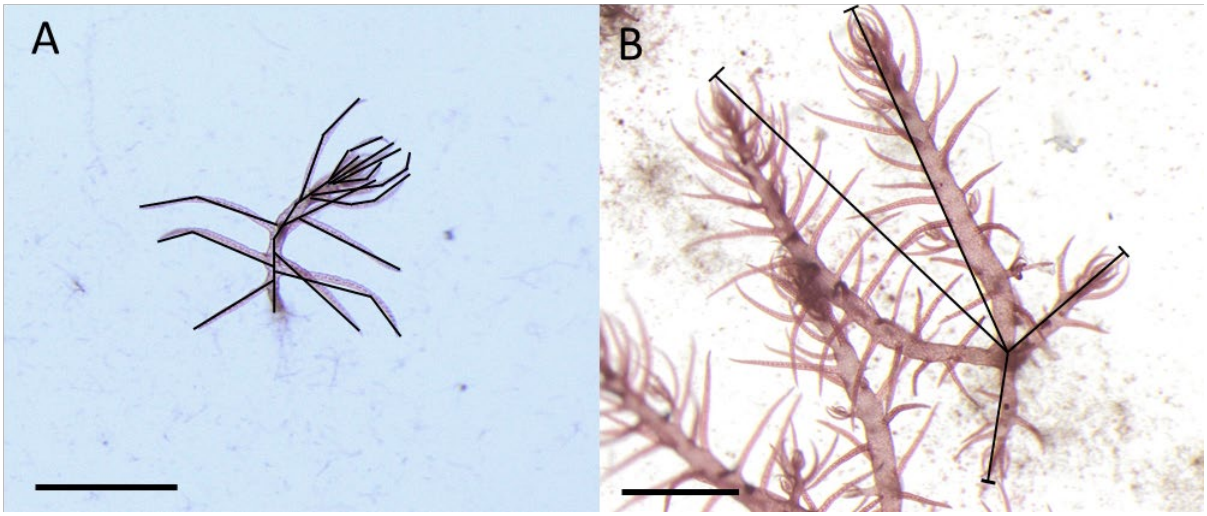

Appendix 3 Examples of how gametophytes were measured during each experiment. Black lines in (A) demonstrate how gametophytes were measured during experiment one, i.e., the combined total length of all branches for each individual. Black lines in (B) demonstrate how gametophytes were measured during experiment two, i.e., the combined total length of determinate branches only for each individual. Scale bar = 1mm.

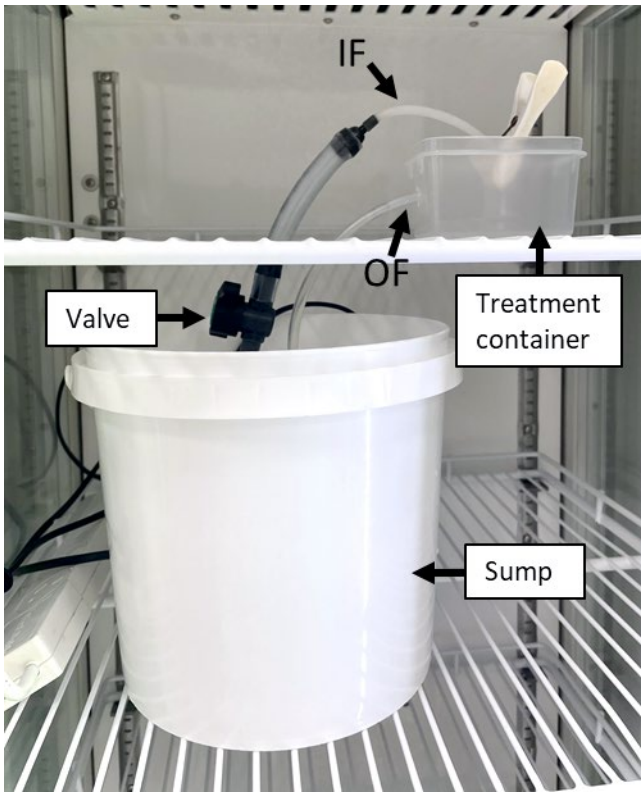

Appendix 4 Individual recirculating flow system used in experiment two. Treatment containers contained individual seeded microscope slides. IF = water inflow, OF = water outflow.

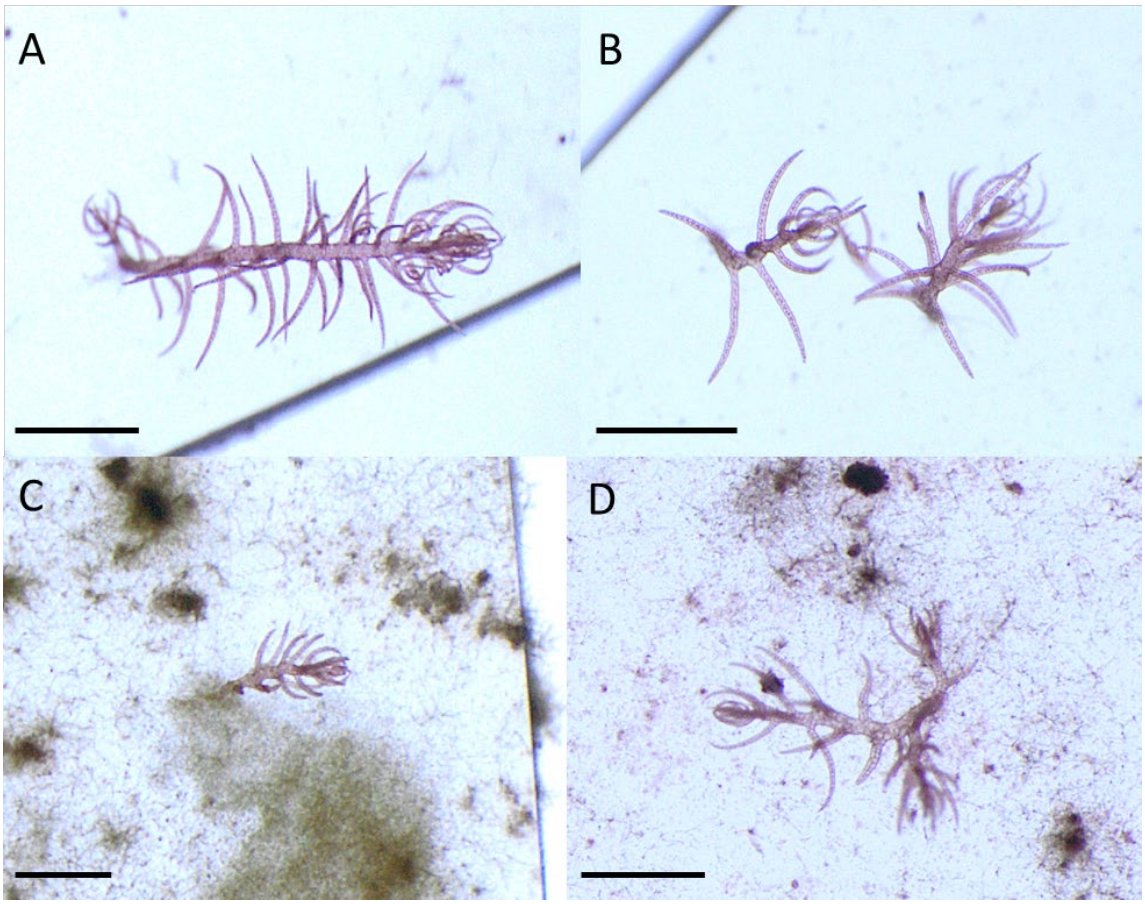

Appendix 5 Examples of increased contamination under high irradiance (30 µmol photons m^{-2} s^{-1}) treatments compared to low irradiance (15 µmol photons m^{-2} s^{-1}) treatments at the end of experiment one testing the effect of temperature (15, 18, and 21 °C), irradiance (15 and 30 µmol photons m^{-2} s^{-1}), and photoperiod (12 h L:12 h D and 8 h L:16 h D) on the development and growth of juvenile gametophytes. (A) 18 °C, 15 µmol photons m^{-2} s^{-1}, 12 h L:12 h D, (B) 15 °C, 15 µmol photons m^{-2} s^{-1}, 12 h L:12 h D, (C) 21 °C, 30 µmol photons m^{-2} s^{-1}, 12 h L:12 h D, (D) 18 °C, 30 µmol photons m^{-2} s^{-1}, 12 h L:12 h D. Scale bar (A) & (B) = 1 mm, (C) & (D) 500 µm.

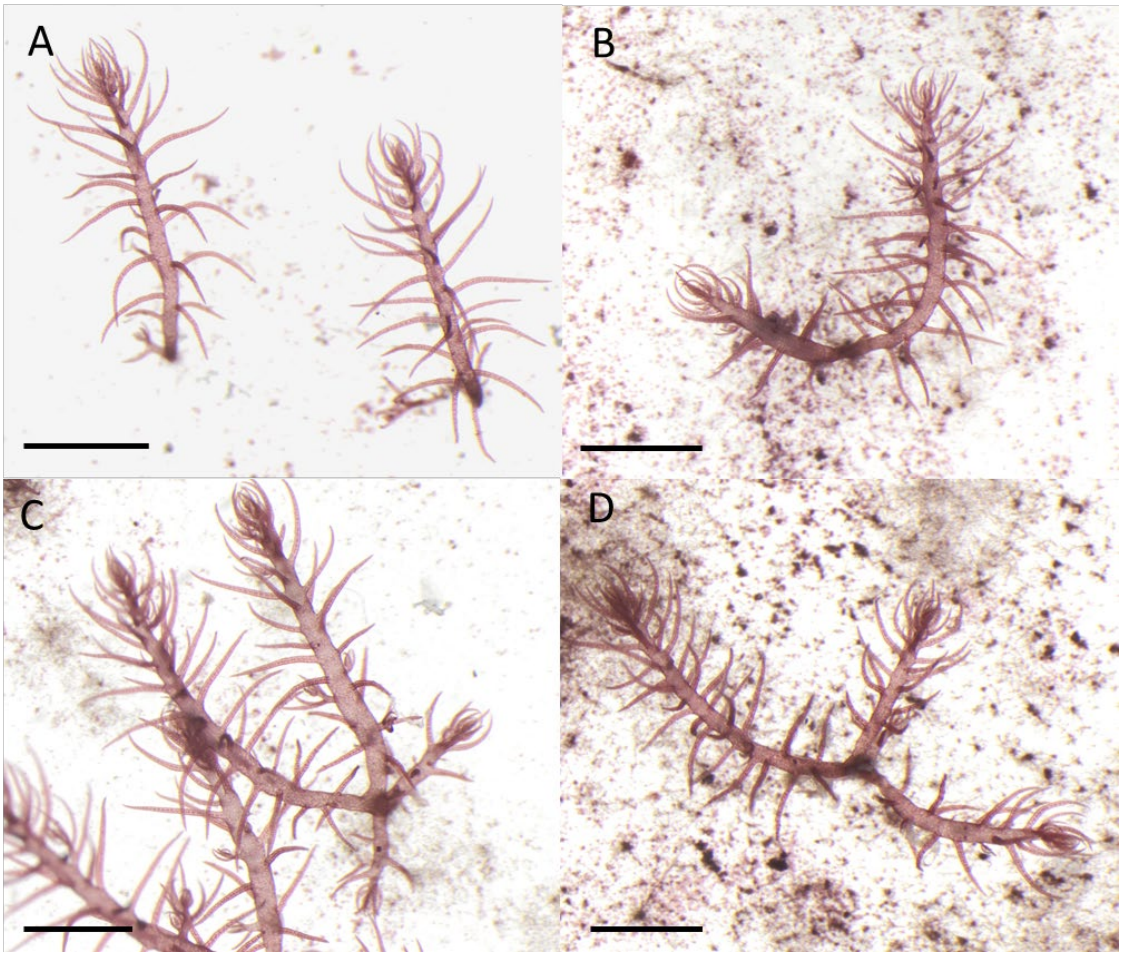

Appendix 6 Examples of gametophytes present under each treatment combination at the end of experiment two testing the effect of nutrient concentration (high = F/4 and low = F/8) and water flow (flow and static conditions) on the development and growth of juvenile gametophytes. (A) Static F/8, (B) Static F/4, (C) Flow F/8, (D) Flow F/4. Scale bar = 1 mm.

Appendix 7 Refer to **Additional File 1** for: Table S1 Summary of total reads per sample (RNA-sequencing data); Table S2 Metabolites identified in *A. armata* by GC-MS (across all samples); and Table S3 Significantly different metabolites ($P \leq 0.05$) between baseline and day 0 samples and between control and induction samples on days 7, 14, and 21.

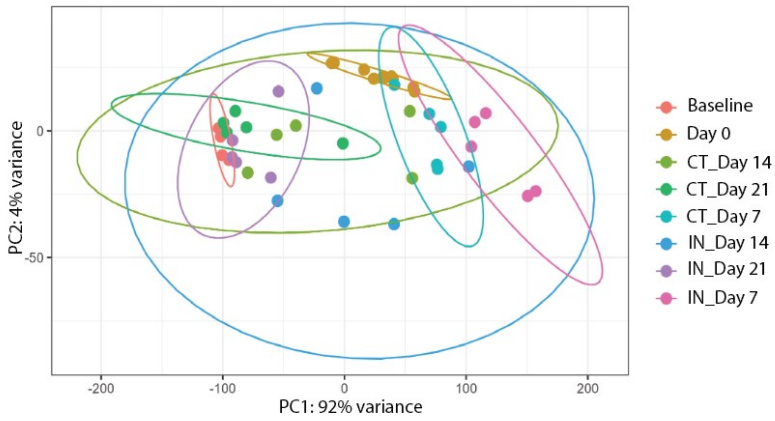

Appendix 8 PCA plot showing the gene expression profiles of *A. armata* during tetrasporogenesis comparing baseline, day 0, and control (CT) and induction (TR) samples on days 7, 14, and 21. Red and orange circles represent baseline (*n* = 5) and day 0 samples (*n* = 10), respectively. Turquoise, light green, and dark green circles represent control samples on days 7, 14, and 21 (*n* = 5), while pink, light blue, and purple circles represent induction samples on days 7, 14, and 21 (*n* = 5), respectively.

Appendix 9 Refer to **Additional File 2** for: Table S1–S4 Results of statistical analysis and gene annotations for differentially expressed genes (DEGs) identified between baseline and day 0 samples and between control and induction samples on days 7, 14, and 21.

Appendix 10 Refer to **Additional File 3** for: Table S1–S4 Enriched GO terms based on differentially expressed genes (DEGs) identified between baseline and day 0 samples and control and induction samples on days 7, 14, and 21, annotated to the category 'biological process'; and Table S5–S8 Enriched KEGG pathways based on DEGs identified between baseline and day 0 samples and control induction samples on days 7, 14, and 21.

Appendix 11 Refer to **Additional File 4** for: Table S1 Details for specific differentially expressed genes (DEGs) associated with photoreceptors on day 7; Table S2 Details for specific DEGs associated with the phosphatidylinositol (PI) signalling system on day 7; Table S3 Details for specific DEGs associated with inositol phosphate (IP) metabolism on day 7; Table S4 Details for specific DEGs associated with polyamine production on days 7 and 14; and Table S5 Details for specific DEGs associated with C21-steroid hormone metabolic process and steroid biosynthetic process on day 14.

Appendix 12 Chapters published as papers

Mihaila, A. A., M. Magnusson, C. R. K. Glasson, and R. J. Lawton. 2023a. The reproductive phenology of Asparagopsis armata in New Zealand - potential shifts 35 years later. Algal Research 76:103318

Mihaila, A. A., R. J. Lawton, C. R. K. Glasson, and M. Magnusson. 2023b. Early hatchery protocols for tetrasporogenesis of the antimethanogenic seaweed Asparagopsis armata. Journal of Applied Phycology 35:2323-2335

Mihaila, A. A., R. J. Lawton, C. R. K. Glasson, and M. Magnusson. 2024. Moderate temperature and water flow increase growth during the nursery phase of Asparagopsis armata. Algal Research 78:103380